

ALMA MATER STUDIORUM UNIVERSITÀ DI BOLOGNA

School of Engineering and Architecture
Department of Electrical, Electronics and Information Engineering
“Guglielmo Marconi”

MASTER DEGREE IN ELECTRICAL ENERGY ENGINEERING

THESIS IN
Predictive Maintenance for Electrical Infrastructures M

THESIS TITLE

Critical points in the More Electric Aircraft (MEA)
converter-machine chain

Author:
Ameet Kumar
Matr.: 0000903127

Supervisor:
Prof. Andrea Cavallini
Co-Supervisor:
Eng. Alberto Rumi

ACADEMIC YEAR 2020/21
First Session

Abstract

Electrical systems are now being used in applications that were formerly powered by hydraulic or pneumatic sources, which have resulted in a dramatic change in aircraft design. These new systems are helping to make future aircraft more fuel-efficient and quieter, improving the environment for everyone by reducing the weight and improving the efficiency and reliability of the aircraft. However, this requires advancements in electrical, electronics, and control systems. This research aims to analyze the critical points of the inverter to machine chain used in the actuation system of MEA. To analyze the critical points, it is necessary to investigate the Partial Discharge Inception Voltage (PDIV) of the printed circuit board (PCB, representative models of the high voltage part terminal part of the inverter) by considering the effects of aerospace conditions like pressure, temperature, and humidity on it. Along with the endurance tests of twisted pairs (TPs, representative models of the turn/turn insulation) at aerospace conditions, this is necessary to investigate the life of the machine when it is stressed by repetitive square wave/sinusoidal AC voltages. These experiments help to find the proper way to design and qualify MEA actuators.

In this research, the effect of AC voltages, space charges at DC, temperature, pressure, and converter waveforms have been analyzed on different PCB models. Results show that an increased temperature decreases the PDIV and a reduction of PDIV is observed due to reduction of pressure. It is also analyzed that space charges play an important role in the measurement of PDIV at DC. Finally, the effect of converter waveforms supplied by SiC is analyzed, where it is observed that there's an 8% increase of PDIV as compared to the PDIV in AC. After these entire tests, it is concluded that the HV terminal part is not critical in the sense of PD occurrence.

After the inverter part, the behaviors of insulation when it is continuously stressed by repetitive square wave/ AC 50 kHz voltages have been analyzed. The results obtained from both the supplies are compared with each other to understand the effect of supply type and frequency on the endurance, finally, the effect of humidity on the endurance of

the twisted pairs has been analyzed. It is observed after all these endurance tests that the corona-resistant wire can endure PD for a long time in aerospace conditions.

Table of Contents

1	Introduction	1
1.1	Objectives and approaches.....	3
2	Theory	5
2.1	Use of Chain Converter-Machine in MEA	5
2.1.1	More Electric Aircraft (MEA)	5
2.1.2	Techniques to decrease the size of electrical equipment in the aircraft.....	19
2.1.3	Importance of Inverters.....	21
2.1.3.1	Three-phase PWM Inverter	21
2.1.3.2	Wide-Band Gap (WBG) semiconductor devices	25
2.1.3.3	Importance of SiC Inverter.....	27
2.1.4	Over-stresses and uneven voltage distribution in converter fed machine.....	27
2.1.4.1	Effects of Wide Band Gap (WBG) converters.....	29
2.2	Partial Discharges (PDs).....	30
2.2.1	Classification of PDs.....	30
2.2.2	Problems and dangers created by PDs.....	31
2.2.2.1	Mechanism of degradation	32
2.2.3	Insulation in low pressure.....	33
2.2.4	Life curves	35
3	Test Setup	38
3.1	Printed Circuit Boards (PCBs)	39
3.1.1	Description of the test samples	39
3.1.2	Testing procedures for PCBs	40
3.1.2.1	Environment for testing.....	40
3.1.2.2	Voltage sources	43
3.1.3	Measurement techniques.....	45

3.1.3.1	Voltage measure	46
3.1.3.2	PD measure.....	46
3.1.4	Equipment for other than PD test.....	51
3.1.5	Experimental setup.....	52
3.1.5.1	Setup for PDIV measurement of PCBs at normal environmental conditions using AC 50Hz voltage supply	52
3.1.5.2	Setup for the measurement of PDIV at different temperatures (25°C, 80°C, and 120°C) using AC 50Hz voltage	53
3.1.5.3	Setup for the measurement of PDIV in DC at ambient condition	54
3.1.5.4	Setup for the measurement of PDIV at lower pressure in the case of AC 50Hz voltage	56
3.1.5.5	Setup for the measurement of PDIV at lower pressure in case of repetitive square wave generated by SiC pulser .	57
3.2	Twisted Pairs (TPs)	58
3.2.1	Construction and Description of TPs.....	59
3.2.2	Concept of the endurance test.....	60
3.2.3	Testing procedure for PCBs.....	61
3.2.3.1	Environment for testing.....	61
3.2.3.2	Voltage sources	61
3.2.4	Measurement techniques.....	62
3.2.4.1	Voltage measure	62
3.2.4.2	Endurance time.....	62
3.2.5	Test setup	62
3.2.5.1	Endurance test of twisted pairs at lower pressure using repetitive square waves generated by SiC pulser	63
3.2.5.2	Endurance test of twisted pairs at lower pressure using AC sinusoidal 50 kHz voltage source	64

4	Results and Discussion	67
4.1	Printed Circuit Boards (PCBs)	67
4.1.1	Analyze the effect of AC voltages on all the PCBs by comparing their Partial Discharge Inception Voltages (PDIVs) at ambient conditions	68
4.1.2	Effect of temperatures on the PDIV of PCBs in case of AC voltages	71
4.1.3	Effect of low pressure on PDIV of three types of PCBs in the case of AC supply	75
4.1.4	PDIV measurement of three kinds of PCBs and the role of space charges in the measurement of PDIV at DC supply	78
4.1.5	The effect of converter waveform on PDIV of PCBs in case of the repetitive square wave at 100 mbar	81
4.2	Twisted Pairs (TPs)	84
4.2.1	Effect of voltages (AC and repetitive square wave) stress on the endurance of the twisted pairs at lower pressure (150 mbar)	84
4.2.2	Effect of supply type (AC or Repetitive square wave) and their frequencies on the endurance of the twisted pairs at lower pressure (150 mbar)	90
4.2.3	Effect of humidity on the endurance of the twisted pairs	91
5	Conclusion	95

Chapter 1

Introduction:

The transportation sector is responsible for roughly a quarter of global greenhouse gas (GHG) emissions, and it is one of the main sectors where emissions are still increasing. A rapidly growing population increases transportation that makes the trend of fossil fuel increase in a faster way. Due to society's persistent reliance on fossil fuels, the reduction of global GHG emissions from transport to limit the magnitude or rate of long-term climate change will be more challenging.

Electrification is widely considered an attractive solution for reducing the oil dependency and environmental impact of transportation. We can say that low-carbon vehicles powered by electricity offer an alternative to conventional fossil fuel technologies and switching to electricity for transport has been proposed as a significant way to reduce direct CO₂ emissions [1].

In More Electrical Aircraft, Electrical systems are also used for aircraft actuation systems, wing ice protection, environmental control systems, and fuel pumping. This makes future Aircraft more fuel-efficient and quieter also improves the environment for everyone. Power Electronics plays an important role to enable the technology for More Electrical Aircraft. Without the use of power electronics to convert and control electrical energy none of the benefits of More Electrical Aircraft would be possible. However, aerospace applications present some challenging operating conditions for power electronics and there are still several areas where improvements must be made in terms of the weight, volume, cost, and reliability of power converters and their associated systems. Moreover, the operating environment can be very harsh and the operating number of hours and expected lifetime, compared to other industrial applications is long.

In conventional civilian aircraft, there are four ways to drive the power from the engine which are: electrical, pneumatic, hydraulic, and mechanical, these powers are then delivered to different non-propulsive loads. However, if we use only one source of power for all the systems, we can reduce the weight and the aircraft would be more efficient and more reliable. The single chosen source is electrical power because it has many

advantages in terms of flexibility and range of applications that's why we have one electrical power source and this concept is used in more Electrical Aircraft [2].

One of the main challenges of the MEA is the reduction of weight and improvement of efficiency and reliability, which can be achieved by replacing the hydraulic actuator (used in modern aircraft to move the control surface to control the plane), with the electrical actuator. In this case, the control surface can simply be controlled by controlling the motor which is fed by the converter. The converter is responsible for the machine's uneven voltage distribution and over-stresses [30], phenomena that are exacerbated by the new generation of wide bandgap semiconductors (WBG, like Silicon Carbide and Gallium Nitrite) based converters. These types of converters can reach higher voltages, temperatures, and switching frequencies. Furthermore, the weakest part of the machine is the insulation and when it is subjected to overstresses can start showing partial discharges (PDs), which means the insulation is partially bridged and if we continuously stress the insulation it will eventually cause a breakdown. This could be very harmful to the machine that carries out critical operations like primary flight surface control.

Many standards related to the converter, such as IEC 62477-1 and IEC 62477-2 apply to the safety requirements of Power Electronics Converter Systems (PECS) and equipment [28] [29] but they do not provide any specific information about the insulation of high voltage part of the inverter, which may create the risk of partial discharges. While IEC standard 60034-18-41 is used for the machines with organic insulation (type-1) fed by the converter to never present PD in their lifetime and explain how to qualify for industrial applications [14]. We can use this standard but the problem is that it applies only to normal environmental conditions and does not consider the aerospace conditions while MEA actuators work in a particular environment with lower pressure due to the altitude of aircraft and different temperatures and humidity. As a result of the existence of high voltages that flow from inverter to machine chain in MEA's electrical actuation system, there may be a risk of partial discharges in the inverter and motor, which could be hazardous to the actuation system.

In order to make the actuation systems free from all these PD problems and make them reliable. It is, therefore, necessary to understand the performance of the inverter to machine chain at aerospace conditions, and to do so, we need to detect the PDs from Printed Circuit Boards (PCBs, which are models of high voltage terminal part) using AC, DC, and voltage pulses of converters at a higher frequency along with the endurance test of twisted pairs (TPs, which are the models of turn/turn insulation of the converter fed-motor). These tests are necessary to understand the consequences of aerospace conditions.

Objectives and Approaches

This thesis has the following objectives:

- I. Analyze the partial discharge inception voltages (PDIV) of printed circuit boards (PCBs) in AC source at:
 - Ambient condition
 - Lower pressure
 - High temperature
- II. Analyze the PDIV of PCBs in case of the repetitive square wave generated by silicon carbide converter at lower pressure.
- III. Analyze the PDIV of PCBs when supplied by DC source at ambient condition.
- IV. Perform the endurance test of twisted pairs, analyze the impact of pressure and stressing voltages on the endurance of twisted pairs in case of:
 - Repetitive square wave voltages.
 - Sinusoidal AC 50 kHz voltages.

The above objectives are obtained with an experimental approach.

Profound research and study have been done to understand the concept behind this work. The experiments have been conducted in the setup realized, using

simultaneously custom software and commercial detection system. The results have been analyzed by understanding the physics behind them and have been compared to what as of now observed in previous consider and by other creators.

Chapter 2

Theory

The more Electrical Aircraft has many advantages by a civilian aircraft so it is necessary to understand the concept, working principle especially the part related to electrical power generation, why it is more efficient to use only electrical energy as a power source by other three sources, techniques to reduce the size of electrical equipment used in aircraft, the use of inverter in MEA, and also the machine insulation are discussed in the first part (2.1) of this chapter. While in the second section (2.2), the concept of partial discharge (PD), problems due to PDs, the effect of PDs on Insulation and life curves are discussed.

2.1 Use of Chain Converter-Machine in MEA

2.1.1 More Electric Aircraft (MEA)

In a conventional aircraft, the engine converts fuel into power in which most of the power is used for propulsive power to move the aircraft while the remaining power is converted in different forms of non-propulsive power since an aircraft is a complex system divided into a lot of subsystems each of which needs to be powered according to their requirement. To feed these subsystems some of the energy generated by the engine is converted into four different forms of non-propulsive power which are:

a) Pneumatic Power:

This power is obtained by bleeding off air from the high or intermediate pressure compressor; this form of energy is used to power:

- The Environmental Control System (ECS) like Cabin pressurization and air-conditioning
- Supply the hot Air for Wing Anti-Icing (WAI).

b) Hydraulic Power:

It is obtained using engine-driven pumps (EDPs) and a gearbox connected to the engines, it is mainly used for the actuation purpose in:

- Flight control surfaces
- Landing gear extension/reaction and steering
- Doors
- Brakes

c) Mechanical Power:

It is mainly transferred (By mechanical gearbox) from the engine to the central hydraulic pumps to be converted into hydraulic power. The mechanical system is used for fuel and oil pumping, mainly local to the engine.

d) Electrical Power:

The electrical power is obtained from the main electrical generators. This power is used for:

- Power the cabins (Lights, gallery, commercial loads, in-flight entertainment, etc)
- Power the Avionics
- Power many pumps and fans

The infrastructure of Electrical power is simpler (no complexity) as compared to the other power sources. The only drawback is a higher risk of fire (in the case of a short circuit) because it has a lower power density as compared to hydraulic power.

The schematic of power distribution in a conventional aircraft is shown below in fig: 2.1

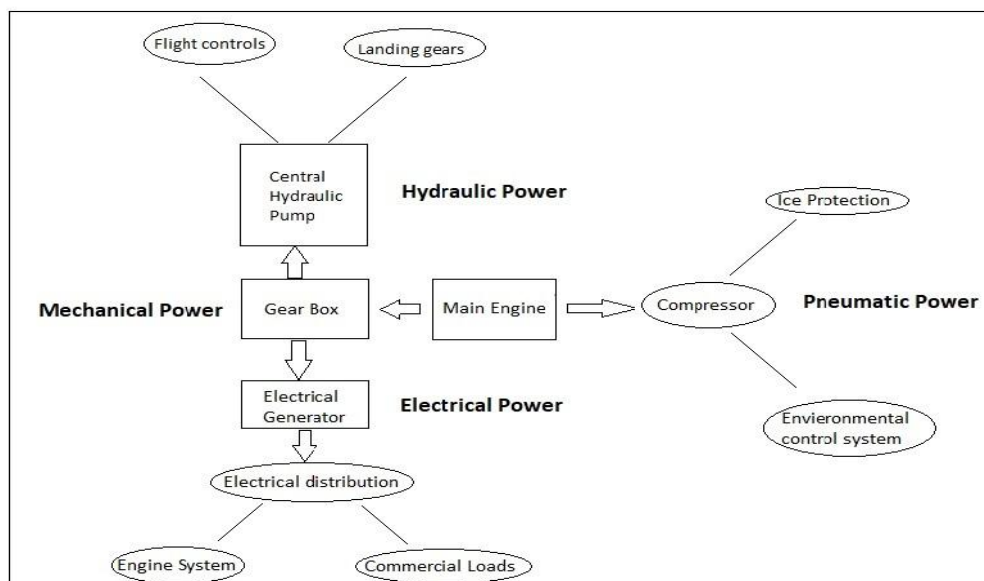


Figure 2.1: Power distribution in a conventional Aircraft.

The system becomes more and more complex and interactions between different pieces reduce the efficiency of the whole system because a small leakage in the pneumatic system may lead to the outage of every user of that network, resulting in grounded aircraft and flight delays.

The trend is to move towards “all-electric “aircraft, which means all power taken from the aircraft is electrical, so there is no need for on-engine hydraulic power generation and bleed air off-takes. The removal of bleed air off-takes requires new high voltage electrical networks and new solutions such as air conditioning, wing ice protection, or electric engine start-up while removal of the engine hydraulic pumps requires electrical power actuators (fully operated) and flight control architecture. The advantage of removing the old hydraulic system and employing a new electric system is to reduce the weight and increase the efficiency. An electrical system that has desirable characteristics of being highly controllable, configurable, and easily monitorable, this architecture needs a greater electrical generation and challenges to find a valid electrical substitute for each of the systems being replaced. The intermediate step is the More Electrical Aircraft where the penetration of the electrical technology is increased step by step. Two are the main ways in which the MEA project is being realized:

- Increase the power generation capability of the aircraft (to feed the new electrical loads). The challenge is to redesign the electrical system of the aircraft from generation to network system and fault protection.
- Substitute the non-electric system with electrical counterparts. The main challenge is the substitution of hydraulic actuators with electromagnetic actuators [3].

The MEA emphasizes the utilization of electrical power by hydraulic, pneumatic, and mechanical power to optimize the performance and life cycle of the aircraft. The MEA requires a highly reliable, fault-tolerant, autonomously controlled electrical power system to deliver higher quality power and electrical levels to the aircraft’s loads. Also, high integration and safety of electrical power systems lead to the use of distributed generation and control architecture. The schematic of MEA power distribution shows in figure 2.2.

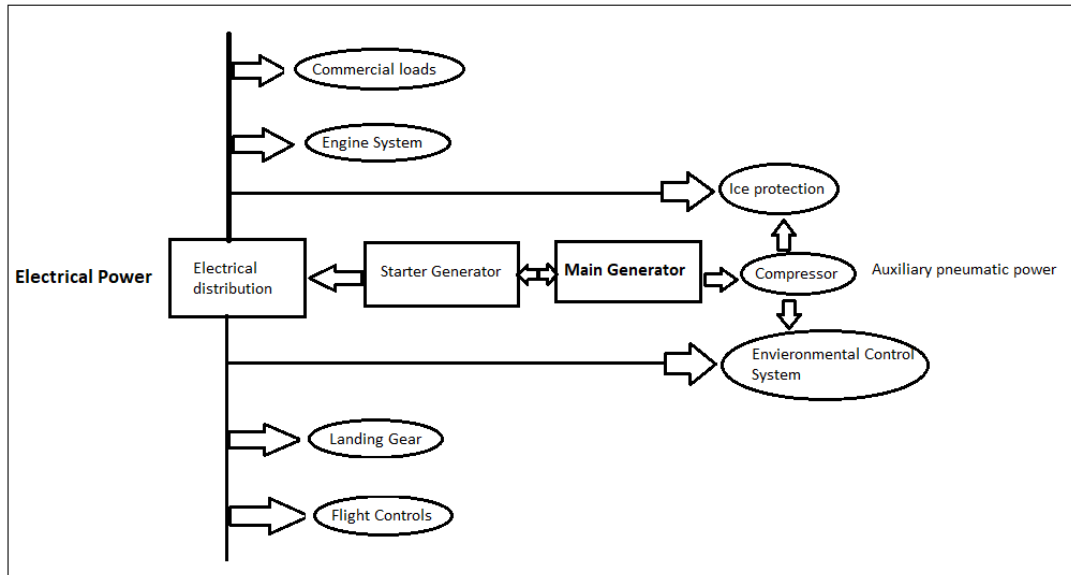


Figure 2.2: Schematic of MEA power distribution

History of Electrical Aircraft:

The concept of "all-electric" aircraft has been considered by military aircraft designers since World War II, but until recently, the lack of electrical power generation capability, as well as the volume of power conditioning equipment and the advanced control required, made the approach unfeasible especially for commercial and civil aircraft. Since the 1990s, research into aircraft power system technologies has been advanced to reduce or eliminate the centralized hydraulics aboard and replacing them with electrical power. Several programs have been done to drive the research in this field such as, Totally Integrated More Electric Aircraft (TIMES), devoted to using previously developed systems into electrical aircraft, the US Air Force MEA program that investigates for providing more electrical capability for fighter aircraft, and power-optimized Aircraft (POA), which tries to optimize the management of electrical power on aircraft to reduce non-propulsive power and reduce fuel consumption while increasing the reliability and safety of onboard systems and reducing maintenance to make the system more efficient. More advanced techniques to onboard energy power management and drive systems have recently emerged as a result of global research into the future development of commercial aircraft (Figure 2.2). These are currently being thoroughly

addressed, and it is anticipated that electrical systems have significantly more room for future improvement in terms of energy efficiency than conventional systems [3] [4].

On-Board Electrical Power Systems in MEA

The development of MEA onboard electrical power systems (EPSs) undergoes significant changes to render considerably increased power demands whilst meeting extremely strict requirements as for weight and volume, safety and reliability, electrical power quality, availability, etc. The changes concern both EPS architectures and individual subsystems responsible for energy generation, distribution, utilization, and storage. The Onboard electrical power system is shown in figure 2.3.

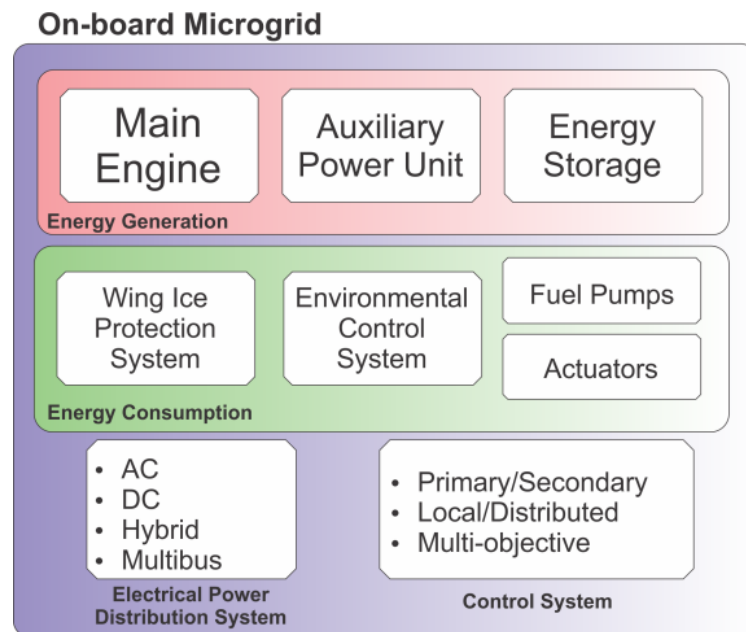


Figure 2.3: On-Board Electrical Power System of MEA

The On-grid electrical power system of MEA divided in:

- I. **Energy Generation:** An aircraft derives power mainly from engines of the main aircraft generator but there are various other sources like:
 - Main Engine (primary source): AC generator
 - Auxiliary Power Unit (Secondary source) generator: an AC turbine gas generator.

- Ram Air Turbine (Tertiary source): an air-driven turbine for emergencies that is deployed when other power generation system fails.
- Energy storage.

II. **Energy Consumption:** The section where different loads which consume energy are discussed. Loads include:

- Wing Ice Protection System
- Environmental control system
- Fuel pumps
- Actuators

III. **Power Distribution and Control system:** This section includes primary and secondary power distribution where the various power inputs are managed and consolidated. In this section, the aircraft needs to convert the power in the forms needed by its systems. The components used are:

- AC – DC
- AC – AC
- DC – DC
- Inverters (DC - AC)

Batteries provide an electrical storage medium independent of the generation sources.

I. Energy generation system in MEA:

Multi-level electrical power generation is typically employed which includes, primary power sources (Main generator typically AC), secondary source (Auxiliary power unit (APU) that is normally employed on the ground but can be used as airborne if other source fails), and the tertiary power source is ram-air turbine (RAT) which can be utilized, in case of multiple failures.

Main Engine (Primary power source):

The three stages synchronous machine is considered as state-of-art technology for the primary power source for MEA application. Composed of:

- a) The Permanent magnet (PM) generator: Generates three-phase electromotive force (emf) in its stator.
- b) The main Exciter: The DC field induces a voltage in the rotating armature of the main exciter that is rectified by a rectifier on the shaft, used to produce the field current for the excitation of the main generator. The generator control unit (GCU) controls the amplitude of the voltage.
- c) The main generator: It produces a voltage whose frequency is dependent on the number of poles and the speed of the shaft.

Different types of electrical power generation architectures can be used from this type of generator, includes:

- **Constant Frequency Drive (CFD):** Since the prime mover of the shaft in the aircraft is the main aircraft engine that has a variable speed. To maintain the constant frequency, the generator is coupled to the shaft via an automatic variable-ratio gearbox that is a complex hydro-mechanical device that is heavy, not reliable, and needs to be correctly maintained in terms of oil clearness and charge level. The system is complex and costly.
- **Variable Speed Constant Frequency (VSCF):** In this case the generator is coupled with the engine directly (without gearbox), avoiding the disadvantages of CFD. The power is produced by the generator is immediately electronically converted, there are two possible approaches to convert the power:
 - DC link: Using a rectifier and an inverter implementing a link between the two, having two stages of conversion AC/DC and DC/AC.
 - Cycloconverter/Matrix Converter: Using a converter capable of an AC/AC direct conversion.
- **Variable Speed Variable Frequency (VSVF):** It's the simplest, cheapest, and most reliable form of generating power since the minimum number of components is present. The generator is coupled directly to the engine and no conversion stage is practiced so that the power is generated with Variable frequency (from 360 to 800 Hz). Both the disadvantages of power electronics and the

gearbox are avoided, but a variable frequency bus is present in the aircraft so that this architecture is also called “frequency wild”. Loads like the wing ice protection, galley ovens, and cargo heaters can be fed directly with the variable frequency due to their frequency insensitivity.

Independently from the generation architecture, the conventional aircraft have a 115V AC bus for AC loads and a 28V DC bus for DC loads. As a consequence of gradually substituting the hydraulic, pneumatic, and mechanical systems, there is a trend of increasing the electrical power demand. Keeping the same voltage levels while increases the power demand will increase proportionally the feeder cable current and this will lead to higher power loss and cable weight. Increasing the voltage level will reduce the feeder cable current so lower cable weight and increase the frequency reduce the size of electrical equipment used in aircraft, with this technique we have lower fuel consumption, environmentally friendly, high efficiency, and reliability (As less number of equipment so lower chances of failure). This process can be carried out by considering the system’s safety.

Some innovative aircraft have been adopted like Boeing 787 with higher wild architecture and higher voltage level (230V at 360-800Hz). HVDC solutions are as well under evaluation, with 270V DC buses. As shown in fig 2.4

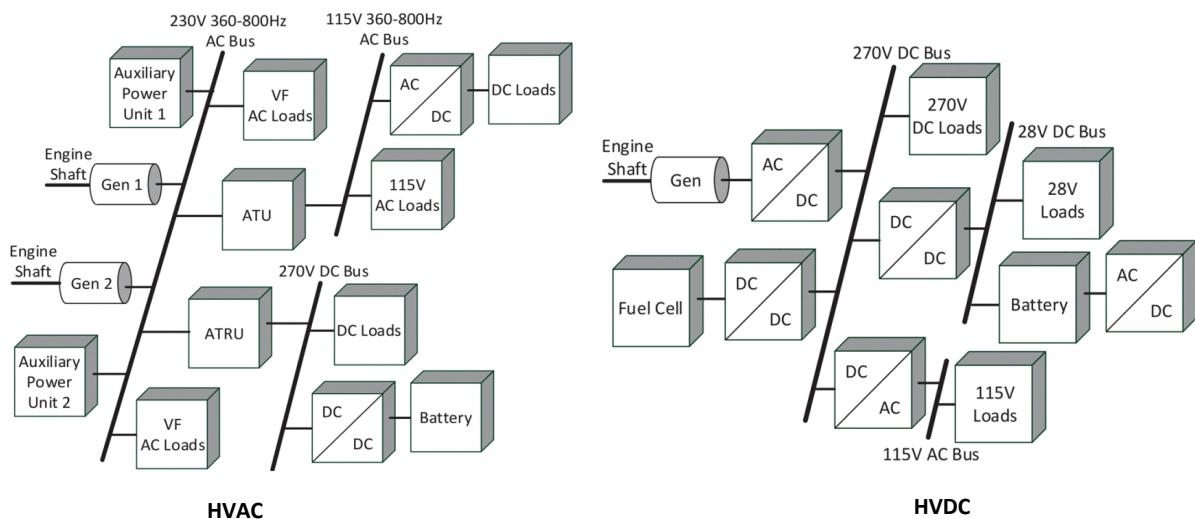


Figure 2.4: High voltage Electrical systems

Case study: The Boeing 787

The Boeing 787 “Dreamliner” shown in fig 2.5 is the most valuable More Electric Aircraft (MEA) ever produced.

The B787 uses a 230V AC phase-neutral voltage that is double of one in conventional 115V AC systems. This higher voltage decreases feeder losses but it requires particular care in the design to avoid corona or partial discharges. A key feature of the B787 is the variable Frequency Generation, the power generates in a range of frequencies spanning from about 360 to 800 Hz.

The electrical power is generated with:

- 2x250kVA starter/generators per engine (500kVA per channel, 1MVA total)
- 2x225kVA auxiliary power unit (APU) starter/generators both connected to the same APU.



Figure 2.5: Boeing 787

Figure 2.5 illustrates this. In addition to powering 230V AC loads, the power is converted into 115V AC and 28V DC to feed many of the subsystems that require more conventional power. The B787 has reduced the air bleed tapping to only the cowl anti-icing, all the other functionality once taken by bleed air are replaced with electric technology. Comparing with the B767 the bleed-less architecture has reduced the fuel consumption at cruise conditions by 2%.

The most relevant more-electric loads of the B787 are:

- **Environmental Control System and Pressurization:** This task is accomplished by four electrically driven compressors for a total power of \approx 500kVA.

- **Wing Anti-Icing:** This task is accomplished by heating mats embedded in the wing's edge and requiring $\approx 100\text{kVA}$ of power.
- **Electric Motor Pumps:** some of the Engine Driven Pumps (EDPs) for the hydraulic system are replaced by four electrically driven pumps, each requiring $\approx 100\text{kVA}$ for a total of $\approx 400\text{kVA}$.
- **Main Engine Start:** The main engine is started using the generators as starters, this operation needs $\approx 180\text{kVA}$ [5].

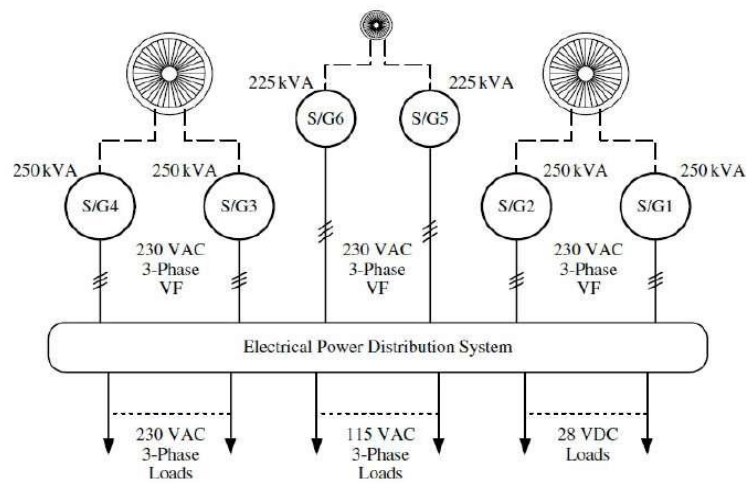


Figure 2.6: Boeing 787 Generators

Figure 2.7 shows the main electrical loads of B787 and their power requirements

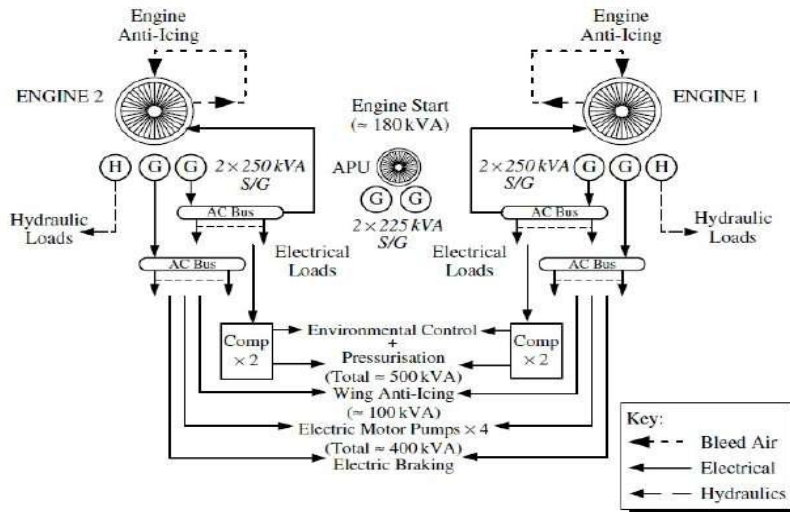


Figure 2.7: Boeing 787 main electrical loads

➤ Main Generator Start (MES):

Before Boeing 787, the main engine of the aircraft starts with the help of a pneumatic system but now this system has eliminated the use of a pneumatic system. The Main Engine Starter (MES) generators have been electrified using main engine generators as motors. Power is produced from the APU generator in AC, converted in DC using converters, and back to AC using inverters to obtain the variable frequency control needed for MES. The challenge lies in sizing all the systems from the MES generator to the APU and its generator passing by converters. The current researches are going on the possible issues caused by the electric start of the engine.

Auxiliary Power Unit (APU):

The Auxiliary power unit is the secondary power source, which is normally employed on the ground but can be used airborne (in the air) in case of other source failures. APU is an AC turbine gas generator usually placed in the aircraft, working at a constant frequency of 400 Hz with a line to neutral voltage of either 115 or 230 V. Its main role is to generate both pneumatic power and electrical power. On the ground, it provides compressed air for the start of main engines, conditioning of cabin air, and generates power for the electrical loads of the aircraft. While during flight it works as a backup or emergency system. APU acts as a backup in case of problems with the main hydraulic system. Examples of using this traditional APU system are Airbus A350 and A380. With the electrification of systems like the main engine start or deicing, the APU is required to change its role, no more providing pneumatic and hydraulic power but generating only electrical power. Since all the power has to be converted into electrical power, a larger generator is needed so the design consideration suggests that a better solution could be the use of two APU instead of a single one, improving also the reliability due to the generator redundancy. Anyway, complex requirements may be present for the ETOPS (Extended-range Twin-engine Operational Performance Standard), the certification that permits twin-engine aircraft to fly long-distance routes that had been off-limits, granting the flight with only one engine active in case of failure of the other. Boeing 787 is an

example of a full-electric APU where two generators are connected to a single APU, to meet the larger electric energy demand of the loads [7].

Ram Air Turbine (Tertiary power source):

A Ram Air Turbine (RAT) is a tiny turbine that is mounted in an airplane and used as a backup or emergency source of hydraulic or electrical power. The RAT, which is coupled to an electrical generator or a hydraulic pump, creates power from the airstream based on the aircraft's speed. In most cases, modern aircraft only use the RAT in an emergency, such as when hydraulic systems fail or when primary electrical power is lost. The RAT will be used to power key systems like flight controls, flight-critical instruments, navigation, and communication devices under certain situations. Some RATs solely provide hydraulic energy, which is then used to power an electrical generator.

Under typical circumstances, the RAT is stored in a fuselage or wing compartment. It can be used manually as needed, or it can be activated automatically in some setups after a total loss of AC power. Aircraft batteries are utilized to power important instrumentation in the time between power loss and RAT deployment [62].

II. Energy Consumption:

New loads in MEA EPS are associated with the application of electrically-driven technologies to replace hydraulic and pneumatic driven systems of traditional aircraft. Loads like:

- **Wing Ice-Protection System (WIPS):** In this system embedded resistive heat mat system has been utilized instead of the circulation of hot air taken from the engine. For mid-size aircraft, this load requires 40-60 KW in de-icing mode and up to 200kW in anti-icing mode. WIPS can be smoothly and efficiently controlled by power electronics, managing either the power delivered or surface temperature.
- **Environment Control System (ECS):** This system employs an electric drive to compress the ambient air and to controls air parameters to provide passengers comfort. For mid-size aircraft several ECSs are required, with the typical rating of each ECS is 70 kW.

- **Fuel pumps:** In the case of traditional aircraft, high-pressure fuel pumps are hydraulic, while in the case of MEA these pumps are electrically driven. This system of pumps is required for transferring and feeding the fuel, for controlling the location of the aircraft, as well as to reduce wing bending and structural fatigue. This system is typically based on an induction motor drive. The total power of fuel pumps on mid-size aircraft is about 200kVA. As a result, these new and traditional loads must be supplied by a power safely and reliably. This is one of the key functions of electrical distribution, which is defined by the EPS architecture.
- **Actuator:** For the majority of the flight time the actuator energy demand is minimal and the conventional hydraulic actuation techniques that require continuously pressurize the actuator result in energy wasting. Nowadays the trend is to substitute this traditional hydraulic system with electro-hydraulic actuators or electromechanical actuators. In any case, both systems require an electric motor and a converter. The EMA rated power depending on flight surfaces, can vary from 2 to 40kW, they are typically based on permanent-magnet machine drives, by considering different factors like (reliability, Power density, safety, weight, and efficiency) permanent magnet machine seems to be the best selection for the actuators, EMAs can also be employed for landing gear operation (steering, retraction, braking). EMAs are more efficient than EHAs (Electro-Hydro Actuators) and do not suffer from any leakage problem. However, the risk of mechanical jumping plays an important challenge that has to be resolved to see the technology applied in critical safety systems like landing gear extraction/retraction and primary surface control.

III. Power Distribution System and Control system:

The inherently hybrid AC and DC characteristics of the EPDS imply power electronics conversion stages. Although a different approach to the distribution (e.g.: DC distribution) would be possible, the fact that electric motors/generators and DC loads must be supplied makes the power conversion necessary. Many power converter

topologies have been proposed and investigated; this section aims at reviewing the most investigated ones for the MEA.

- **Rectifier (AC-DC):** AC to DC power conversion is needed in applications such as connecting an AC generator to a DC electrical system as well as front-end power converters for back-to-back AC to AC power converters. Due to low-frequency current harmonics, 12 and 18 pulses diode bridge rectifiers are the preferred solutions. The addition of more diodes eliminates lower frequency harmonics in AC. Hydraulic and fuel pumps are directly connected to the distribution (variable AC or DC) without power electronics, the hydraulic systems control the flow.
- **Direct (AC-AC) converter:** In motor drive applications on an aircraft with an AC Power system, it is possible to convert the electrical energy and control the load in a single-stage converter. This can be a very advantageous solution to enable the weight and volume of the converter to be minimized when compared to the back-to-back connection of an AC to DC and a DC to AC power converter. For a 3-phase AC to AC power converter, the Direct Matrix Converter uses nine bi-directional switches to ensure that each output phase can be connected to each input phase. Multi-level Matrix Converters do exist, but their topologies are too complicated for aerospace applications. In terms of waveform efficiency for a specific semiconductor device switching frequency, these topologies are identical to the NPC converter.
- **DC-DC Converter:** DC-DC conversion is needed in the MEA framework to:
 - Step down the voltage level to feed the low voltage avionics
 - Regulate the power flow among DC buses.
 - Interface the storage.

There are hundreds of topologies used for DC/DC conversion both isolated and non-isolated, but the most investigated topology is Dual Active Bridge, which features two H-bridge coupled via a high-frequency transformer. This converter has excellent power control and galvanic isolation (a fault on the LV side does not

affect the entire HV bus). The basic modulation entails the generation of symmetrical square waves at the transformer's primary and secondary, with the phase shift between the square waves regulating the transfer of power. The theory of operation is similar to that of AC inductive transmission lines, in which the voltage angle controls active power and the difference in voltage magnitude controls by reactive power. The major disadvantage is the high current ripple in the input/output capacitors, which is particularly important for avionic applications, where electrolytic capacitors are not used.

- **Inverter (DC-AC) converter:** The DC to AC power converter can be one of the most prevalent applications for power electronics on a More Electric Aircraft. For the control of AC loads such as electrical machines, these DC to AC power converters are required. In many applications the common six-switch voltage source inverter topology dominates. This topology is widely used in many industrial applications so there is a large amount of knowledge and experience in applying, modulating, and controlling this power converter topology and associated loads.

Despite recent advances in power semiconductor devices with the recent practical introduction of Silicon Carbide (SiC) and Gallium Nitride (GaN) materials for switching semiconductor devices, there are applications of higher speed electrical machines where the compromise between switching loss and output waveform quality is far from ideal. In these high-speed electrical machine applications where high-frequency fundamental AC waveforms are required, there is, therefore, consideration for using the three-level Neutral Point Clamped (NPC) power converter topology [7].

2.1.2 Techniques to decrease the size of electrical equipment in the aircraft:

Historically, aircraft engines have generated and delivered electrical power at low voltage levels because it has been a safe and reliable method of energy transfer. After the introduction of technology like the More Electric Aircraft, the engine's electrical power

consumption has increased. The replacement of heavy non-propulsive systems with electrical systems has resulted in an increment in electrical power demand. The replacement will significantly improve aircraft efficiency and improve environmental performance due to lower fuel use. Maintaining the same voltage levels while increasing the power demand will raise the feeder cable current correspondingly, resulting in increased power losses and cable size/weight. An increase in the level of voltage and fundamental frequency would solve these problems [31].

1. Increase the voltages:

Increasing the voltage level will reduce the feeder cable current which allows for the reduction of cable weight and power losses. For example, in a 115 V system, the current value is halved at 230 V for the same amount of electricity. Because of the lower cable loss, high-voltage aircraft have higher efficiency. High voltage aircraft architectures favor the use of more electrical energy than others such as hydraulic and pneumatic energy. But this would increase the probability of electrical discharges, therefore, the use of higher voltage systems in aircraft can be achieved as long as criteria can be defined that allow aircraft electrical systems to be designed safely and in which electrical discharge can be avoided [31] [32]. Saving weight has an impact on aircraft performance and a huge impact on eco-efficiency and fuel consumption. Saving one kilogram of weight will reduce costs by approximately 4500 \$ at a short and midrange aircraft over 20 years of operation [33].

2. Increase the fundamental frequency:

To reduce the weight and volume of the starter/generators, electrical machines with higher speed are preferable for the desired power capability. Therefore, the power converters play a very important role to convert electrical power from one form to another with wide fundamental frequency variation to reduce the volumes and sizes of electrical equipment. Increase the fundamental frequency helps to achieve high specific power, minimize the magnetic circuit of the motor, reducing the amount of heavy metal in the design, and consequently, reduce the size of electrical equipment used in aircraft [34] [36].

2.1.3 Importance of Inverters:

Inverters are power converters that are used to convert DC voltage into AC voltage with the possibility to control the frequency and voltage amplitude at the output. By changing the width of the pulse, we can control the output voltage and, by changing the modulation cycle, we can control the output frequency of the circuit. They are classified according to their AC output, depending on the number of phases (single-phase or three-phase), the number of levels (two (Bipolar) or three (unipolar)), and stages (half bridge or full bridge).

In low voltage industrial drive the usual choice is the two-level voltage source inverter operating at switching frequencies between 4 and 16 kHz with a DC link up to 600V. The purpose of its operation is to obtain the output as a set of three sinusoidal voltages shifted by 120° from each other, with the possibility of control their amplitude and frequency.

2.1.3.1 Three-phase PWM Inverter:

The three-phase inverter is based on a half-bridge structure and a full-bridge structure. In half-bridge, there are four possible switching configurations in which two are not used where both switches turned on at the same time which generates a short circuit and must be avoided while the configuration where both switches are turned off leaves the output terminal flying and shall be present only in transient conditions. For this reason, in each leg one of the switches is on and the other is off and the pole voltage (output of the leg concerning the DC bus) is set accordingly.

In the three-phase inverter, three legs are connected to bus DC. The schematic diagram of a three-phase inverter is shown in Fig. 2.8. The three legs with two possible states, each define eight possible configurations of the switches (2^3) of which two are null. Null configurations are the ones where the load voltage is zero on all phases.

The relationship between pole (v_{ok}) and phase/phase v_{kj} and load voltages e_k are:

$$\begin{aligned}v_{12} &= e_1 - e_2 = v_{o1} - v_{o2} \\v_{23} &= e_2 - e_3 = v_{o2} - v_{o3} \\v_{31} &= e_3 - e_1 = v_{o3} - v_{o1}\end{aligned}\tag{2.1}$$

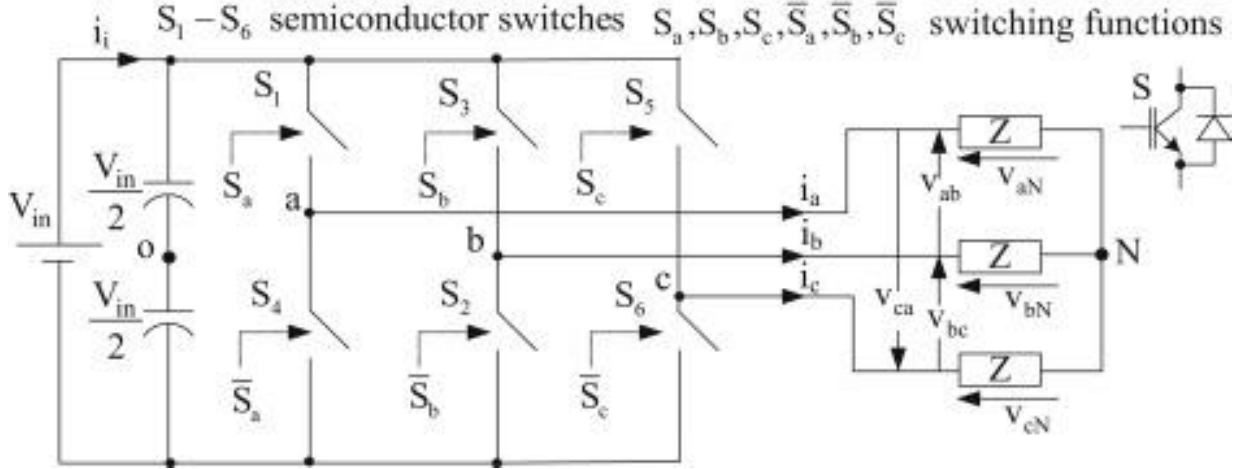


Figure 2.8: Schematic of a three-phase Inverter

Thanks to Kirchoff's voltage law. This determines in standard condition (balanced load,

$$i_1 + i_2 + i_3 = 0 \text{ as well as } e_1 + e_2 + e_3 = 0 \text{ since } e_k = Ri_k + L \frac{di_k}{dt}$$

The load voltages are:

$$\begin{aligned} e_1 &= \frac{V_{12} - V_{31}}{3} \\ e_2 &= \frac{V_{23} - V_{21}}{3} \\ e_3 &= \frac{V_{31} - V_{23}}{3} \end{aligned} \quad (2.2)$$

So from two possible values for the pole voltages, each phase/phase voltage can have three values meaning that the load voltages can have six possible values. Output values of three-Phase inverter represented by 6 steps of operations as shown in the table: 1.1 there are 5 levels of Load voltages and 3 levels of Line voltages

V_{1n}	V_{2n}	V_{3n}	V_{12}	V_{23}	V_{31}	e_1	e_2	e_3
+ Vdc	0	0	+ Vdc	0	- Vdc	+ 2V _{dc} /3	- Vdc/3	- Vdc/3
+ Vdc	+ Vdc	0	0	+ Vdc	- Vdc	+ Vdc/3	+ Vdc/3	- 2V _{dc} /3
0	+ Vdc	0	- Vdc	+ Vdc	0	- Vdc/3	+ 2V _{dc} /3	- Vdc/3
0	+ Vdc	+ Vdc	- Vdc	0	+ Vdc	- 2V _{dc} /3	+ Vdc/3	+ Vdc/3
0	0	+ Vdc	0	- Vdc	+ Vdc	- Vdc/3	- Vdc/3	+ 2V _{dc} /3
+Vdc	0	+ Vdc	+ Vdc	- Vdc	0	+ Vdc/3	- 2V _{dc} /3	+ Vdc/3
0	0	0	0	0	0	0	0	0
+ Vdc	+ Vdc	+ Vdc	0	0	0	0	0	0

Table 1.1: Step operations represent the output values of a three-phase inverter

The switches are controlled to achieve the selected voltage through the Pulse Width Modulation (PWM) technique. PWM is a technique used to generate a predetermined output waveform starting from a reference signal that pilots the turn on and off of the switches. Pole Voltages can be obtained by taking a reference point which is between two switches of any leg and the upper or lower line of Vdc. (upper line positive pole voltages and lower line negative pole voltages).

The waveforms of pole voltages and line voltages are shown below:

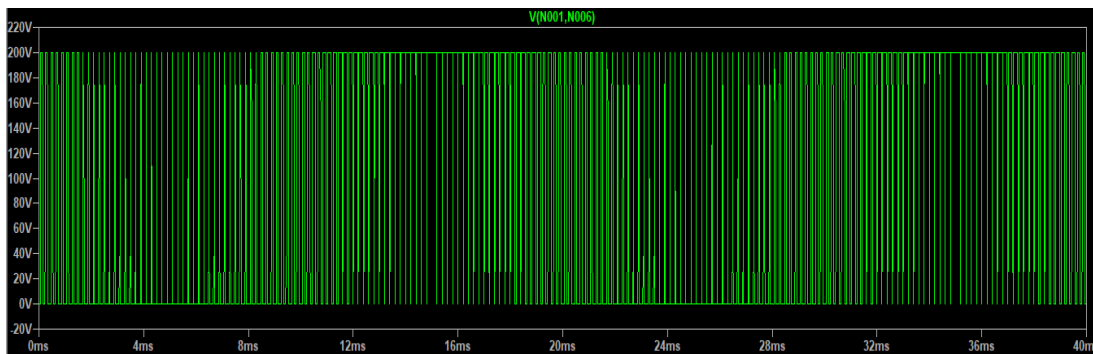


Figure 2.9: PWM controlled Pole voltages

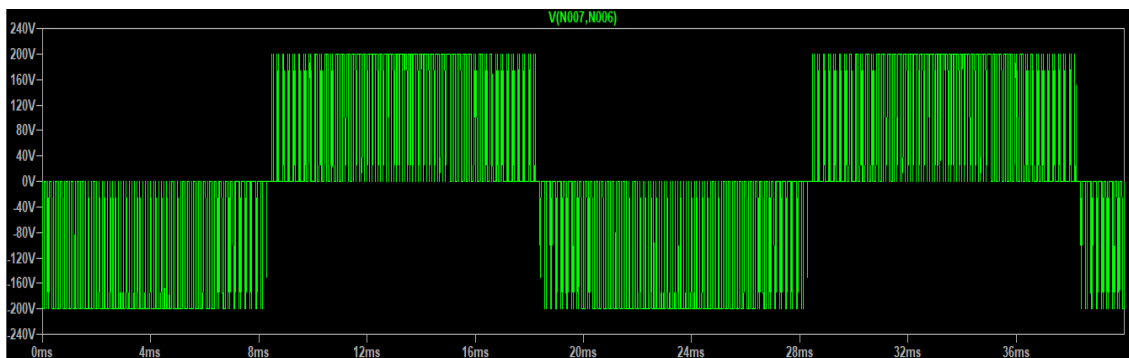


Figure 2.10: PWM controlled Line voltages

In PWM the time is discretized, in each time step T the switches of the leg will be turned on and off, having always one switch is on while the other is off (for the reasons already explained above). The output voltage has to follow the average value of the reference signal in each time period.

The time duration of switches (On and off) is selected using the duty cycle so that in each time period T , the voltage is the average between the two levels of the DC bus. For instance, let's consider E_{DC} and 0 as the two possible voltages at the output of the leg

and V_0 the reference signal in a given time step. The duty cycle ($d = \frac{T}{T}$) is calculated from:

$$d = \frac{T}{T} = \frac{V_0}{E} \quad (2.3)$$

Where T is the time during which the voltage is at its peak value (and $T - T$ the one during which is in the low value).

This duty cycle can be calculated digitally or obtained analogically using carrier signals and the switches are turned on and off according to the calculated time. Different PWM control strategies can be actuated on the same machine only changing the control stage. The most popular are the sinusoidal PWM (SPWM) and the space vector modulation (SVPWM). An example of the voltage waveform produced by a three-phase two-level inverter is in Fig. 2.9, Fig. 2.10, and Fig. 2.11. It must be highlighted that the PWM produces a voltage waveform that is made of pulses and that's there is only the average of each time step that follows the sinusoidal voltage. While the current result of the sinusoidal waveform is due to the filter action of the inductance of the motor, the voltage remains Impulsive and presents a high harmonic content. Figure 2.12 represents an example of the harmonic content in such a converter [14].

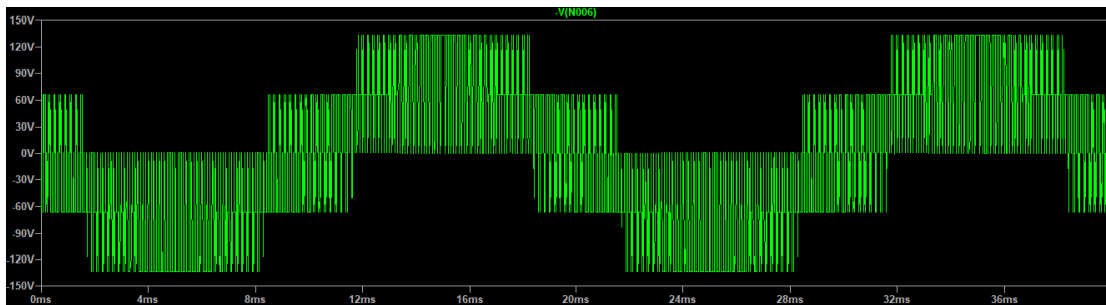


Figure 2.11: PWM controlled Load voltages



Figure 2.12: FFT of load voltages.

2.1.3.2 Wide-Bandgap (WBG) semiconductor devices:

The bandgap is defined as the energy difference between the top of the valence band and the bottom of the conduction band. The energy required promoting a valence electron to an atom to become a conduction electron and so conduction starts in semiconductors. The WBG semiconductors have a larger bandgap compared to the normal semiconductors, over 3eV vs. 1.1 eV of Silicon.

The new generation of wide bandgap semiconductors is already showing its advantages and could start replacing silicon in some places, like one of the power switches for converter applications. Advances in power electronics lead to high-temperature capabilities, reductions in weight and volume, and improvements in efficiency, which are of extraordinary interest for MEA applications.

The Wide Bandgap (WBG) device features, low specific on-resistance, fast switching speed, high breakdown electric field, and high junction temperature capability. All these characteristics are beneficial for the efficiency, power density, specific power, and reliability of power converters so power semiconductors based on WBG materials like Silicon carbide (SiC) and Gallium nitride (GaN) can accomplish the increasing demand for power density and high efficiency, and it also provides more flexible operation in a rough environment.

The wider bandgap gives SiC and GaN semiconductors several advantages:

- Due to thermal excitation of the electrons happens at higher temperatures, there is an errant activation of the semiconductors, with a temperature range up to 300°C versus 150°C of Si for safe operation.
- These materials have strong and high Debye temperature that ensures higher melting temperature and high thermal conductivity, which promotes the extraction of heat (so a larger power can be handled by the device at a given junction temperature). In this case, GaN is an exception with conductivity one-fourth of the SiC.
- WBG devices can work at much higher voltages because a larger electric field is required to generate carriers (A large number of carriers causes breakdown), For the same reason higher doping levels can be achieved and the width of the drift

region can be reduced by having thinner layers, also on-resistance of the drift region is ten times smaller than Si.

- Switching frequencies can be raised thanks to fast response time due to higher saturation velocity (the drift velocity is twice the one of Si) without having heating problems owing to the already cited advantages in heating and temperature management. For the same reason, the reverse recovery current is smaller and the reverse recovery time is shorter.

In short, we can say, SiC devices offer low specific on-state resistance, fast switching speed, high operating temperature, and high voltage capability.

The properties and the comparison between Si, SiC, and GaN materials are schematized in Fig. 2.13.

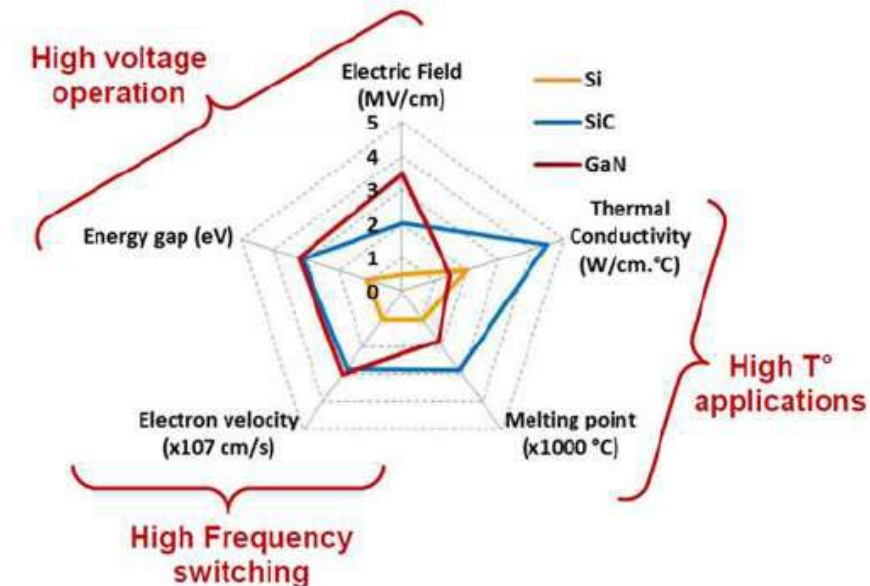


Figure 2.13: Properties of WBG semiconductors

While GaN and SiC devices have similar switching properties, but GaN exceeds SiC as the frequency increase, but from the manufacturing point of view, it is more complex to handle, starting from the fact that it doesn't have a native oxide, which is required for the production of MOS devices [8][41].

2.1.3.3 Importance of SiC Inverter:

Recent trends toward power converter miniaturization are to operate power converters at high switching frequencies to reduce the volumes and sizes of the passive components used in filters. However, the switching frequency of silicon (Si) insulated gate bipolar transistors (IGBTs) is limited below 20 kHz. In addition, there is a trend to directly mount the Electric Starter/Generator (ESG) with the power converter on the shaft of a gas turbine engine, which will subject the power converter to high ambient temperature exceeding 200 °C. However, the maximum junction temperature of Si-based power devices is normally below 150 °C, which is unacceptable for the embedded ESG in aircraft. Silicon carbide (SiC) is considered as next-generation wide bandgap material for power semiconductor devices used in high power density and harsh environment applications. SiC power devices permit high switching frequency and high junction temperature theoretically up to 600 °C [37].

High power density is required for a power converter in more electric aircraft due to the strict demands of volume and weight, which makes silicon carbide (SiC) extremely attractive for this application. Since these types of power devices can operate at high switching frequencies and high voltages while still maintaining high efficiency. Moreover, SiC power devices can operate at high junction temperatures, which is beneficial for embedded power converter applications such as for an electric starter/generator on the shaft of a gas turbine engine. Nevertheless, a trade-off should be made between size, cost, and losses, as size miniaturization leads to cost reduction but usually increases system losses [36].

2.1.4 Over-stresses and uneven voltage distribution in converter fed machines:

The insulation systems of rotating machines driven by power electronics are subjected to high frequency and rapidly changing stress, which can hasten insulation aging. When rotating machines are connected to an inverter, the impedance mismatch between the machine and the connecting cable causes overvoltage at the machine terminal. This overvoltage can be more than two times higher than the DC bus voltage, depending on

the inverter rise time and cable length. Due to the non-uniform distribution of the overvoltage inside the stator, the first one or more turns of the insulation will be stressed by significantly high impulsive voltages. When this voltage is higher than partial discharge inception voltage (PDIV), PD will occur with high probability and hastening the insulation aging of rotating machines [38].

The disadvantage of converters comes from the high-frequency content of the impulse signals which leads to overvoltage. Machines that use converters are subjected to greater electric stress. The severity of this over-stress is determined by several factors, including:

- Operating line voltage of the converter.
- Architecture and control regime of the converter (rise time and switching frequency).
- Filters between the converter and machine.
- Length and type of cable between the converter and machine.
- Design of the machine winding.
- Design and configuration of the installation.

The factors indicated to play a role in defining the rise time, overshoot factor, and impulse repetition. These three factors are the main causes of overstraining:

- Short rise time, resulting in voltage gradients and an uneven voltage distribution
- Voltage overshoots, resulting in higher voltages.
- Increased losses and degradation due to high switching frequency [40].

As we have seen in the previous section that there are many advantages of using wide bandgap semiconductor devices (SiC and GaN) due to high frequency. While these types of high-frequency converters accelerate the insulation aging of the machine at a higher rate due to shorter rise time and high switching frequency. The effect of wide bandgap converter is discussed below:

2.1.4.1 Effects of Wide BandGap (WBG) converters:

Wide bandgap converters can generate surges with very short rise time and high repetition frequencies. The short rise time favors an uneven distribution of the turn voltage but as the rise time becomes smaller and smaller seems also to start influencing the discharge mechanism. The results of the experiments reported in [38] reveal that the effects of rising time on PDIV are greatly influenced by the overshoot of impulsive voltages. Impulsive voltages with a rise time of 20 ns have a higher PDIV, whereas those with a rise time of more than 20 ns have a lower PDIV. Other researches in [39] show that a high commutation frequency can result in a significant reduction in the estimated inception voltage. This effect is especially concerning when combined with a higher magnitude of the discharge, because the insulation degradation from the PD is stronger (due to the higher PD magnitude), faster (due to the high repetition rates), and present itself at voltages smaller than the expected (due to reduction of the PDIV). Another issue arises from the use of such converters. To qualify a machine the PD must be detected (and detectable). This operation becomes more and more difficult when the impulses generated by the converter having tens of nanoseconds of rising time and a repetition rate of hundred of kilohertz. The converter pulses in this situation become identical to the discharge pulses. If it is possible to keep the system PD-free as required by the standard, the effect of frequency on the inception voltage must be taken into account in some way; one option is to introduce enhancement factors similar to those already included in the standard. The change of the inception voltage as a function of frequency, as well as the effect of aging, must be examined to determine a meaningful factor.

Many IEC standards, about the safety requirements of Power Electronics Converter Systems (PECS) and equipment, and IEC 600034-18-41, which describes how machines can be qualified for converter operation, can be used in the MEA's actuation system. But MEA actuators have special requirements and the standards exclude the issues that can arise when using wide bandgap converters in peculiar environments such as, low pressure at high altitude, which causes the occurrence of partial discharges (PDs). To make the actuation system reliable, it is necessary to perform the PD test on PCBs and twisted pairs to understand the behavior of inverter to machine chain in MEA while considering all of

the aspects that cause problems in the MEA actuation system which were not addressed in the standards earlier.

2.2 Partial Discharges (PDs):

Partial discharge (PD) as its name represents, partially bridges a small portion of electrical insulation between phase and ground conductor or between two high voltage conductors. PDs can occur at any point of insulation when the electrical system experiences HV stress.

The partial discharge causes insulation failure and failure of electrical equipment like power transformers, HV cables, switchgear, motors, and generators. Measurement of PDs allows the operator to perform effective and reliable insulation testing of high voltage equipment. PD analysis techniques must stick to IEC 60270, which is the international standard for the measurement of electrical discharges in the insulation.

According to IEC 60270:

Partial Discharge (PD) is a localized electrical discharge that only partially bridges the insulation between conductors and which can or cannot occur adjacent to a conductor [9].

2.2.1 Classification of PDs:

PDs can be recognized on their occurrences as surface discharge, internal discharge, corona discharge, or treeing phenomena.

- **Internal discharges:** These kinds of discharges occur in solid and liquid dielectrics due to the presence of voids or cavities. PD due to an air void inside the insulating material is considered the most dangerous defect during manufacturing [10].
- **Surface discharges:** It is generated by an electrical field along with the interaction between gas and a solid dielectric. It occurs at the boundaries of different insulation materials

- **Corona discharges:** They are low-power electric discharges that occur at atmospheric pressure. Corona is generated when a strong electric field occurs at the sharp edge of an electrode [11].
- **Treeing phenomena:** This phenomenon happens in solid dielectrics before breakdown. When continuous discharges occur in solid dielectrics, a channel is formed and the shape of that channel is like a tree that's why it is called treeing phenomenon.

2.2.2 Problems and dangers created by PDs:

PDs are localized discharges that do not bridge the insulation. However, their continued activity causes a progressive deterioration which leads to breakdown. The repetition rate of PD is very high in the case of power converters since a PD event is likely to take place at both flanks of the voltage impulses. Because the switching frequencies of SiC can be as large as 100 kHz, which enhances the effect of PD so failure can occur in short times, e.g. a few minutes, because of the organic nature of the insulation [41].

Once PD sets out, it causes progressive deterioration of insulating materials, finally electrical breakdown. The consequences of PDs in high voltage equipment and cables can be very dangerous, which leads to complete failure. The cumulative effect of PDs in solid dielectrics is the formation of infinite branches which are partially conducting discharge channels called treeing. Repetitive discharge events induce irreversible mechanical and chemical deterioration of the insulating material. Damage is caused due to the energy dissipated by high-energy ions or electrons, ozone attaching the void walls, ultraviolet light from the discharges, and cracking because the chemical breakdown processes release gases at high pressure. The electrical conductivity of dielectric material surrounding the voids increases due to chemical transformation. This enhances the electrical stress in the unaffected gap region and accelerates the breakdown process. Inorganic dielectrics which include, glass, porcelain, and mica, provide more resistance to PD damage than organic and polymer dielectrics.

Partial discharges (PDs) disperse energy in the form of heat, sound, and light. Localized heating from PD causes thermal degradation of the insulation. In the case of

DC and power line frequencies, the degree of PD heating is generally lower, but it is higher in the case of high voltage high-frequency equipment, which accelerates the failure rate.

The integrity of insulation in high voltage equipment can be confirmed by monitoring the PD activities that occur throughout the equipment's life. In order to ensure supply reliability and long-term operational sustainability, PD in high-voltage electrical equipment should be monitored closely with early warning signals for inspection and maintenance. PD can be prevented by careful design and material selection. In critical high voltage equipment, the integrity of the insulation is confirmed using PD detection equipment during the manufacturing stage as well as periodically through the equipment's useful life (Life curve). PD prevention and detection are necessary to ensure the reliability and long-term operation of high voltage equipment used by electric power utilities [12].

2.2.2.1 Mechanism of degradation:

The insulation wire in low voltage machines has a small thickness and air bubbles can be constituted due to imperfect impregnation. A sufficiently high electric stress, between phase and phase, phase and ground or between turns causes the breakdown of air so insulation bridging partially. Such kinds of discharge are a partial discharge that doesn't suddenly break the insulation but can degrade through chemical erosion and electronic bombardment of the insulation. Organic insulation is particularly sensible to PD activity so the insulation is easily pitted, eventually causing an insulation failure and short circuit. The repetition of the PD, once incepted, depends on the repetition frequency of the stressing voltage that is very high for converter-operated machines. That's why for Type I insulation systems, the PD is prohibited, it may cause a breakdown in a short time while for Type II insulation systems the repetition frequency of the pulses is considered a critical parameter to evaluate the system.

The high-frequency content of the pulses may influence the life of the insulation, causing overheating and degradation in the dielectric. Stray capacitances to the ground (even of a really small magnitude) can cause a significant current flow when the voltage gradient ($\frac{dv}{dt}$) is high enough, like during the turn-on and the turn-off of the switches.

These transitions are therefore associated with capacitive currents $I_c = \frac{dv}{dt}$ that flows through the ground. And these currents are responsible for the increased heating of the insulation. Both the repetition frequency and the frequency associated with the rise time of the leading edge will create extra heating through the dielectric losses.

2.2.3 Insulation in low pressure:

The aerospace industry is moving towards More Electrical Aircraft with the replacement of heavy non-electrical systems with electrical systems. The insulation system used in the electrical system is going to face more challenging environmental conditions which include, extreme temperature, low pressure, etc (The pressure range can vary from 100 mbar to 400 mbar). The effect of this pressure range can be considered as an important factor; it causes electrical degradation of insulation and reduces the insulation life.

According to the experiments performed in [42], lowering the pressure reduces the PDIV significantly. Lower pressures are projected to result in a longer mean free path for electrons. This lowers the breakdown field required to start an electronic ionization avalanche because free electrons have more physical space to accelerate and accumulate enough kinetic energy from the applied electric field to launch an ionization process after colliding with a neutral. When the pressure is lessened, lower field intensity will be required to trigger the initial electronic avalanche [42].

Paschen's law gives an approximation of system voltage that is required to cause partial discharge as a function of pressure. Figure 2.14 shows the analysis when 0.04mm thick insulation is considered as a function of pressure. As we can notice that when pressure decreases, the voltage required to start partial discharge is also reduced.

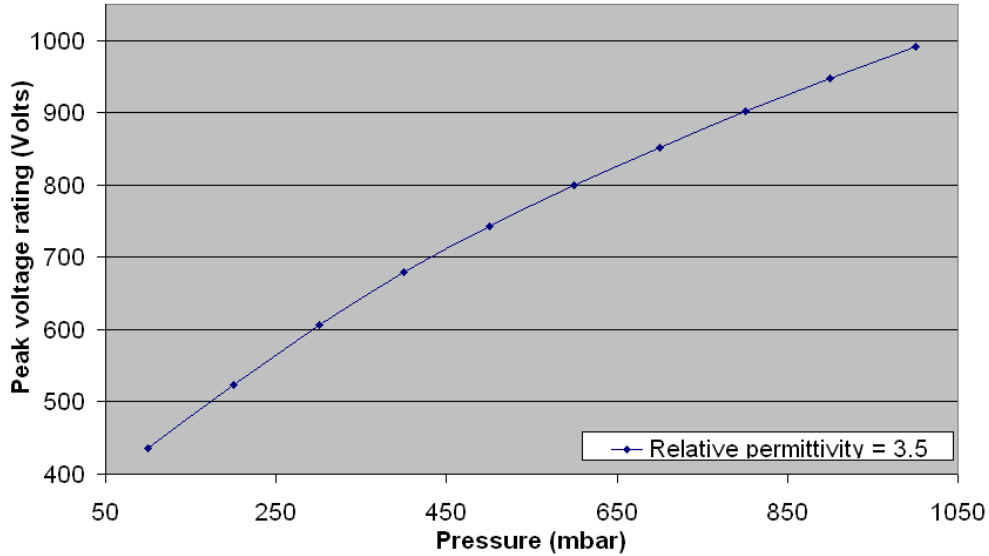


Figure 2.14: Reduction of breakdown voltages as a function of pressure.

The endurance test of wire is carried out at atmospheric pressure to ensure that it will meet the lifetime requirements of the machine at different voltage levels while other conditions are kept constant. It will cause degradation at the start but ultimately leads to failure. It is not certain that such wire will also have a similar lifetime in the case of a low-pressure environment, its lifetime decreases due to reduction of pressure.

An experimental result shows in figure 2.15. The partial discharge measurements have been accomplished in the pressure range of (100 mbar to 1000 mbar). There are three samples of twisted pairs are considered which show how linearly inception voltages decrease as pressure reduces from 1000 mbar to 100 mbar. From these results we can conclude that the insulation system of a machine is more likely to suffer partial discharge in an aerospace environment where the ambient pressure can go as 100 millibar therefore damages due to partial discharge can start at a lower voltage level also that increases the risk factor for machine used in aircraft.

A definition based on PD energy appears to be far more accurate in forecasting the dangers of this occurrence. Carrying out these types of emission spectroscopy tests indeed adds difficulties, but it is a necessary advancement for reliable testing of these types of insulations [13][42].

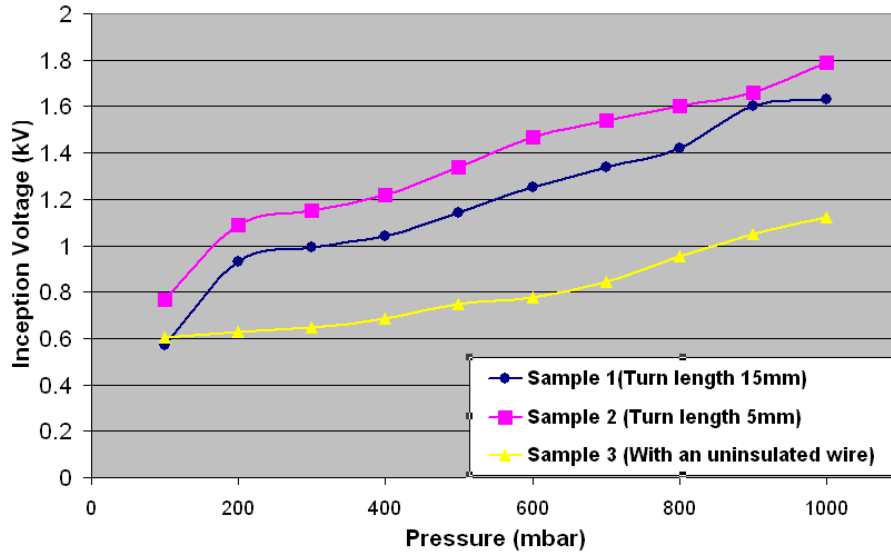


Figure 2.15: Inception voltages at pressure ranges from 100 mbar to 1000 mbar

2.2.4 Life Curves

The electrical failure is caused by a short circuit between a phase and ground or between two phases, which causes the winding insulating system to fail. During normal operation, the motors are typically supplied by pure sinusoidal voltage could be subjected to electronic converter power supplies, resulting in potential overvoltage of various natures and amplitudes. PD activity will start if the overvoltage amplitude exceeds the partial discharge inception voltage (PDIV) level. The electrical insulation of the winding wires in Type I [14] motor stator winding is organic enamel, also packed with nanoparticles. Partial discharge operation erodes organic enamel, causing irreversible deterioration that leads to a breakdown in a short time. Inverter-driven motors are exposed to high-frequency harmonics and pulses, putting a lot of strain on the first winding turn [16].

A test campaign has been implemented to investigate the performance of wire wound insulation when it is subjected to PD stress. There are four different forms of voltages considered as shown in figure 2.16. The results demonstrate that the exact waveform shape can have a significant impact on the actual degradation in the presence of the partial discharge event.

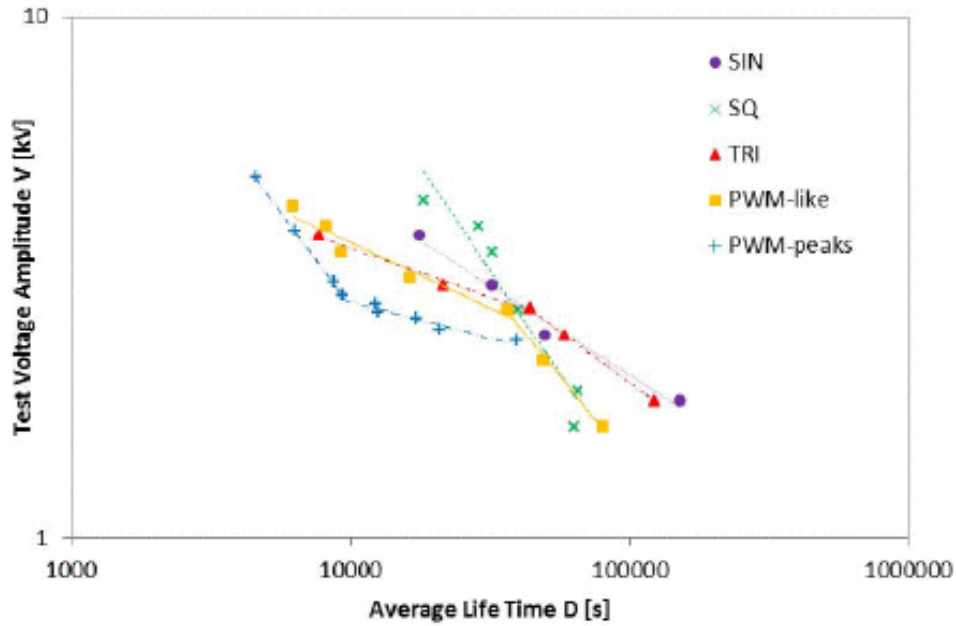


Figure 2.16: Life curve relevant to different voltage waveforms

The inverse power law, as shown in the equation, can be used to relocate the average lifetime D to the applied voltage amplitude V .

$$D = KV^{-n} \quad (2.1)$$

the coefficients K and n are dependent on the applied voltage waveform. The slope of the straight line in a bi-log plot corresponding to the linearization of the equation is defined by n , which is called "voltage endurance coefficient (VEC)." When comparing the different voltage waveforms, it is possible to notice a significant difference that how PD behavior changes when the voltage amplitude is increased. In the case of SIN and SQ the PD amplitude and number increase with the test voltage amplitude in a regular way. While, in the case of switching waveforms like, (TRI, PWM) a threshold effect is observed.

The worst behavior has been attributed to the PWM-peaks waveform, which has a higher PD activity than the other waveforms. The results show that when designing a research protocol for twisted pair specimens, the waveform of the applied voltage must be taken into account since the shape affects both the degradation processes and the voltage amplitude [15].

Another life curve is shown in figure 2.17, where the average lifetime of two different wires (standard and corona resistant) has been tested at four voltages levels. The same inverse power law described above in Eq. (2.1) is valid in this case as well.

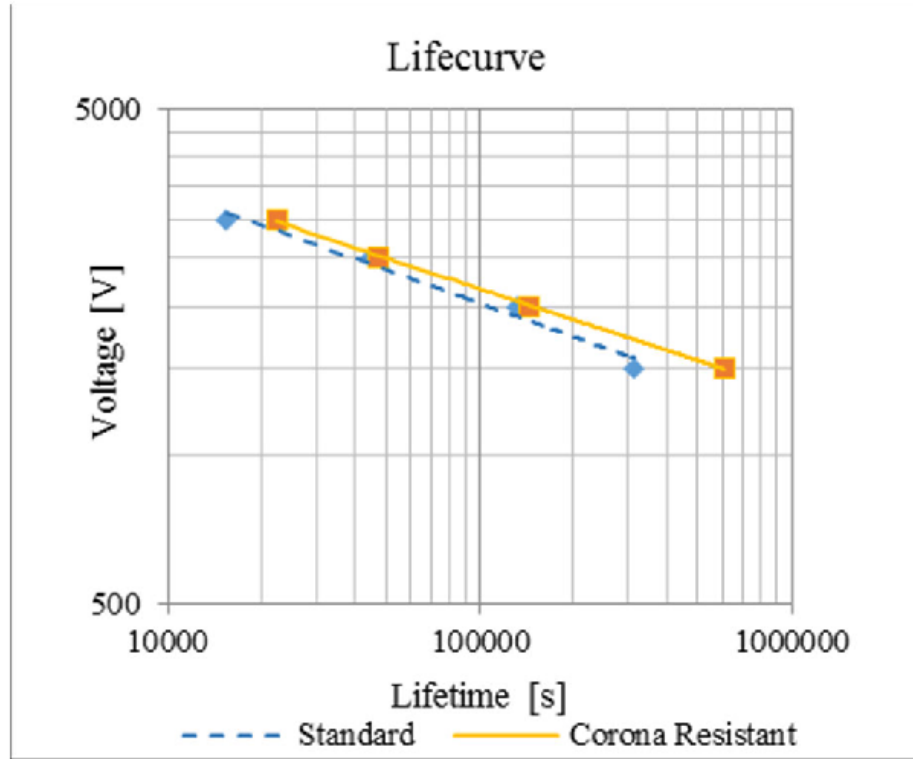


Figure 2.17: Life curves of two insulating enamels, standard and corona resistant

When comparing the different voltage levels, it is possible to notice that how the life of insulation material decreases as voltage increases and vice versa. The behavior of the corona resistant wires ensued better than the relevant standard wires especially if medium–long term is considered [15].

Chapter 3

Test Setup

In this chapter, we will create the test setup for PDIV and Endurance tests. The experiments aim to find the inception voltage of the PD in Printed Circuit boards (PCBs) that are models for testing the high voltage terminal part of the inverter, and the Endurance tests of twisted pairs, which are models for testing the turn/turn insulation of rotating machines fed by the converters. Understand the influence of temperature, humidity, pressure, and switching frequency is important, which helps to find the proper way to design and qualify MEA actuators especially when fed with converters based on wide bandgap semiconductors. In this case, it is important to ensure that the converter to machine part should be free from PDs, otherwise, it creates problems in the plane's surface control, also this part is important because it permits the reduction of weight and improves efficiency and reliability of MEA.

To study the influence of such parameters the experiments have been conducted in two different environments (vacuum tank and climatic chamber), using three voltage sources (AC power frequency voltage, DC voltage source, and unipolar repetitive square wave voltage) for PDIV test of PCBs, and two voltage sources (Sinusoidal AC 50 kHz voltage source and unipolar repetitive square waves) for the Endurance test of twisted pairs. There are three possibilities of the PD detection system: an optical system and two electrical systems (an antenna, a high-frequency current transformer).

Various instruments have been interfaced with the PC through MATLAB ®, to have the possibility to control them remotely and to create an automatic or semi-automatic measurement system. A suite of such software has been already coded on the PC of the laboratory. MATLAB has been selected as the software environment for its versatility, power, diffusion in the technical world, and the expertise already present in the laboratory.

3.1 Printed Circuit Boards (PCBs)

Printed Circuit boards (PCBs) are the models for testing the high voltage terminal part of the inverter.

3.1.1 Description of the test sample:

There are six different kinds of PCBs has been used, all of them are made up of glass fiber reinforced epoxy FR4 but they are different by their corresponding conducting parts which are coated with solder mask. The PCBs are shown below:

i. A hole between two parallel tracks:

The PCB with a hole (without any material) between two parallel conducting plates/tracks with the model number “E6” is shown in figure 3.1. The distance between the two conducting plates is around 1.5 mm.



Figure 3.1: Hole between two parallel tracks (E6)

ii. Two parallel tracks (larger gap):

The PCB with two conducting parallel plates/tracks separated by a creepage distance (distance between two conducting parts) of around 1.5 mm with the model number “C6” is shown in figure 3.2. The material used between two conducting plates is FR4.



Figure 3.2: Large gap between two parallel tracks (C6)

iii. Two parallel tracks (smaller gap):

The PCB with two conducting parallel plates separated by a small gap with the model number “D6” is shown in figure 3.3. The creepage distance (distance between two conducting parts) is very small, around 0.3 mm.



Figure 3.3: Smaller gap between two parallel tracks (D6)

iv. A hole between a track and points:

The PCB with a hole (without any material) between a conducting track and five points with the model number “B6” is shown in figure 3.4. All the points are at equidistance from the plate/track. The distance between the track and each of the points is the same, which is around 1.5 mm.

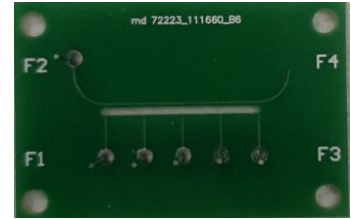


Figure 3.4: Hole between track and points (B6)

v. A larger gap between a track and points:

The PCB with a larger gap between a track and five points with the model number “F6” is shown in figure 3.5. The distance between the track and each of the points is around 1.5 mm.



Figure 3.5: Large gap between a track and points (F6)

vi. A smaller gap between a track and points:

The PCB with a smaller gap between a track and five points with the model number “A6” is shown in figure 3.6. The distance between the track and each of the points is smaller, which is around 0.3 mm.



Figure 3.6: Smaller gap between a track and points (A6)

3.1.2 Testing procedure for PCBs

The testing procedure to perform the tests on PCBs described below:

3.1.2.1 Environment for testing

The two environments (climatic chamber and vacuum tank) in which experiments can be accomplished.



Figure 3.7: ACS Climatic Chamber [17]

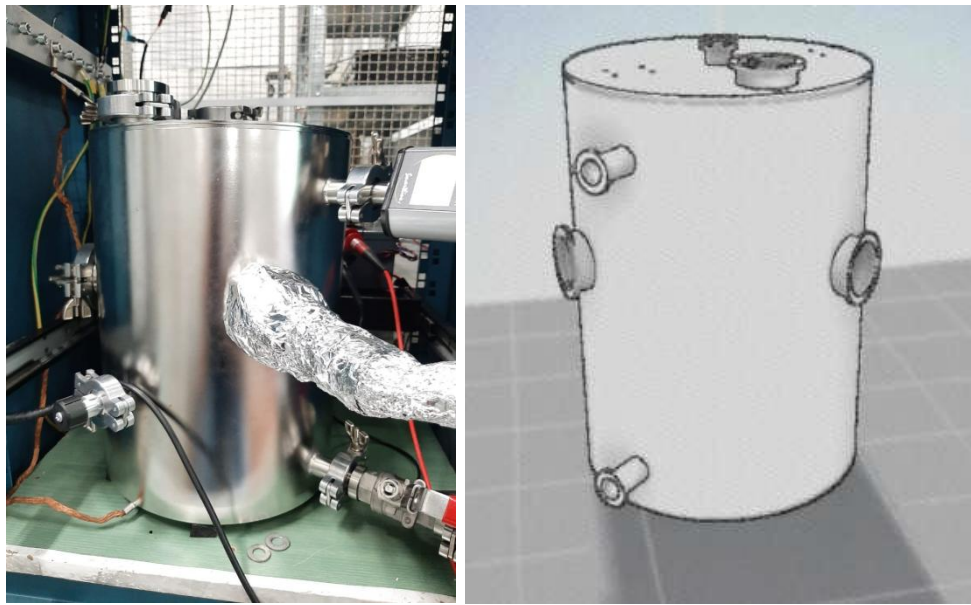
- Climatic Chamber:

In the ACS DY200C Climatic Chamber (Fig. 3.7) it is possible to change the temperature in the range $[-70^{\circ}\text{C}; 180^{\circ}\text{C}]$ and the relative humidity in the range [10% to 95%]. Since the only possible detection methods in the climatic chamber are the electromagnetic ones and the noise generated by the switches is comparable with the PD signal (the optical detection needs a completely dark environment to be used) measurements of PD with the SiC pulser cannot be performed here.

- Tank:

The tank has been custom designed in the laboratory to serve all the needs. It has several flanges where different feedthrough can be mounted in a modular way. Some of them we have available and mounted are

- High Voltage Feedthrough.
- High Current Feedthrough.
- Four BNC Signal Connectors Feedthrough.



(a) Picture of Vacuum Tank

(b) Model of Vacuum Tank

Figure 3.8: Vacuum Tank

The photon counter head has to be placed outside the tank because it can work only in standard ambient conditions, for this reason, quartz windows can be mounted on the flanges. A fixture to hold the counting head in front of the window has been realized with a 3D Printer. Quartz windows are better than glass windows since they don't alter the UV spectrum that should be detected by the photon counter. The flanges have different positions so that the photon head can be mounted in various positions. The tank is chrome plated, to reflect the photon produced by the discharge so that the maximum number of photons can reach the photon counter head that ideally is the only escape way of the photons in the tank. The tank offers the possibility to change the pressure, thanks to a pump. The minimum pressure that can be reached (0.5 millibar to be conservative) is well under the ones in our needs. The complete dark environment permits the optical detection of PDs and the BNC feedthrough allows the simultaneous use of HFCT and antenna sensors. The high voltage feedthrough permits to bring the supply voltage from the generators to the samples inside the tank.

3.1.2.2 Voltage sources:

Three voltage sources have been used in our experiments: AC voltage source at 50 Hz, DC voltage source, and repetitive square wave generated by a silicon carbide converter.

I. AC Source (50 Hz):

The variable 50Hz AC voltage source is generated by using a small transformer cascaded with a variable autotransformer. We have noticed the waveform is slightly distorted caused by the saturation of the small transformer core but this won't affect the results since the essential parameter is the peak/peak value of the voltage. The waveforms generated by the above-discussed system can be observed in figure 3.9.

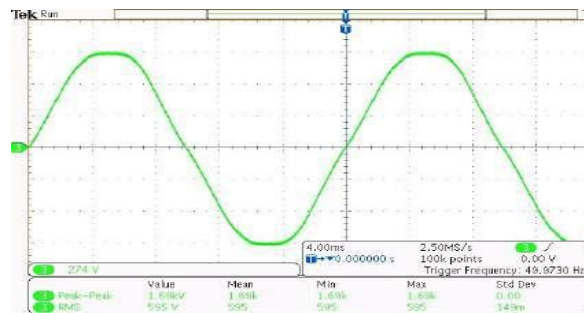


Figure 3.9: Waveforms generated by AC system

II. DC Supply:

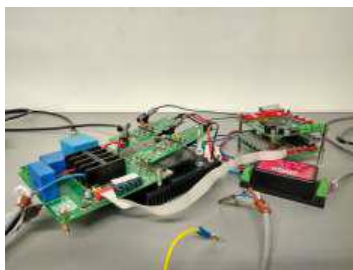
The DC voltages are generated by a Fug HCN 35-20 000 DC generator. This generator has many features like compact size, lightweight, efficiency is about 90%, short circuit and flashover proof, control mode indicated by LED, and can go up to 20 kV (DC). The input is connected to the AC supply 220/230 V and the body of the generator should be connected to the ground because of safety reasons. This generator can go higher than the required voltages for the experiments. The generator is shown in figure 3.10.



Figure 10: Fug HCN 35-20 000 DC generator

III. SiC Pulsar:

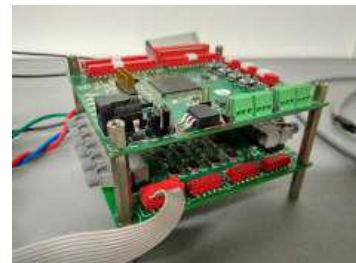
The unipolar repetitive square wave voltage is produced by a silicon carbide-based pulser (unipolar inverter). The pulser in our possession has been custom realized by the University of Parma and is shown in Fig. 3.11.



(a) SiC Pulsar



(b) Power stage and the gate drivers



(c) Control stage

Figure 3.11: SiC Pulsar realized by UinPa

The converter has SiC MOSFET and is characterized by:

- Maximum 1 kV bus DC.
- Up to 200 kHz settable switching frequency.
- Around 20 ns rise time.



Figure 3.12: The Alintel SHV4000, high voltage DC generator

The Alintel SHV4000 shown in fig. 3.12 has been selected as the high voltage DC generator, to serve as a variable DC bus for the SiC pulser. It can reach 4000VDC, far more than the pulser capability. The generator can be controlled by MATLAB through Arduino using the programming of the relative object.

The pulser produces a waveform characterized by very fast rise time and not negligible overshoots. A picture of it can be seen in fig. 3.13.

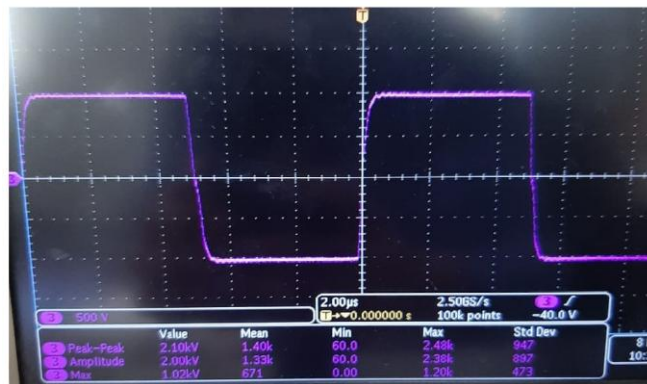


Figure 3.13: Waveform produced by SiC Pulser

3.1.3 Measurement techniques:

Two main quantities have to be measured by the instrument, the supply voltage, and discharges. That's because the voltage at which the first discharges are detected is the PDIV, the parameter we are looking for in our experiments.

3.1.3.1 Voltage Measure

For the voltage measurement in our system, Tektronix MD03054B Oscilloscope (fig. 3.14) has been used. This model has four channels, 500 MHz bandwidth, and up to 5 Giga Samples per second (GS/s). The instrument has been interfaced with MATLAB.

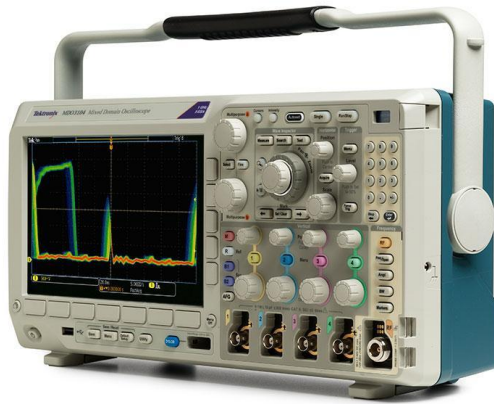


Figure 3.14: Tektronix MD03054B Oscilloscope [18]

3.1.3.2 PD Measure

Electrically, two distinct sensors are used to detect PDs, and optically, a custom-designed system is used to detect them.

PD Base II: Electrical detection of PDs is performed by the “TECHIMP PD Base II”, a commercial Ultra Wide Band instrument, shown in figure 3.15. An ultra-wideband digitizer and integrated processing capabilities are included in the PDBaseII. A large number of digitized PD pulse waveforms are evaluated and pulse features are recorded for subsequent processing leading to the ultimate PD source identification thanks to its fast sampling rate (200 MS/s) and on-board processing capabilities.

The sensors that could be used to capture the PD signals are High-Frequency Current Transformer (HFCT), and antenna.



Figure 3.15: TECHIMP PD Base II [19]

- **HFCT:** The Technimp High-Frequency Current Transformer (fig. 3.16) is the inductive sensor for Partial Discharge (PD) measurement. It is used for PD tests on many electrical systems (cables, transformers, rotating machines, etc.). The high-frequency current transformer is a particular current transformer made of ferrite materials that has a wide bandwidth and can measure high frequency or pulsed current waveforms.

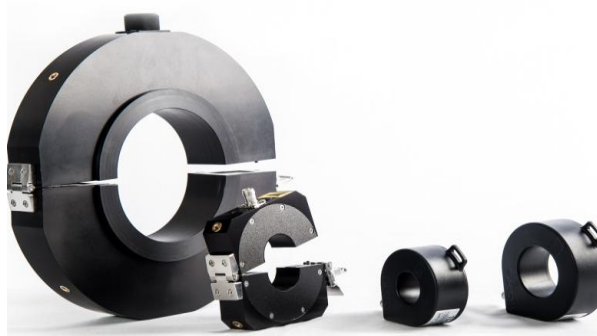


Figure 3.16: Technimp HFCT [19]

- **Antenna:** PD pulses can be detected by using an Ultra High Frequency (UHF) horn antenna shown in figure 3.17. It is a high-performance partial discharge sensor, which is designed to detect electromagnetic (EM) emissions from a PD in electric assets. Horn antenna is a broadband antenna with a flat response, making it useful for a variety of applications. It was developed to provide maximum sensitivity and high gain while operating in a frequency band ideal for PD activity monitoring [19].



Figure 3.17: UHF horn antenna [19].

- **Capacitor divider:** Capacitive Couplers for on-line and off-line PD tests on rotating machines, as well as spot measurements and monitoring. To connect the coupler to a coaxial cable, a BNC termination is offered. The voltage tap on the top is used to apply the high voltage to the coupler. A measuring impedance is included at the base of the capacitive divider, allowing both PD and synchronization signals (i.e. reference voltage) to be calculated. A surge arrester is also included in the base, which restricts the maximum transient output voltage [23].



Figure 3.18: Capacitor divider [23]

- **PD Calibrator (PDCAL):** The scale factor of a PD measuring system is determined by calibration. IEC 60270 provides a calibration method that uses an externally fitted PD calibrator to simulate the internal charge transfer between the PD source and the HV equipment terminals. The comparison method is the primary approach for calibrating PD calibrators, in which a reference source is utilized to create a charge that is measured with suitable PD measuring equipment. The charge produced by the calibrator under test is then measured using the same PD system. Using a reference calibrator with well-established characteristics and traceable calibration ensures the traceability of the calibration [42].

The scale calibration factors are permanently maintained inside PDCAL's flash memory, giving it outstanding pulse-width stability. The PDCAL output pulse can be synchronized with the actual line frequency through external electrical light source systems thanks to the onboard photocoupler. PDCAL has many benefits like it is a portable source reference for a PD measurement, its plus version able to perform up to 800 pC, and it is IEC 60270 certified [43].



Figure 3.19: PD calibrator [43]

Optical detection: This kind of detection is only possible in a dark environment. An optical detection system based on photo multiplication has been selected for PD detection through the photons produced in the discharge.



(a) Photon counting head Hamamatsu H1870-091 [20]



(b) Pulse counter Hamamatsu C8855-01 [21]

Figure 3.20: Photon counting instruments

The photon-counting system is composed of a photon-counting head Hamamatsu H11870-09 shown in Fig. 3.20(a) and pulse counter Hamamatsu C8855-01 shown in Fig. 3.20(b). The H11870-09 is a photon-counting head with a 25 mm diameter head-on

photomultiplier tube, a power supply circuit, and a photon-counting circuit with a wide sensitive area. The equipment can detect UV light, and its sensitivity is a function of photon wavelength, having a peak in the 200-300nm range (Fig. 3.21). The C8855-01 is a counting unit with a USB interface and can be used as a photon counter when combined with a photon-counting head, etc. It has two counter circuits (double counter method) that allow it to count input signals without any dead time [20][21].

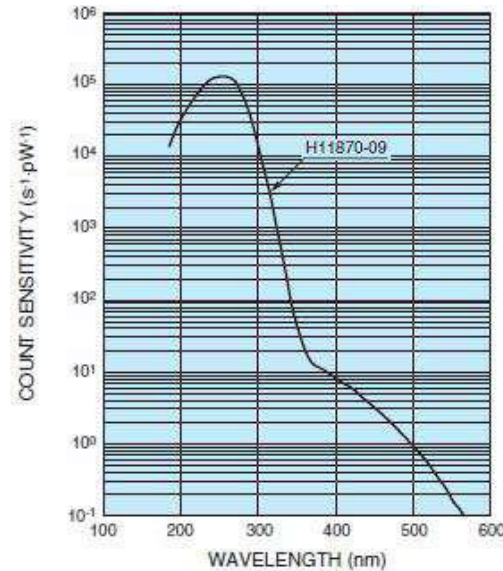


Figure 3.21: Sensitivity of Photon counting head [20]

When light enters the photomultiplier tube, it is detected and produces an output signal, which is then counted by the counting circuit using the methods below:

1. Light passes through the input window.
2. The photocathode's electrons are excited by light, causing photoelectrons to be emitted into a vacuum tube (this is known as the external photoelectric effect).
3. The focusing electrode accelerates and focuses photoelectrons onto the first dynode (a secondary emissive surface), where they are multiplied by means of secondary electron emission. At each of the subsequent dynodes, the secondary emission is repeated.
4. The multiplied secondary electrons emitted from the last dynode are then collected by the anode.

5. The electrons collected produce an output signal, made of pulses. The discrimination of these pulses at a proper binary level, producing a digital signal, is referred to as photon counting.

3.1.4 Equipment for other than PD test

The equipment necessary before performing any PD test is the humidity tester device because humidity affects the PDIV a lot, which causes the difference in the results. It is then necessary to use the humidity checker before performing any experiment.

- The humidity measurement instrument (Testo 635-1)

The measurement of humidity is required before performing any experiment because it affects the PDIV. Temperature, air humidity, and dew point may all be measured with the testo 635-1 temperature and humidity measurement equipment shown in figure 3.22. It is used to measure temperature, air humidity, and dew point even in compressed air. This extensive range of measuring options is made possible by cutting-edge technology and a huge number of optional probes [22].



Figure 3.22: Testo 635-1

3.1.5 Experimental setup

Different experimental setups of PCBs that have been developed are discussed and shown below:

3.1.5.1 Setup for PDIV measurement of PCBs at normal environmental conditions using AC 50Hz voltage supply

Figure 3.23 demonstrates the setup for the measurement of Partial Discharge Inception Voltage (PDIV) of all types of PCBs under normal ambient conditions using AC 50Hz voltage. The purpose of this test is to understand the effect of voltages on various types of PCBs and select some particular PCBs that have higher PDIV to perform further tests at aerospace conditions and propose the selected PCB models for the high voltage terminal part of the inverter used in the actuation system of MEA. The test of each PCB follows the same procedure described below:

- At the start, the PCB is placed in the high voltage cage where the PCB connects to the step-up transformer through a coupling capacitor. One terminal of PCB connects to the ground and the other to the high voltage source, as shown in figure 3.23.
- A transformer is used to step up the grid supply voltages (230 V, 50 Hz), which is cascaded with a variable auto-transformer (VARIAC) used to vary the voltages manually.
- The voltage is manually increased, slowly and continuously until the first discharge is detected.
- The oscilloscope is used to measure the test voltages (peak-peak, Maximum, Amplitude, and RMS).
- A ground cable (connected to LV of PCB) passes through a High-Frequency Current Transformer (HFCT), which senses the PDs and shows the PD waves on the screen of the PC connected through PDbaseII.

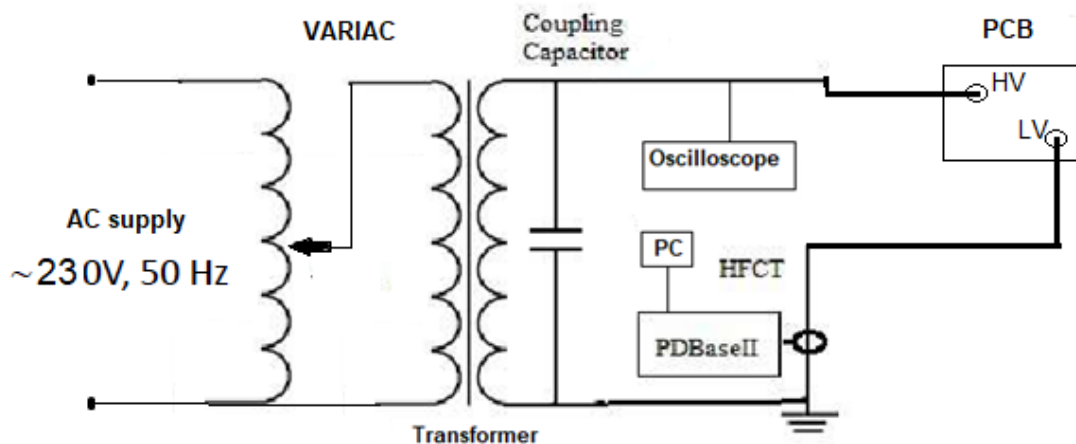


Figure 3.23: Set up for the PDIV measurement of PCB at normal conditions using AC source

3.1.5.2 Setup for the measurement of PDIV at different temperatures (25°C, 80°C, and 120°C) using AC 50Hz voltage

The setup to measure the PDIV of all kinds of PCBs at 25°C, 80°C, and 120°C using AC 50Hz voltage is shown in figure 3.24. The goal of this test is to understand the behavior of PCBs at different temperatures, which is necessary because MEA actuators work in a particular environment (lower pressure and different temperature). The test of each PCB follows the same procedure, which is described below:

- At the start, the PCB is placed inside the climatic chamber where one of its terminals connects to the ground and the other to the high voltage source, as shown in figure 3.24.
- A transformer is used to step up the grid supply voltages (230 V, 50 Hz), which is cascaded with a variable auto-transformer (VARIAC) used to vary the voltages manually.
- The climatic chamber is then set to the desired temperature (25°C, 80°C, and 120°C) and waits until it reaches the required temperature.

- The voltage is manually increased (with the help of VARIAC), slowly and continuously until the first discharge is detected.
- The oscilloscope is used to measure the test voltages (peak-peak, Maximum, Amplitude, and RMS).
- A ground cable (connected to LV of PCB) passes through a High-Frequency Current Transformer (HFCT), which senses the PDs and shows the PD waves on the screen of the PC connected through PDBaseII.

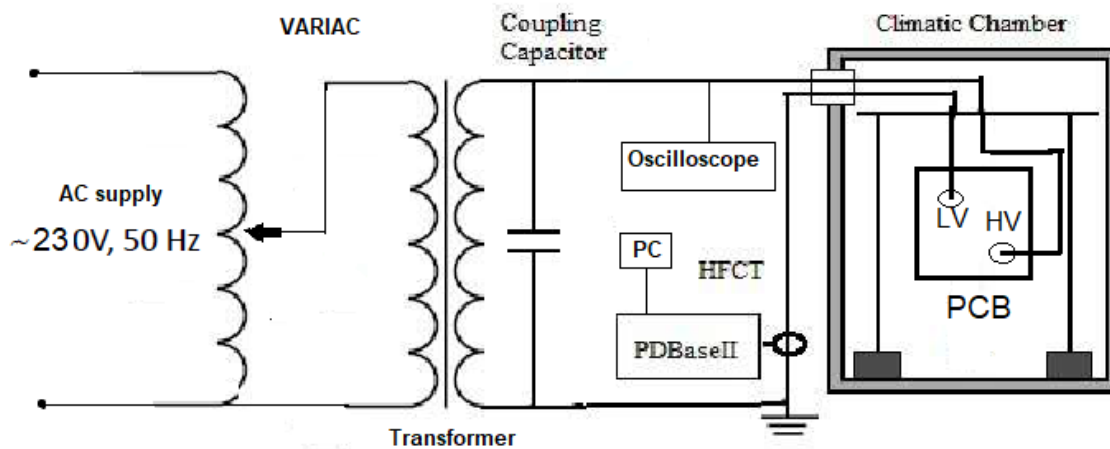


Figure 3.24: setup to measure the PDIV of PCBs at 25°C, 80°C, and 120°C using AC 50Hz voltage.

3.1.5.3 Setup for the measurement of PDIV in DC at ambient condition

This test has been performed to understand the behavior of PDIV in the case of DC supply at normal environmental conditions. The setup to measure the PDIV of PCBs using a DC voltage source is shown in figure 3.25. This is the most difficult kind of PD test because PD detection in DC is not as simple as in AC, the PDs don't appear all the time after we reach the inception voltage, but only one PD pulse occurs at a time and then after some time it occurs again and so on. So while performing this test it is important to have enough knowledge of PD detection. The test procedure is described below:

- Before performing the test, we first clean the PCB with alcohol and leave it for 10 to 15 minutes, which is necessary to be sure that the PCB doesn't have any space charges accumulated on its surface.
- After that, we put the PCB inside the shielded cage (it is important to avoid the environmental effects, which creates difficulties in the PD detection process) where the PCB is connected to the DC generator, as shown in figure 3.25.
- A DC generator has been placed outside to increase the voltages manually until discharge occurs. The voltages supplied to the test object can be examined on the LCD of the DC generator.
- A ground cable (connected to LV of PCB) passes through a High-Frequency Current Transformer (HFCT), which senses the PDs and shows the PD waves on the screen of the PC connected through PDBaseII.

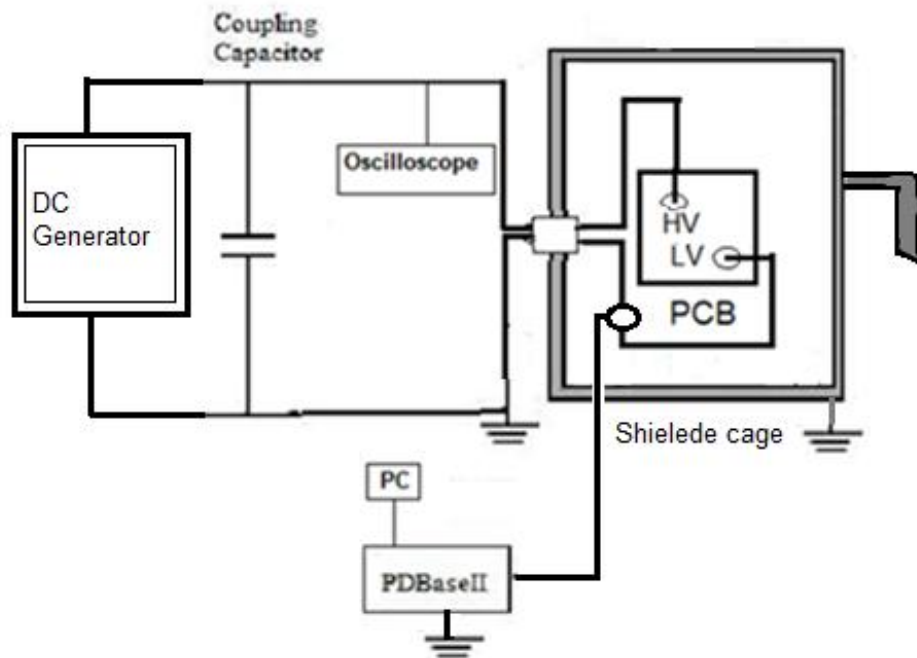


Figure 3.25: Setup for PDIV measurement of PCBs using DC source

3.1.5.4 Setup for the measurement of PDIV at lower pressure in the case of AC 50Hz voltage

The setup for the PD measurement of PCBs at lower pressure (150 mbar) by using AC 50 Hz voltage supply is shown in figure 3.26. The purpose of this test is to understand the effect of reduced pressure on PCBs, which is necessary because MEA actuators work in a particular environment (lower pressure due to altitude of aircraft). The test of each PCB follows the same procedure, which is described below:

- First, the PCB is placed inside the vacuum tank where one of its terminals connects to the ground and the other to the AC sinusoidal voltage source, as shown in figure 3.26.
- The tank is then pressurized and monitored by using a pressure gauge attached to the tank and set the desired pressure (150°C) while for the other condition (at ambient) the tank is left open without reducing any pressure.
- A transformer is used to step up the grid supply voltages (230 V, 50 Hz), which is cascaded with a variable auto-transformer used to vary the voltages manually.
- The voltage is manually increased, slowly and continuously until the first discharge is detected.
- The oscilloscope is used to measure the test voltages (peak-peak, Maximum, Amplitude, and RMS).
- A ground cable (connected to LV of PCB) passes through a High-Frequency Current Transformer (HFCT), which senses the PDs and shows the PD waves on the screen of the PC connected through PDbaseII.

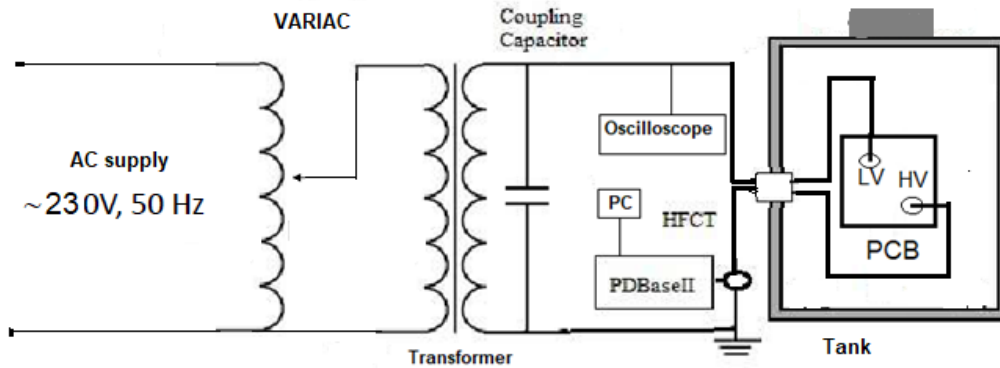


Figure 3.26: Setup for the PDIV measurement of PCBs at lower pressure by using AC 50 Hz voltage source.

3.1.5.5 Setup for the measurement of PDIV at lower pressure in case of repetitive square wave generated by SiC pulser:

The setup for the PDIV measurement of PCBs at lower pressure (150 mbar) by using SiC pulser is shown in figure 3.27. The purpose of this test is to understand the effect of high switching frequency on the PDIV of PCB at lower pressure. Only one PCB (A shorter gap between points and plate shown in fig.3.6) has been tested because of the limitations of the inverter. The test procedure is described below:

- First, the PCB is placed inside the vacuum tank where the PCB is connected to the SiC supply, as shown in figure 3.27.
- The tank is then pressurized and monitored by using a pressure gauge attached to the tank and set the desired pressure (150°C).
- The DC generator is connected to the SiC inverter as a supply source and then the SiC inverter converts DC into repetitive square waves, which is then supplied to the test equipment (PCB).
- The test is performed automatically with the help of the software PhotonUp+. This application acquires the voltage applied and photon emitted and controls the voltage of the bus DC of the pulser.

- The gate time set for the photon acquisition is 500 ms, also rise time, step increment voltages start voltages, and stop voltages are sated before the test. The application allows the voltages to be supplied to the test sample when we press the start button on the bottom of the application. While the test is stopped by us manually when we examine the discharges on the screen.
- The oscilloscope shows the test voltages applied to the test sample.

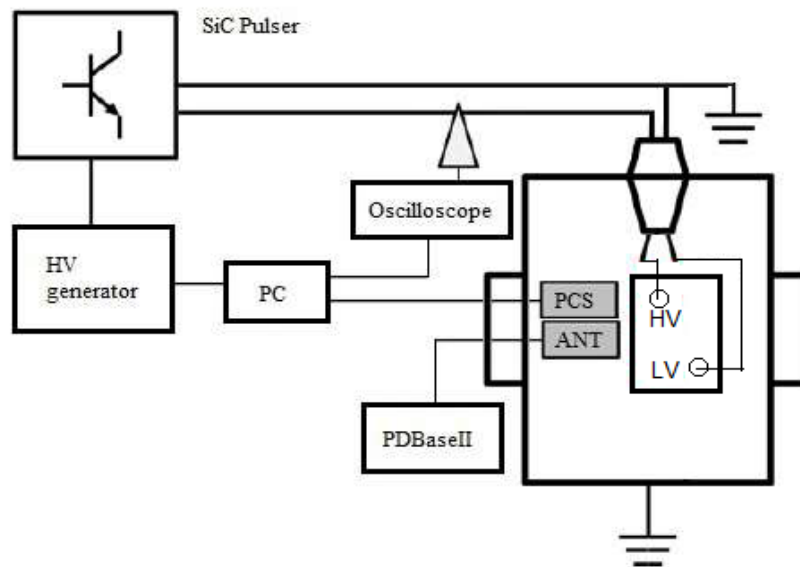


Figure 3.27: Setup for the PDIV measurement of PCBs at lower pressure by using SiC pulser.

3.2 Twisted Pairs (TPs)

Twisted pairs are models for testing the turn/turn insulation of rotating machines fed by the converters. As far as, the material of the twisted pairs is concerned there are three different types of corona resistance wires are used:

Sample 1: The wire used for the twisted pair is DAMID 200 GR2 0.56mm round enameled winding wire of copper. The diameter of the wire is 0.56mm and the insulation thickness is 35um (being of grade 2).

Sample 2: The wire used for the manufacturing of twisted pair (sample 2) is of grade-2 round enameled winding wire having a diameter of 0.63 mm.

Sample 3: The wire used for the manufacturing of twisted pair in the case of sample 3 is ZTERM200NT GR2 of round enameled winding wire having a similar diameter as sample 1 (0.56 mm), but it differs by the insulation because nanotechnology particles are present on the insulation in order to ensure a good resistance to the corona effect.

These wires are sold with declared properties of:

- High heat resistance
- High-speed machine windings suitability
- Very good resistance to transformers oils
- Very good resistance to typical solvents
- Freon resistant
- Excellent resistance to mechanical stress

And to be utilized among others fields in electrical motors.

The insulation is composed of two coats, one internal, the basecoat in THEIC-modified polyester or polyesterimide, and one external, the overcoat of polyamide-imide. It has a temperature index of 200°C.

3.2.1 Construction and description of (TPs)

They are manufactured by a specialized machine built in our lab, as seen in Fig. 3.28. The machine is made up of a step-by-step drive that is controlled by an Arduino Nano and allows selecting the rotation speed and number of revolutions. The machine starts with a piece of straight wire long around 70cm and twists it 12 times, to obtain 12 nodes and 10 antinodes. The wire is bent in a U shape and the curve part is attached to the rotating shaft of the motor while the two open extremities are attached to a counterweight using two pulleys to maintain constant tension on the wire while it is twisted. Depends on the need it is possible to regulate the distance between the pulleys and the shaft as well as to change the counterweight, different wires may require different settings. TPs realized in such a way for this thesis have a twisted region of length around 11cm. The reason to have a machine that produces TPs is to have samples as much homogeneous as possible. One of the samples of twisted pairs after manufacturing is shown in figure 3.29.



Figure 3.28 Twisted Pairs (TP) manufacturing machine (Luppatore)

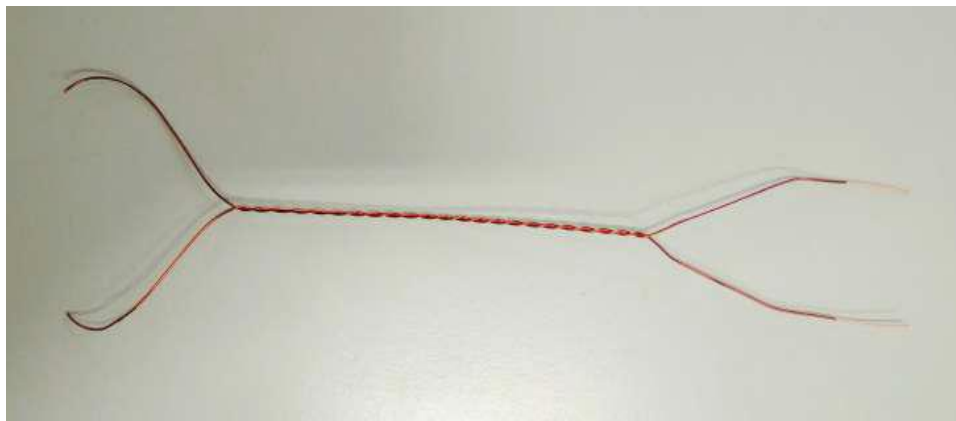


Figure 3.29: Picture of twisted pair

3.2.2 Concept of the endurance test

In inverter-fed motors, the over-voltages induced by impedance mismatch at the motor/cable interface and the uneven distribution of turn voltages can cause partial discharge (PD) in the motor insulation system, causing insulation degradation to accelerate significantly [24] [25]. The International Electrotechnical Commission (IEC) has issued two technical specifications, TS 60034–18–41 and 42, to address this issue and improve inverter-fed motor insulation system reliability.

The qualification and acceptance tests for form-wound motors (Type II) are addressed by IEC TS 60034–18–42 [27]. According to the TS, endurance tests on insulation models are required to compare new and proven insulation systems. sinusoidal voltages can be used to test the lifetime of insulation because it is assumed that sinusoidal and square

wave voltages will provide comparable results if they have the same peak-to-peak voltage and frequency.

As we know the turn/turn insulation is the critical part of the inverter fed machine and TPs are models for testing the turn/turn insulation. The purpose of the endurance test is to figure out how the machine reacts when it is continuously stressed by the voltages at high frequency, as well as how long it can withstand the stress under aerospace conditions (lower pressure).

The experiments have been conducted in a vacuum tank using two voltage sources (Sinusoidal AC 50kHz voltage, and unipolar repetitive square wave voltage). Various instruments have been interfaced with the PC through MATLAB ®, to have the possibility to control them remotely and to create an automatic system. A pre-build MATLAB code has been used which helps to perform the endurance test by connecting all the equipment when the “Run” button has been pressed and starts/stops the test when Endurance occurs.

3.2.3 Testing procedure for PCBs

The testing procedure to perform the endurance test on twisted pairs is described below:

3.2.3.1 Environment for testing

The vacuum tank is used in which experiments can be accomplished at lower pressure.

Tank:

The tank has been custom designed in the laboratory to serve all the needs, which is already defined in section 3.1.2.1.

3.2.3.2 Voltage sources:

Two voltage sources have been used in our experiments: AC voltage source at 50 kHz and repetitive square wave generated by a silicon carbide converter.

I. Sinusoidal AC supply (50 kHz):

The sinusoidal 50 kHz AC voltages are generated by using a resonant generator board manufactured by the University, which generates the square wave pulses of 50 kHz. The 50 kHz waves are supplied to the twisted pairs through the transformer. As between the two open terminals of twisted pairs, there is a capacitor of around 10-30pF (capacitive effect due to open ends), the circuit diagram shown in the figure. 3.31. The output waveforms are the same as shown in fig. 3.9 has been generated in this case as well; the only difference is the higher frequency. Here also the waveforms have slightly distorted but this won't affect the results because the essential parameter is the voltage value.

II. SiC Pulser:

The unipolar repetitive square wave voltage is produced by a silicon carbide-based pulser (unipolar inverter) has been already defined in section 3.1.2.2.

3.2.4 Measurement techniques:

Two main quantities have to be measured by the instrument, the supply voltage, and endurance time. These two quantities are important to measure because the voltage stress and the time the material takes to endure at that particular voltage stress is necessary to understand the material strength, the parameter we are looking for in our experiments.

3.2.4.1 Voltage Measure

For the voltage measurement in our system, Tektronix MD03054B Oscilloscope (fig. 3.14) has been used, which is already defined in detail in section 3.1.3.1.

3.2.4.2 Endurance time:

Endurance time can be measured with the help of a pre-build MATLAB code, which starts counting the seconds when the test starts and stops the time when endurance occurs. This process is performed automatically using MatLab code. It also stops the test (generate a train sound) and stops applying the voltages when endurance occurs.

3.2.5 Test setup

The experimental setups for the endurance test have been developed and discussed below:

3.2.5.1 Endurance test of twisted pairs at lower pressure using repetitive square waves generated by SiC pulser

The setup for the Endurance test of twisted pairs at lower pressure (150 mbar) supplied by SiC pulser is shown in figure 3.30. As we know the turn/turn insulation is the critical part of the inverter fed machine, therefore, the purpose of this test is to figure out how the machine reacts when it is continuously stressed by the inverter, as well as how long it can withstand the stress under aerospace conditions (lower pressure). The test procedure is described below:

- First of all, the twisted pair is placed inside the vacuum tank where it is connected to the SiC pulser, as shown in figure 3.30.
- The tank is then pressurized and monitored by using a pressure gauge attached to the tank and set the desired pressure (150°C).
- The DC generator is connected to the SiC inverter as a supply source, which converts DC into repetitive square waves, these waves are then supplied to the test equipment (twisted pair).
- The test is performed automatically with the help of the MATLAB code, named “Endurance”. This code helps to connect all the equipment (using Arduino) to the PC and controls automatically.
- The Endurance code opens and sets to “1” and presses the run button for connecting all the equipment once all types of equipment are connected successfully, we set “0” and run the endurance test.
- The test sample can be seen from the “Silica window” during the test. It glows when high voltages are flowing through it and generates a spark when endurance occurs.

- The Endurance time is calculated by the MATLAB code. It stops the test and generates a train sound when endurance occurs.
- The oscilloscope is used to measure the voltages applied to the test sample.

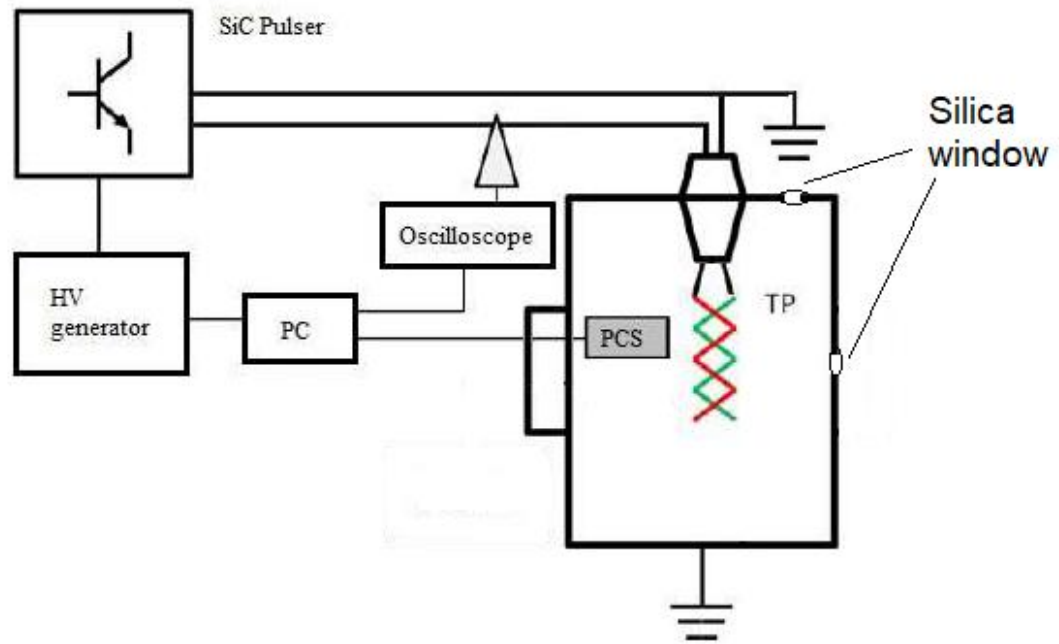


Figure 3.30: Endurance test of twisted pairs at low pressure supplied by SiC pulser

3.2.5.2 Endurance test of twisted pairs at lower pressure using AC sinusoidal 50 kHz voltage source

The setup for the endurance test of twisted pairs at lower pressure (150 mbar) using a sinusoidal AC 50 kHz voltage source is shown in figure 3.31. As mentioned above that the turn/turn insulation is the critical part of the inverter fed machine, therefore, the purpose of this test is to understand the behavior of the machine when it is continuously stressed by sinusoidal waveforms at a higher frequency (50 kHz) along with the effect of frequency on the endurance of the twisted pairs, in other words, how long they can sustain the stress at aerospace conditions (lower pressure). The test procedure is described below:

- At the start, the twisted pair is placed inside the vacuum tank where it is connected to the resonant generator through a transformer, as shown in figure 3.31.
- The tank is then pressurized and monitored by using a pressure gauge attached to the tank and set the desired pressure (150°C).
- The resonant generator generates square waves of 50 kHz. These waves are supplied to the twisted pairs through the transformer. As between the two open terminals of twisted pairs, there is a capacitor of around 10-30pF (capacitive effect due to open ends). In the end, the capacitive effect cancels by the resonant waveforms and we have sinusoidal waveforms on the screen of the oscilloscope.
- The test is performed automatically with the help of the code written on the Python program. This code helps to connect all the equipment to the PC and controls automatically.
- The code runs, after running the code resonant generator should be turned on and when endurance occurs it automatically disconnects the resonant generator from the system.
- The test sample can be seen from the “Silica window” during the test. It glows when high voltages are applied through it and produces a spark when endurance occurs.
- The Endurance time is calculated by the Python program. It stops the test when endurance occurs.
- The oscilloscope is used to measure the voltages applied to the test sample.
- At the time just a bit before the endurance the waveforms completely distort, which can be analyzed on the screen of the oscilloscope this is because the twisted pair is aged and about to endure.

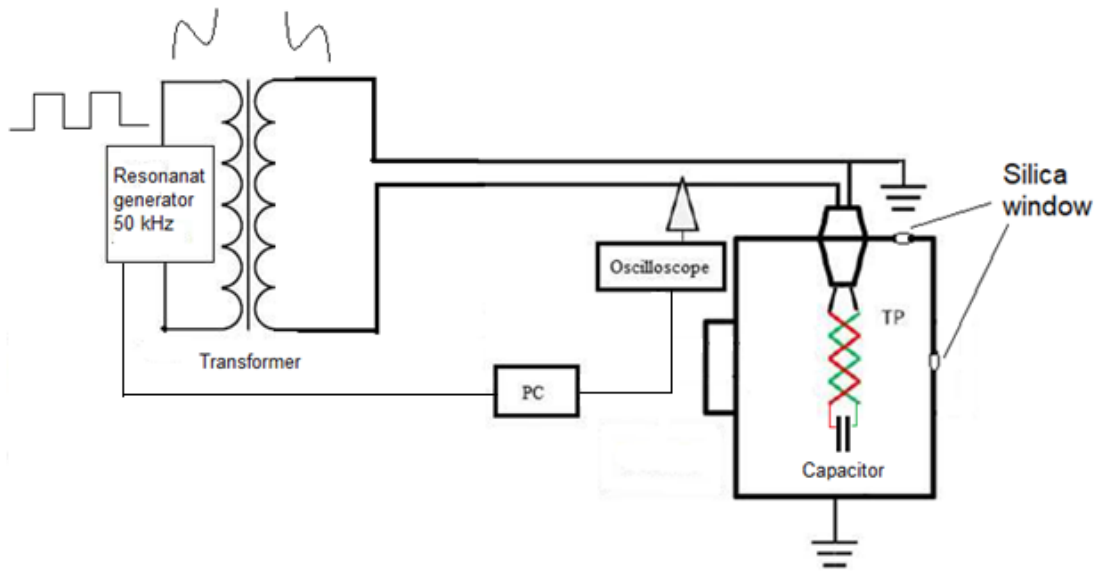


Figure 3.31: Endurance test of twisted pairs at low pressure using sinusoidal AC 50 kHz source

Chapter 4

Results and Discussion

In this chapter, the results of all the experiments performed on PCBs and twisted pairs have been discussed with a brief discussion on each experiment.

4.1 Printed Circuit Boards (PCBs)

The increasing use of electrical rather than pneumatic or hydraulic power in aircraft systems has resulted in a rise in demand for power electronics that operate with greater power densities. Electrical failure risk exists in all industries that use high voltages and power electronic equipment; however, the aircraft industry is especially vulnerable because circuit boards are exposed to lower pressures than those found at ground level, lowering partial discharge inception voltages. Protective polymers are often applied to printed circuit boards to increase dielectric performance. However, in the event of a partial discharge, the coating might degrade, diminishing protective capability and breakdown strength, as well as limiting board lifetime. Therefore, PD prevention and detection are necessary to ensure the reliability and long-term operation of power electronic equipment [44].

In this section, PCB models described in section 3.1, which are used to simulate the discharges within an inverter. In the inverter fed machine, the high voltages supplied to the machine pass through the inverter so if the inverter fails it causes problems in the machine and consequently actuation system of MEA fails. Therefore, it is important to ensure the reliability of the inverter to the machine chain. It is, therefore, necessary to perform the PD test on the models of the high voltage terminal part of the inverter (PCBs) at aerospace conditions (high temperature and low pressure) when they are supplied by high voltages (AC, DC, Square waves).

4.1.1 Analyze the effect of AC voltages on all the PCBs by comparing their Partial Discharge Inception Voltages (PDIVs) at ambient conditions

The purpose to perform the PDIV test on many PCB models is to examine the effect of AC voltages on different PCBs (different by their creepage distance). And propose the PCBs, which can be used for other experiments in order to find the PCB which is best suited for the high voltage terminal part of the inverter that has a lower or zero probability of occurrence of the partial discharge. The experimental setup for PDIV measurement of PCBs in AC has been already shown in figure 3.23. While the Partial discharge Inception Voltages (PDIVs) of all kinds of PCBs are shown in Figure 4.1.

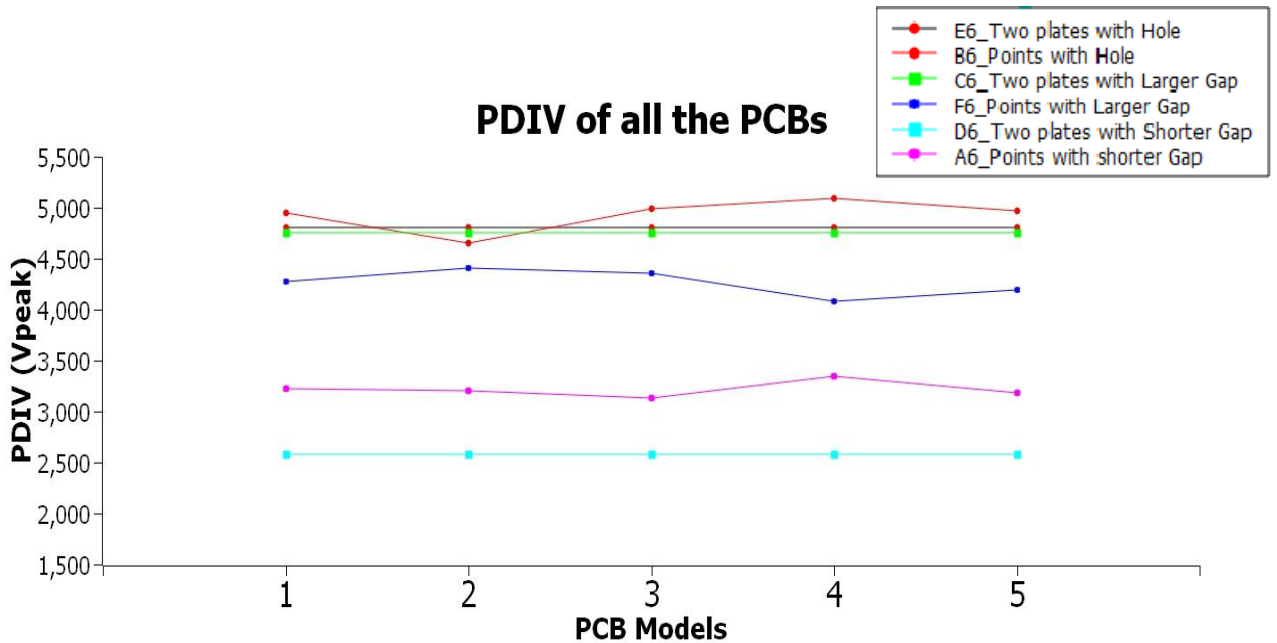


Figure 4.1: PDIV of all the PCBs at ambient conditions in case of AC supply

From this diagram, we can examine that:

- The numbers in the X-axis of the graph indicate the five points of the PCBs (only for PCBs with points). For the PCBs having two parallel plates, the numbers have no meaning (a single PDIV value was measured instead of five).
- PDIV values of PCBs with points have a fluctuation around the PDIV of their corresponding PCBs with two plates as shown in the figure above where the

PDIV of PCB model B6 fluctuates around E6, F6 fluctuate around C6, and D6 fluctuates around A6 but these models are similar by their creepage distance as shown in figure 4.2. The PCB with two parallel plates separated by a hole (E6) is similar to the PCB having a hole between a plate and 5 points (B6) with a creepage distance of (≈ 1.5 mm). In the same way, the PCB F6 is similar to C6 with a creepage distance of (≈ 1.5 mm) and the PCB D6 is similar to A6 with a creepage distance of (≈ 0.3 mm). The description of all the PCB models is present in section 3.1.1.

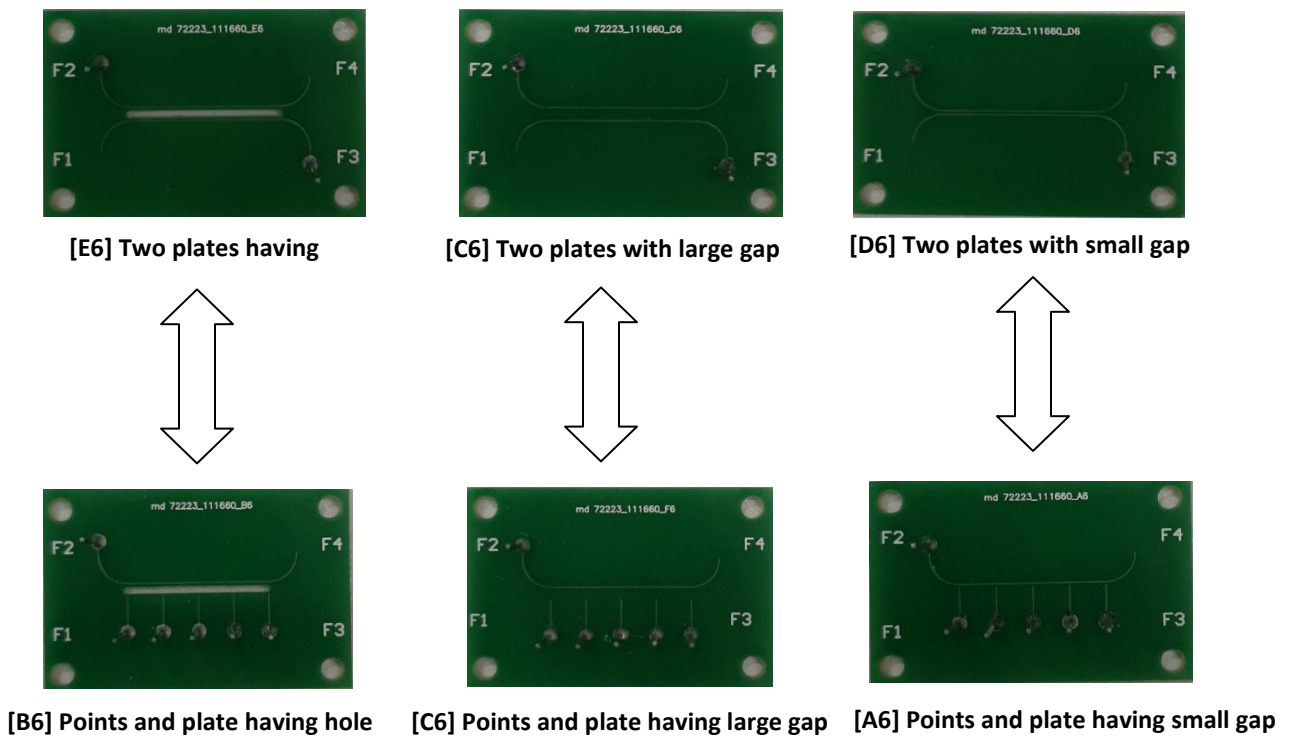


Figure 4.2: PCB pairs with the same creepage distance.

- The fluctuations are due to the space charges accumulated on the surface of PCBs because of multiple testing on the same PCB without giving enough delay. Also, some small variations in their creepage distance could be observed (within manufacturing tolerance, some points have a bit higher distance from the plate and some have lower).
- By considering the above points it is better for simplicity, to skip the results of PCBs with points (because their results are almost similar and fluctuating to their

corresponding PCBs with two parallel plates) and consider only the results of the remaining three PCBs with parallel plates, the new diagram is shown in figure 4.3.

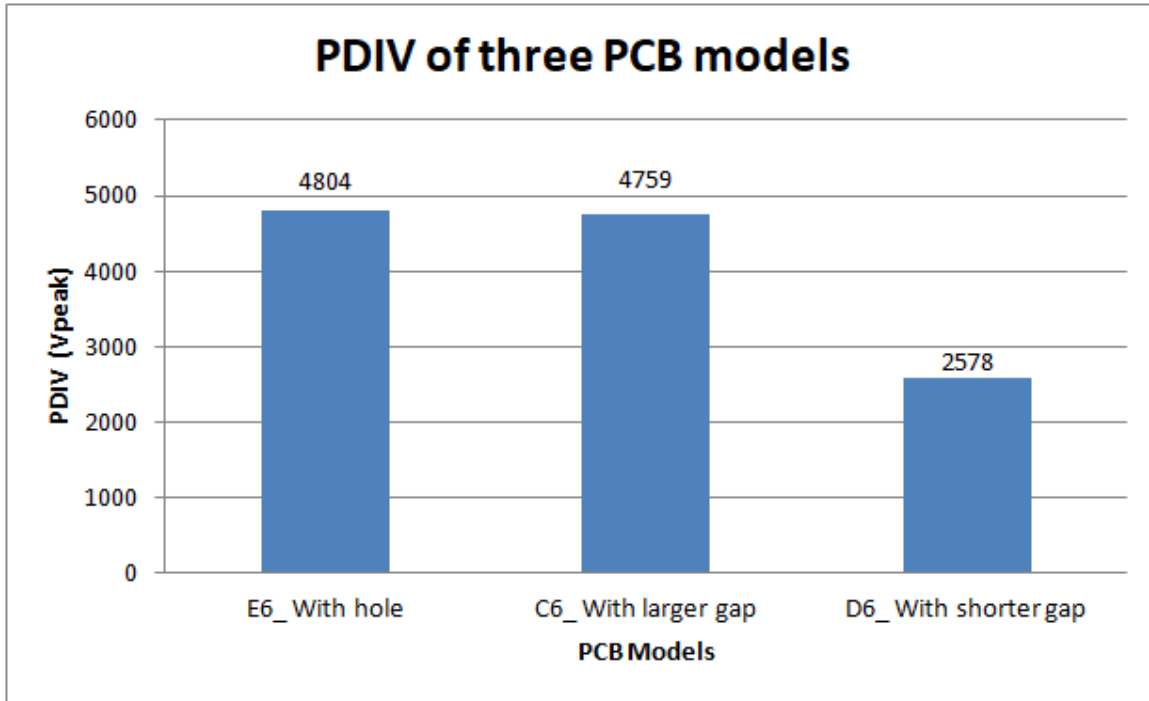


Figure 4.3: PDIV of three PCBs (Two parallel plates)

- The PCB with a hole between two plates (E6) and PCB with a larger gap between two plates (C6) have similar creepage distances (around 1.5 mm). Their PDIV is almost the same, indicating that the holes have a limited impact on PDIV.
- The PCB with a shorter distance between two plates having a creepage distance of 0.3 mm has the lowest PDIV compared with the other two PCBs.

In figure 4.4 we can also analyze that the creepage distance of PCBs (E6 and C6) are the same and their PDIV is also the same, while the creepage distance of PCB D6 (short gap) is smaller so the PDIV is also lower as compared to other PCBs.

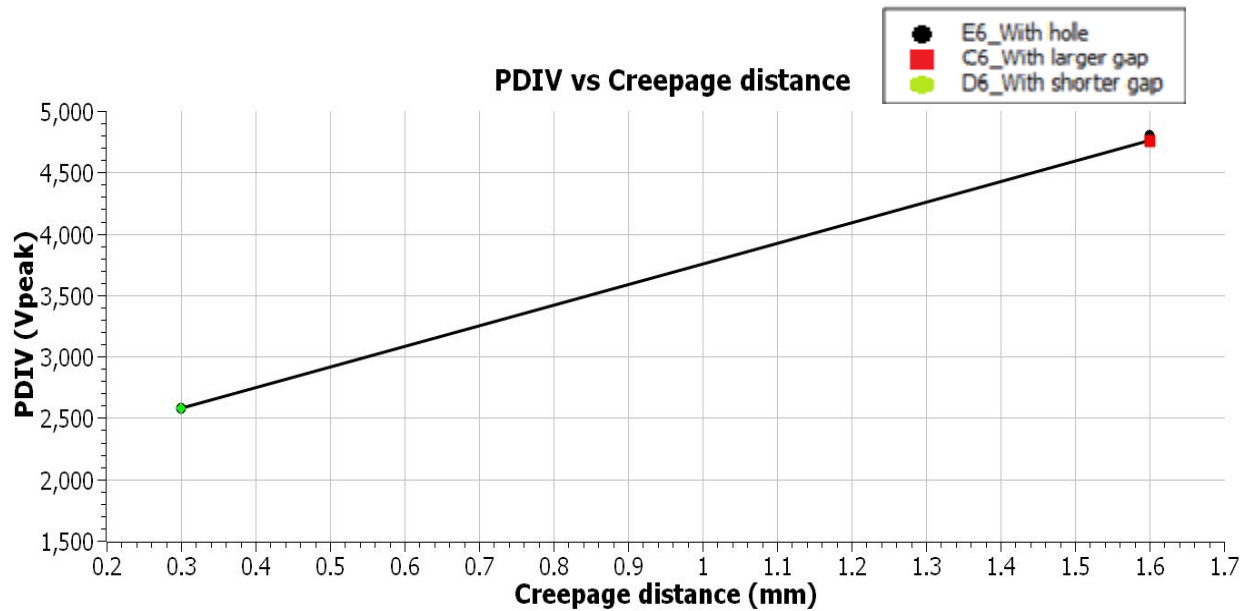


Figure 4.4: PDIV vs. Creepage distance of three parallel plate PCBs

Thus, the PDIV in AC at ambient conditions decreases if the creepage distance decrease, however, the creepage distance adopted typically seems more than adequate to prevent PD inception during operation, at least for new PCBs.

4.1.2 Effect of temperatures on the PDIV of PCBs in case of AC voltages

To understand the behavior of temperature on PDIV of the PCBs in the case of AC supply, different temperatures have been used to perform the PDIV test. The climatic chamber is used to set the temperatures and PCBs are placed inside it to perform these tests. The experimental setup for this kind of test has already been shown in chapter 3 in figure 3.24. The graph between PDIV and temperatures (25°C, 80°C, and 120°C) is shown in figure 4.5.

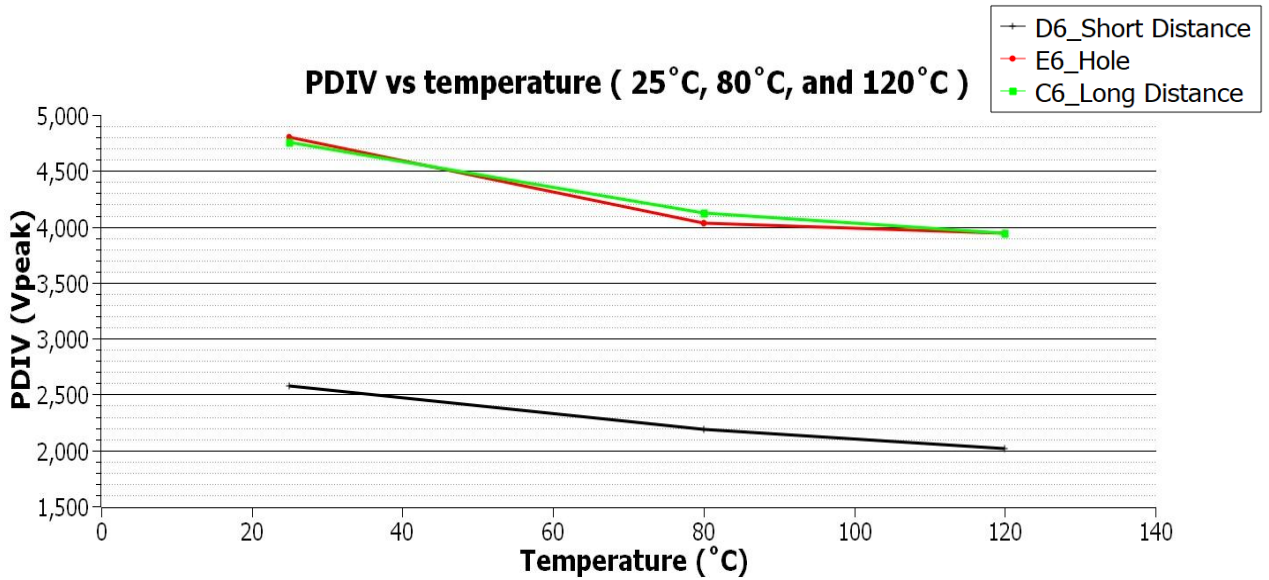


Figure 4.5: PDIV vs. Temperature

From fig 4.5, it is easy to conclude that temperature affects the PDIV of all three PCBs. There is an inverse relationship between PDIV and temperature, when temperature increases from 25 to 120°C, PDIV decreases and vice versa. Figure 4.6 shows the percentage decrease of PDIV when temperature increases from 25 to 120 °C.

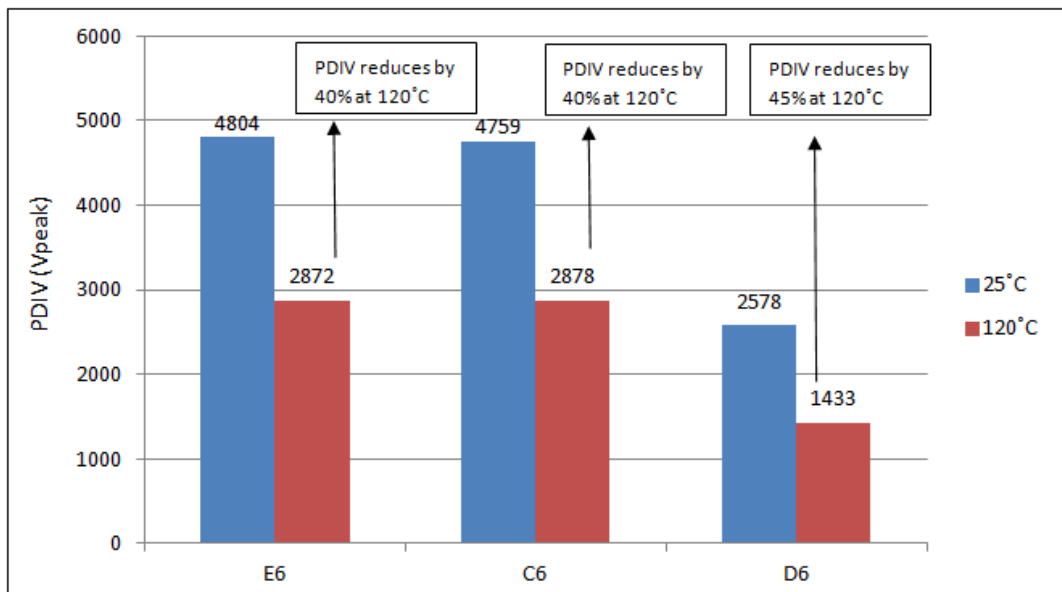


Figure 4.6: Comparison between PDIVs of three PCBs at 25°C and 120°C

It can be shown that at 120°C, the percentage decrease in PDIV is 40%, which is the same in both PCBs (hole between plates (E6) and the gap between plates (C6) \approx 1.5 mm), whereas the percentage drops in PDIV is 45% in PCBs with short creepage distance of around 0.3 mm. In all the above experiments, the humidity is kept constant, which was around 50% because humidity also affects the results.

The physics behind the reduction of PDIV can be understood with the help of ideal gas law

$$PV = nkT \quad 4.1$$

If we consider an environment with fixed pressure and volume then we can keep P and V constant in equation 4.1 because we are interested in the relationship between the number of molecules and atoms (n) and temperature (T) while k is Boltzman constant then the equation 4.1 can be rewritten as:

$$\frac{\text{Constant}}{T} = n \quad 4.2$$

From equation 4.2 we can say that as the temperature increases the number of molecules decreases in an environment.

This means that an electron travels higher distances before colliding with a molecule (the mean free path becomes longer) and the average electron can be accelerated for a longer time and indeed needs a smaller electric field to reach the speed (and energy) capable of ionizing a molecule. A lower electric field is needed to have ionization compared to the case where the temperature is lower. A lower electric field means smaller voltages when the geometry is unchanged.

Equation 4.3 relates mean free path to the temperature comes from the law of ideal gases (Eq. 4.2) and the definition of the mean free path

$$\lambda = \frac{kT}{P\sigma} \quad 4.3$$

Another impact of temperature is that the permittivity of the polyimide increases leading to a higher electric field in the air. As a result, higher temperatures can both increase the field in the air while reducing the air density, both phenomena leading to lower PDIV values [45].

To understand which factor is predominant in the reduction of PDIV (an increase of permittivity or reduction of air density) we normalized the data based on the temperature

utilized for testing. Table 4.1 shows, all the PCB models, their PDIV values at (25°C, 80°C, and 120°C), and the procedure to normalize the data based on the temperature utilized for testing:

$$\text{PDIV Theoretical} = \frac{\text{Temperature (K) of that test}}{\text{Temperature at 25°C}} \times \text{PDIV (Experimental) of that test}$$

PCB Model	PDIV (Experimental)	Temperature (°C)	Temperature (K) = (°C+273)	PDIV (Theory)	PDIV ratio (EX/TH)
E6	4804	25	298	4804	1
C6	4759	25	298	4759	1
D6	2578	25	298	2578	1
E6	4031.5	80	353	5690.6	0.70844
C6	4123.5	80	353	5637.3	0.73146
D6	2183	80	353	3053.8	0.71484
E6	3944	120	393	6335.5	0.62252
C6	3845	120	393	6276.1	0.61263
D6	2013.5	120	393	3399.8	0.59223

Table 4.1: Data normalization based on the temperature utilized.

Figure 4.7 shows the temperature normalization curves for all three PCBs at 25°C, 80°C, and 120°C.

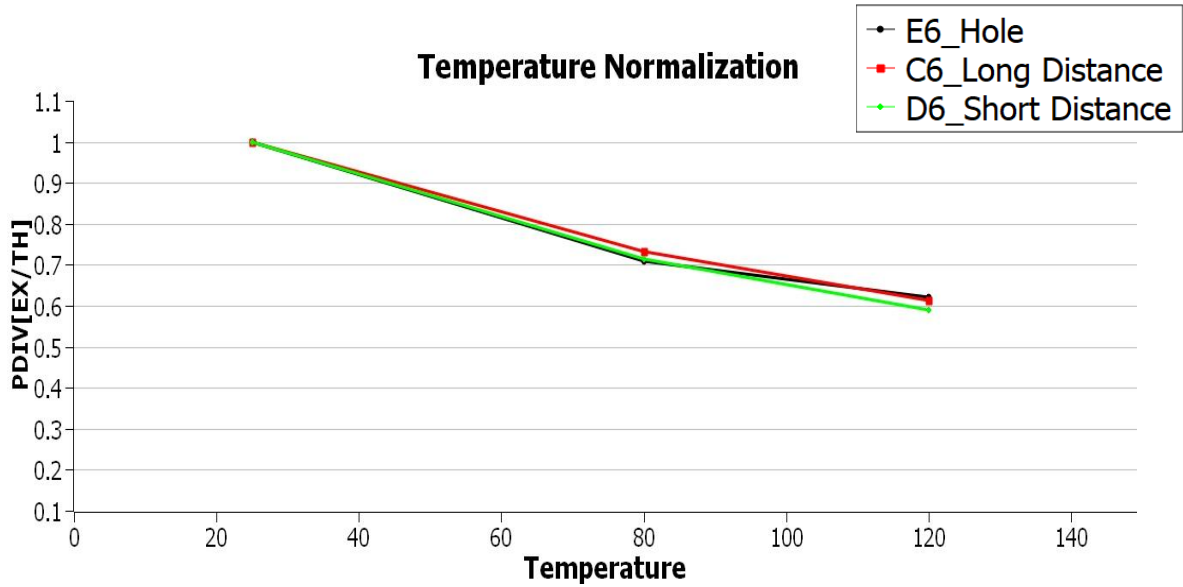


Figure 4.7: Temperature normalization

As we can see, the PDIV drop due to temperature effect is linear but not exactly; if the effect was solely due to air density reduction, the curve should be linear and equal for all PCBs, but there are some deviations, implying that the effect of PDIV drop due to temperature is caused by something other than air density reduction. This could be due to permittivity. However, the influence of permittivity seems limited because the non-linearity is moderate.

4.1.3 Effect of low pressure on PDIV of three types of PCBs in the case of AC supply

The effect of low pressure on PDIV of PCBs in the case of AC supply can be examined by using the tank, the experimental setup is shown in figure 3.26. The purpose of this test is to examine the effect of low pressures on the PDIV of the PCBs and compare the results to the ambient pressure (1013 mbar). Humidity also affects the PDIV, which can be controlled by placing Silica gel inside the tank.

These experiments have been performed on six sets of three PCBs (to ensure the test results are similar) to understand the behavior of low pressure on the PDIV of PCBs. Figure 4.8 shows the graph between PDIV and pressure.

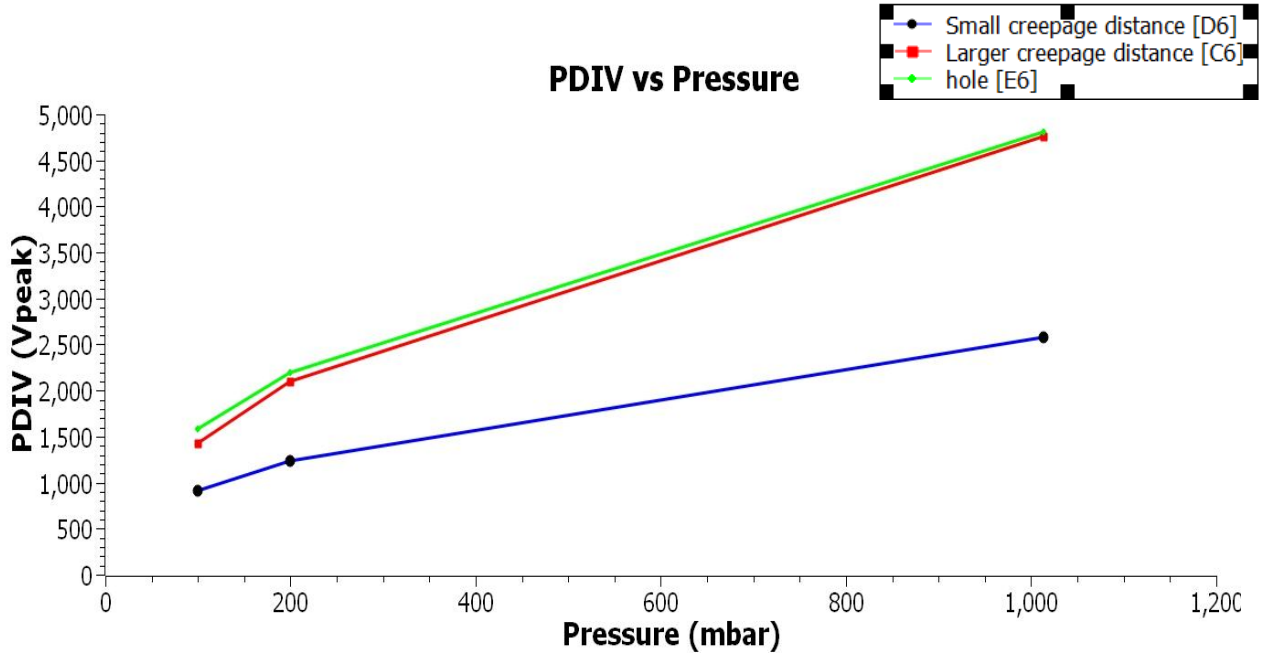


Figure 4.8: PDIV vs. Pressure

It can be analyzed that, the pressure and PDIV have a direct relationship, if the pressure goes down from (1013 – 200 mbar) PDIV decreases linearly while if we further decrease the pressure from 200 mbar, PDIV decreases in a faster way.

Rui and Ian Cotton in [13] performed many tests on the different twisted wire samples to understand the effect of low pressure on PDIV in the case of AC supply. In that paper, many experiments have been performed considering different pressure levels (1013 to 100 mbar) but the results (shown in fig. 2.15) at the end are somehow similar to what we got in this experimental part. This shows that under low-pressure, insulating systems are more vulnerable. Partial discharge activity and, as a result, the damage will begin at a lower voltage level in an aircraft environment where ambient pressure can drop to as low as 150 mbar.

The effect of low pressure on the reduction of PDIV is due to the lower number of molecules at constant temperature and air volume, equation 4.4 derived from ideal gas law, discussed above:

$$\lambda = \frac{kT}{P\sigma} \quad 4.4$$

Lower pressures are projected to result in a longer mean free path for electrons this lowers the breakdown field required to start an electronic ionization avalanche because

free electrons have more physical space to accelerate and accumulate enough kinetic energy from the applied electric field to launch an ionization process after colliding with a neutral. When the pressure is lessened, lower field intensity will be required to trigger the initial electronic avalanche [42].

The comparison between the PDIVs at atmospheric pressure (1013 mbar), 200 mbar, and 100 mbar is shown in figure 4.9

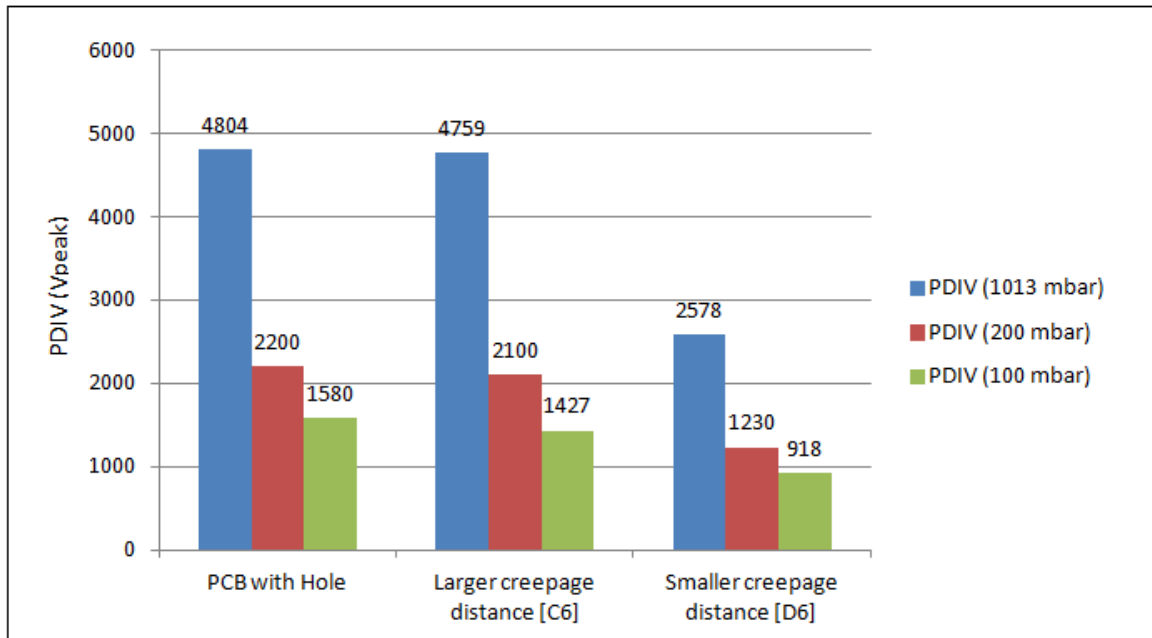


Figure 4.9: Comparison of PDIVs at 1013 mbar, 200 mbar, and 100 mbar

- The percentage decrease of PDIV at 200 mbar is 55% while at 100 mbar there's a 68% reduction of PDIV in E6 PCB.
- The percentage decrease of PDIV at 200 mbar is 55% while at 100 mbar there's a 70% reduction of PDIV in C6 PCB.
- The percentage decrease of PDIV at 200 mbar is 54% while at 100 mbar there's a 65% reduction of PDIV in D6 PCB.

In all these cases, it can be said that the percentage reduction of PDIV at 200 mbar is around 55% while the reduction at 100 mbar ranges between 65% – 70%, which is huge.

4.1.4 PDIV measurement of three kinds of PCBs and the role of space charges in the measurement of PDIV at DC supply

The experimental setup used for these tests is depicted in figure 3.25, which shows the measurement of PDIV of three PCBs (E6, C6, and D6) in the case of DC supply at ambient conditions. The goal of this test is to figure out how PCBs react when they are exposed to DC voltage.

The findings of multiple studies are not very convincing since when we approach the inception voltage, there are only a few PD pulses with very low repetition rates. This complicates PDIV determination; also, the PDIV of PCB with a larger creepage distance (C6) has the same PDIV as PCB with a smaller creepage distance (D6), which seems illogical. This was eventually revealed to be due to space charges accumulating on the PCB's surface, as well as other environmental factors influencing our results. The findings are still inconclusive even after performing several tests and following some strict procedures such as cleaning the PCB before performing any test to drain off the charges from the surface of the PCBs, increasing the voltages in steps, and so on. Figure 4.10 show some results, which gives a range of voltages where we found PDs according to the PD pulses we are interested in (bigger or smaller).

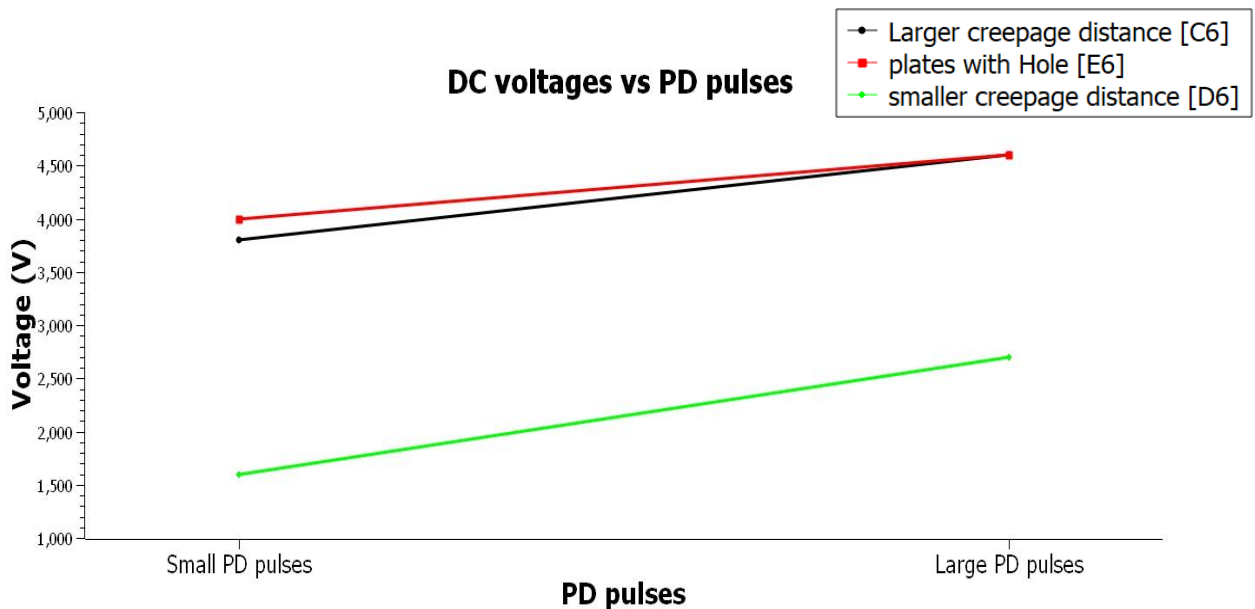


Figure 4.10: Voltages vs. PD pulses in case of DC supply

From figure 4.10, the following results are analyzed:

- The small PD pulses appear at 1600 V (DC) in the case of PCB with a small creepage distance, if we continue to increase the voltages (random step time) then at around 2700 V large PD pulses appear once and then disappear.
- In the case of larger creepage distance PCB (C6), small PDs appear at 3800 V. Around 4600 V large PD pulses appear (once/twice) and do not appear again even after a long wait. The same happens in the case of PCB with hole (E6).
- Large PD pulses appear sometimes after a long delay (30 minutes or maybe more).
- We were interested to see big PD pulses more frequently to ensure whether these are PDs or noise, the PCB (C6) has been tested again by increasing the voltages higher than 4600 V while reaching at 5700 V, many large magnitude PDs appear and in a few seconds breakdown occurs. It is analyzed here that we have PDs in the range of (3800 – 4600) voltages and if we go beyond this, breakdown occurs.
- From all these experiments, it is concluded that in the case of PCBs with a small creepage distance, the PDIV ranges between 1600 – 2700 V. In the case of the other two PCBs, the PDIV ranges between 3800 – 4600 V. If we go beyond this, breakdown occurs. Some small and large PD pulses, which were observed during the experiments, are shown in figure 4.11 (a) and 4.11 (b) below:

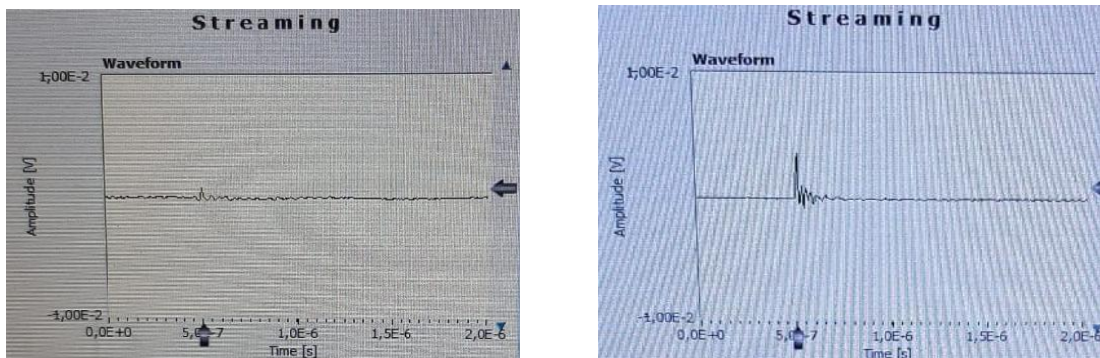


Figure 4.11: (b) Small PD Pulses

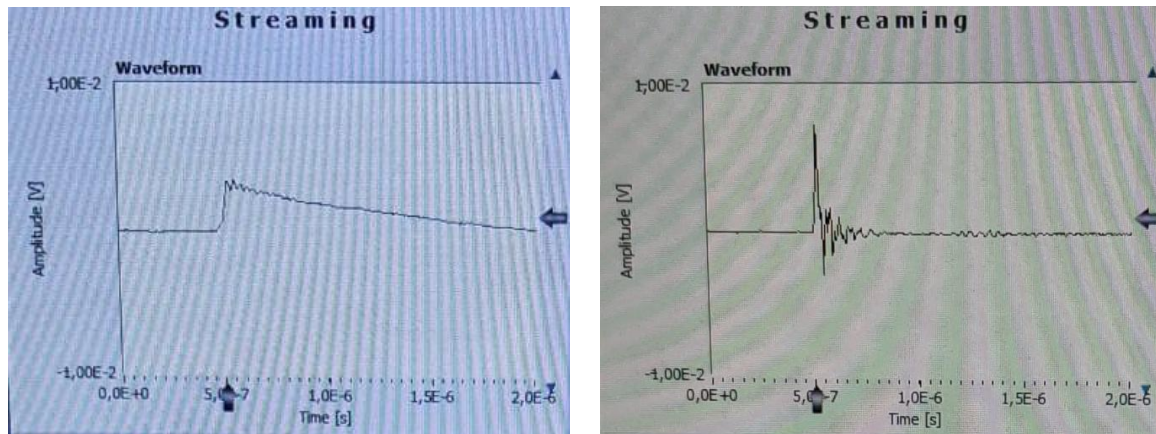


Figure 4.11: (b) Large PD Pulses

The above results are recorded without giving any proper delay (random step time) to increase the voltages. When we reach the inception voltage (where small PD pulses start appearing) space charges can influence the results. As we don't know how much time the space charges take to drain out from the surface of the material it is difficult to decide the step time. If we increase the voltages and there are still some space charges present on the surface of the PCB then these charges try to oppose the applied field and we will not be able to find the exact value of PD inception voltages.

According to U Fromm in [46], the PD occurrence causes accumulation of charge near to the location where discharges occur. This leads to a drop of the local field strength below the minimal breakdown field strength (E_{min}), so that the discharge extinguishes [46].

As a result, it's important to comprehend the role of space charges in PD measurement. This allows us to better understand the behavior of the material used in PCBs under a DC power source, as well as how long it takes for space charges to drain from the PCB's surface and, eventually, how to determine the necessary step time for increasing voltages to get meaningful results.

Role of space charge in the measurement of PD:

Due to electrode injection and/or ionic species, the presence of space charge (SC) in insulation cavities can influence PD activity. On the one hand, due to the space charge, the field inside the dielectric can be enhanced in comparison to the Laplacian field created by the electrodes. The action of electric field and temperature, on the other hand,

can extract SC deposited at the cavity-insulation interface, providing starting electrons that increase the probability of PD inception. These events are likely to change the PD inception voltage (PDIV), as well as the magnitude and phenomenology. These considerations need, however, to be supported by evidence, since the way space charge affects PD activity cannot be predicted easily.

Results from PD measurements performed on nonpolarized and DC polarized specimens have been presented in [47]. The results show that space charge can change significantly PD activity, even if in a way that cannot be predicted easily. This is due to the fact that especially in the first hour of PD activity, it is quite difficult to distinguish the effects associated on one side with the natural reduction of space charge density, on the other side with changes in the chemical-physical properties of the cavity [47].

The Pulsed Electro-Acoustic (PEA) method, which is used in [47] for the detection of space charges can also be employed in our case to detect the space charges because it is one of the most largely, used techniques to detect space charges trapped in the insulation. Once we know the nature of space charges behaves in the material of our test sample we can easily drain them out or we can increase the step time to rise the voltage until all the space charges are drained out from the surface of PCB.

4.1.5 The effect of converter waveform on PDIV of PCBs in case of the repetitive square wave at 100 mbar

The goal of this experiment is to see how the converter waveform affects the PD inception voltage of PCBs in the case of a repeated square wave. In this case, PCB is placed inside the closed tank, where the PCB is connected to the inverter, which uses a DC generator to supply repeating square waves to the PCB. The setup has been already demonstrated in figure 3.27.

In [52] it has been observed that PD detection under power electronic converter interference with the PD detection system in a frequency band where PD have their spectral content due to the large slew rate of WBG switches. As a consequence, it is hard to distinguish between PD and interference. To solve this problem an optical and a UHF system were used.

In our case as well, the optical system has been used to detect the PDs. The optical detection is based on the ability to detect photons created during the discharge by collision events (ionization, recombination, attachment, etc.). This method eliminates nearly all electromagnetic noise, but it necessitates a completely dark environment and a clear line of sight between the specimen and the detector.

To examine the effect of converter waveform (repetitive square wave) on PDIV of PCB at lower pressure, four same types of PCBs (small creepage distance D6) are considered for the experiment. This is because other PCBs have higher PDIVs, which are above the inverter limit. The four same types of PCBs have been tested and their results are plotted in the Weibull chart, shown in figure 4.12. The results of the experiments seem to have an overall good fit in the Weibull chart meaning that all the tests are performed well.

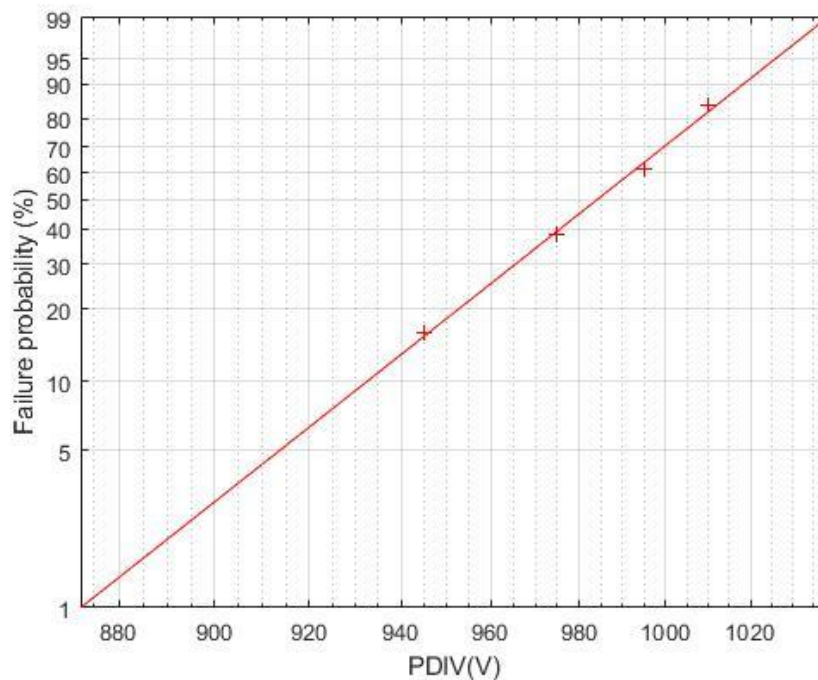


Figure 4.12: Weibull chart shows the PDIV of four small creepage distance PCBs at the repetitive square wave

If we want to compare these results with the one which we got in AC to see the effect of the repetitive square wave on PDIV of PCB then we should consider the mean of all four above PCBs and compare it to the mean of PDIVs obtained from the same type of PCBs in AC. As a result, the PDIV under repeating square wave is found to be higher than

under AC waveform (variation of 8%, 981 at 10 kHz converter against 900 at 50 Hz AC), which is shown in figure 4.13. This is because the repetitive square wave voltage is affected by an overshoot during the turn on and off flanks. The probability of PD inception during the overshoot is limited to the inherent randomness of free electrons able to start a PD. Since the applied voltage is ramped during the tests, this delay tends to provide a higher PDIV. Besides, the PCB permittivity at the largest frequencies of the inverter voltage might be lower (due to dipole inertia) than that at AC 50 Hz. Consequently, lower electric fields can be expected in the air, leading to larger PDIV values.

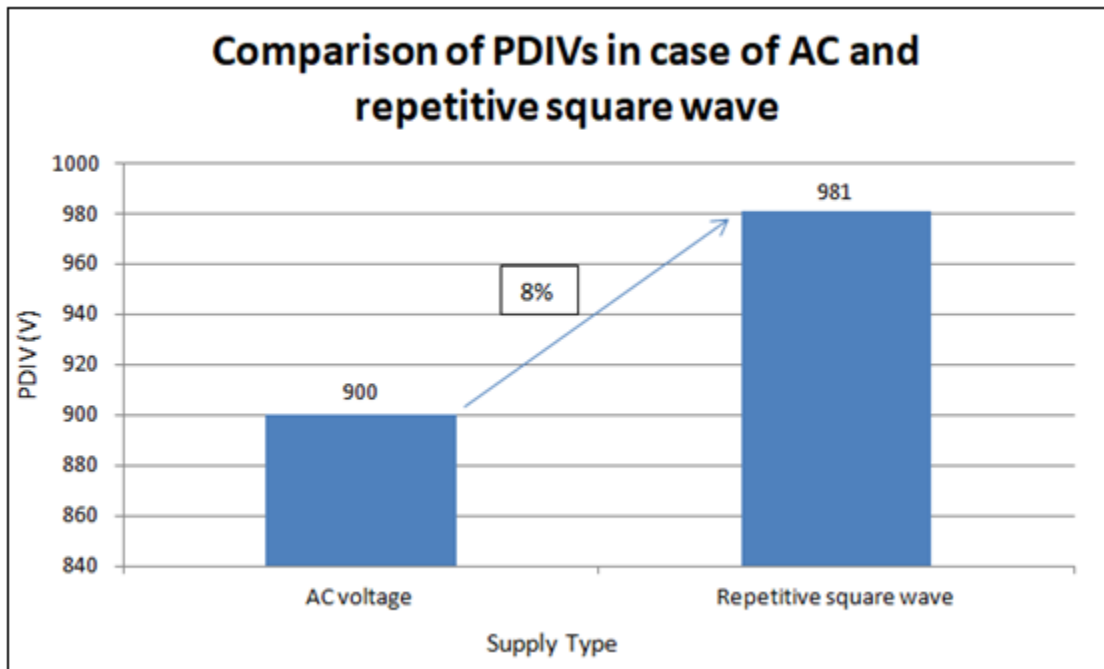


Figure 4.13: Comparison of PDIVs in case of AC and repetitive square wave

After performing all the tests on different types of PCBs, it is now easy to answer the question, which we had previously at the start of this research work, whether the converter part in the converter to machine chain is critical or not? The answer is, no it is not the most critical item in the system; however, it is important to remember that the proper creepage distance in the high voltage terminal part of the inverter is necessary to avoid PDs and ensure the inverter to machine chain's reliability.

4.2 Twisted Pairs (TPs):

As we already know the turn/turn insulation is the critical part of the inverter fed machine and TPs are models for testing the turn/turn insulation. The purpose of the endurance test is to figure out how the machine reacts when it is continuously stressed by the voltages at high frequency, as well as how long it can withstand the stress under aerospace conditions (lower pressure).

Two voltage sources (repetitive square wave at 100 kHz and sinusoidal AC at 50 kHz) are used to perform the endurance test on three different corona-resistant wires.

4.2.1 Effect of voltages (AC and repetitive square wave) stress on the endurance of the twisted pairs at lower pressure (150 mbar)

The purpose of this test is to examine the effect of both AC and repetitive square wave voltages on the endurance of the twisted pairs at lower pressure (150 mbar). In this test different voltage levels are applied to twisted pairs to calculate the time taken by the twisted pairs to the breakdown. There are three different types of corona-resistant wires are used to manufacture the twisted pairs. At each voltage level, endurance tests have been performed on at least 5 times of the same wire (for the accuracy of the results) which means 15 tests have been performed at the same voltage level and then again voltage level changes for another 15 tests and so on.

The twisted pairs are placed in the vacuum tank, where the twisted pairs are connected to the supply voltages either repetitive square wave or AC 50 kHz. All the instruments have been interfaced with the PC to have the possibility to control them remotely and to create an automatic system. This system stops supplying the voltages to twisted pairs when the breakdown occurs; two different setups for different voltages supplies are used to examine the effect of voltages on the endurance of twisted pairs. The setup for repetitive square waves is shown in figure 3.30 while the setup for AC 50 kHz voltage supply is shown in figure 3.31.

The test results after performing multiple tests on each wire sample at a voltage level of (700, 756, and 1050 V) in the case of repetitive square wave voltage with 100 kHz frequency is shown in figure 4.14, where the average of results having the same sample, same voltage level, and same humidity are shown in the figure to make the results simple to understand. Furthermore, the rise time and frequency are the same in all the experiments.

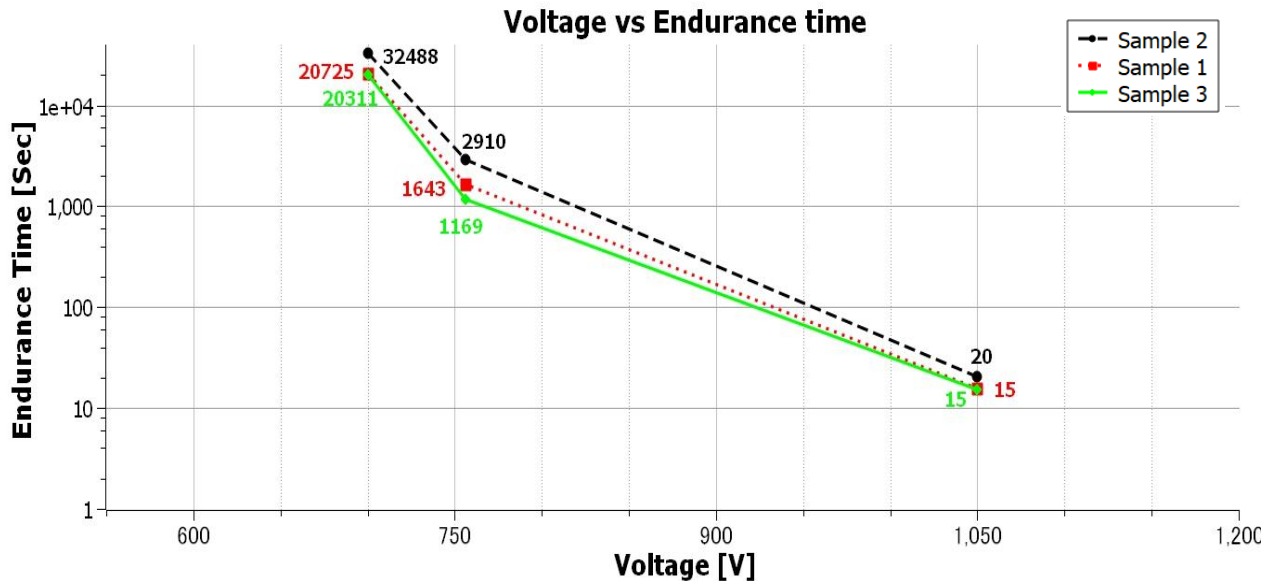


Figure 4.14: Graph between voltage and endurance time of three different wire types of twisted pair in the case of repetitive square wave 100 kHz voltage under 150 mbar.

The results clearly show that in the case of all three samples, as the voltage stress increases the endurance time decreases, implying that if we increase the voltage level of an inverter fed machine at a lower pressure, it will take less time to the breakdown. The tests were not performed higher than 1050 V because of the lower endurance time observed at 1050 V.

Furthermore, it is shown that the endurance time of sample #2 TP is higher compared with others. This is because the wire used to manufacture this TP has a higher diameter (thus, thicker insulation) than the other two wire samples. We can also notice that a voltage level of (700 V \approx 1400 Vpk-pk) has an endurance time of 32488 sec \approx 9 (hours), which is not that much if compared to the duration of a transcontinental flight, these experiments have been performed at relatively large relative humidity (\sim 40%). If we consider lower humidity, longer times can be expected.

Some experiments have also been performed on other days without reaching the endurance of the sample. This was because of low humidity; the effect of humidity and on the endurance of the twisted pairs will be discussed in the following sections of this chapter.

The endure twisted pairs in case of repetitive square wave voltage shown in the figures below

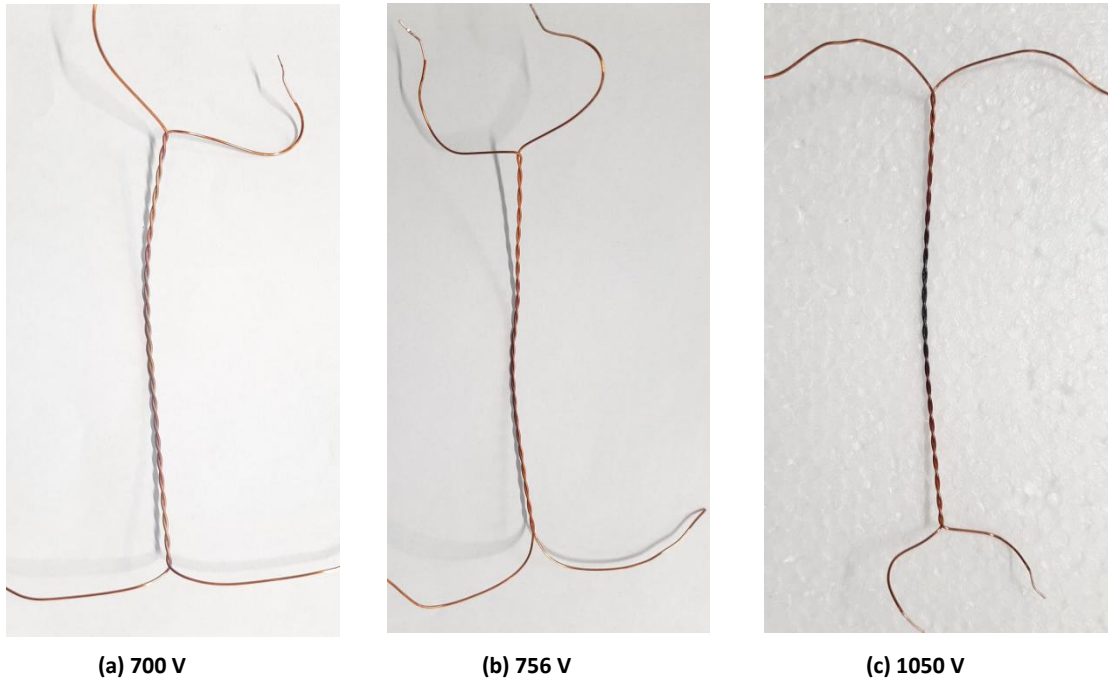


Figure 4.15: Twisted pairs of Sample #1 wire after the endurance test at a repetitive square wave



(a) 700 V



(b) 756 V



(c) 1050 V

Figure 4.16: Twisted pairs of Sample #2 wire after the endurance test at a repetitive square wave



(a) 700 V



(b) 756 V



(c) 1050 V

Figure 4.17: Twisted pairs of Sample #3 wire after the endurance test at the repetitive square wave

A similar effect is observed when Sinusoidal AC 50 kHz voltage supply is used. In this case, different voltage levels were chosen for three different twisted pair samples, and 15 tests were performed on each wire type at voltage levels of (875, 1050, and 1400 V), as shown in figure 4.18, where the average of results having the same sample, same voltage level, and same humidity are shown in the figure to make the results simple to understand.

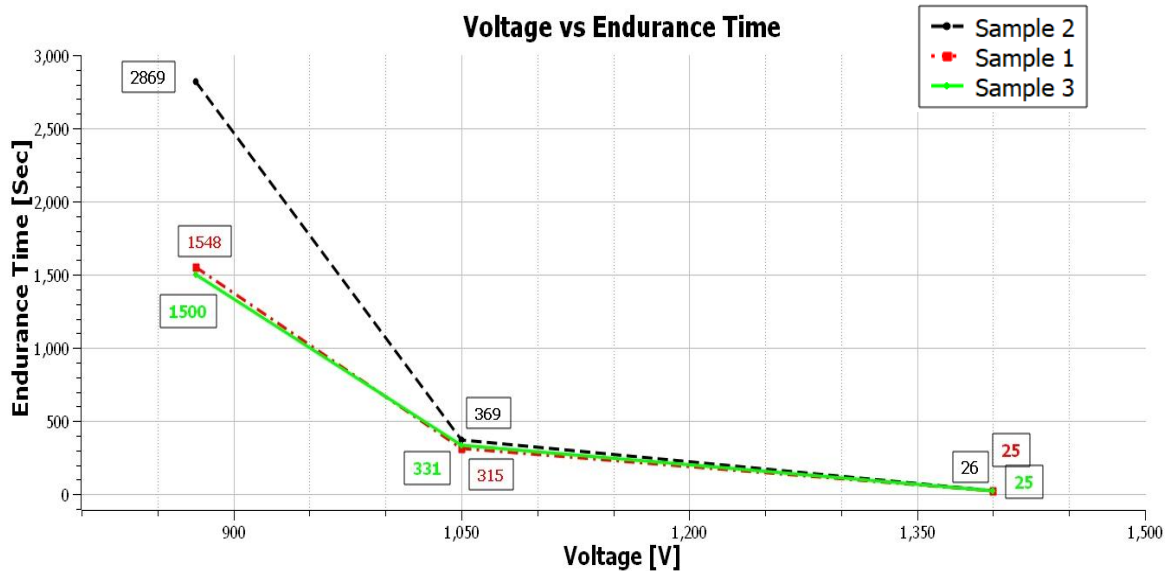


Figure 4.18: Graph between voltage and endurance time of three different wire types of twisted pair in the case of AC voltage supply

The results in this case as well are the same, as the voltage level increases, endurance time decreases. In this case, the endurance time is shorter as compared to the previous case, this is because here the voltage stress is higher.

In the instance of Sinusoidal AC 50 kHz supply voltage, the twisted pairs after the endurance test are depicted in the figures below: The location where the insulation cracks are also indicated in some diagrams with a circle around it.



(a) 875 V



(b) 1050 V

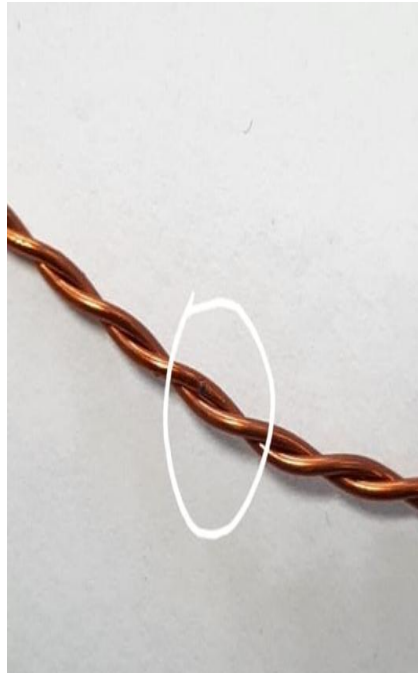


(c) 1400 V

Figure 4.19: Twisted pairs of Sample #1 wire after the endurance test in case of sinusoidal AC 50 kHz voltage supply



(a) 875 V



(a) 1050 V



(a) 1400 V

Figure 4.20: Twisted pairs of Sample #2 wire after the endurance test in case of sinusoidal AC 50 kHz voltage supply.

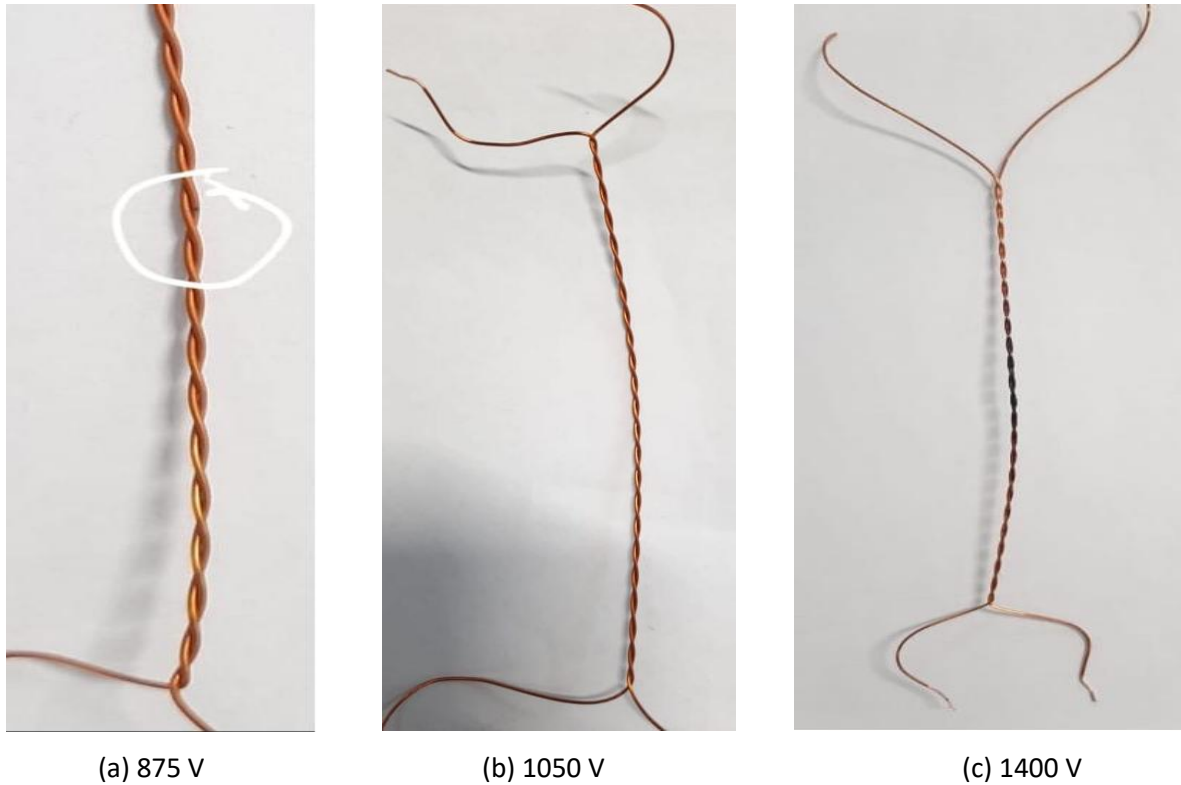


Figure 4.21: Twisted pairs of Sample #3 wire after the endurance test in case of sinusoidal AC 50 kHz voltage supply.

4.2.2 Effect of supply type (AC or Repetitive square wave) and their frequencies on the endurance of the twisted pairs at lower pressure (150 mbar)

Until now we have noticed that endurance of the twisted pair decreases as the voltage level increases either repetitive square wave or sinusoidal AC wave. Now let's look at the influence of the supply frequency on the twisted pair's durability while maintaining constant voltage stress.

Apart from the voltage stress, there may be the effect of frequency, which changes the endurance time. There is a direct effect of frequency on the PDIV, which changes when frequency changes.

The effect of repetitive square wave 100 kHz and sinusoidal AC 50 kHz on the endurance of the twisted pairs is shown in figure 4.22, where it can be observed that endurance time

in the case of repetitive square wave 100 kHz voltage is higher than the sinusoidal AC 50 kHz by keeping the same voltage level of $1050 V_{peak}$ and the same humidity in both cases. This is because, in the case of repetitive square wave voltage supply, the frequency is 100 kHz causes a huge amount of discharges per period as compared to the discharges in sinusoidal AC 50 kHz voltage supply. This increase of discharge when frequency increases, decreases the lifetime of the insulation, which is clearly shown in the figure below where endurance time decreases as frequency increases from 50 kHz to 100 kHz.

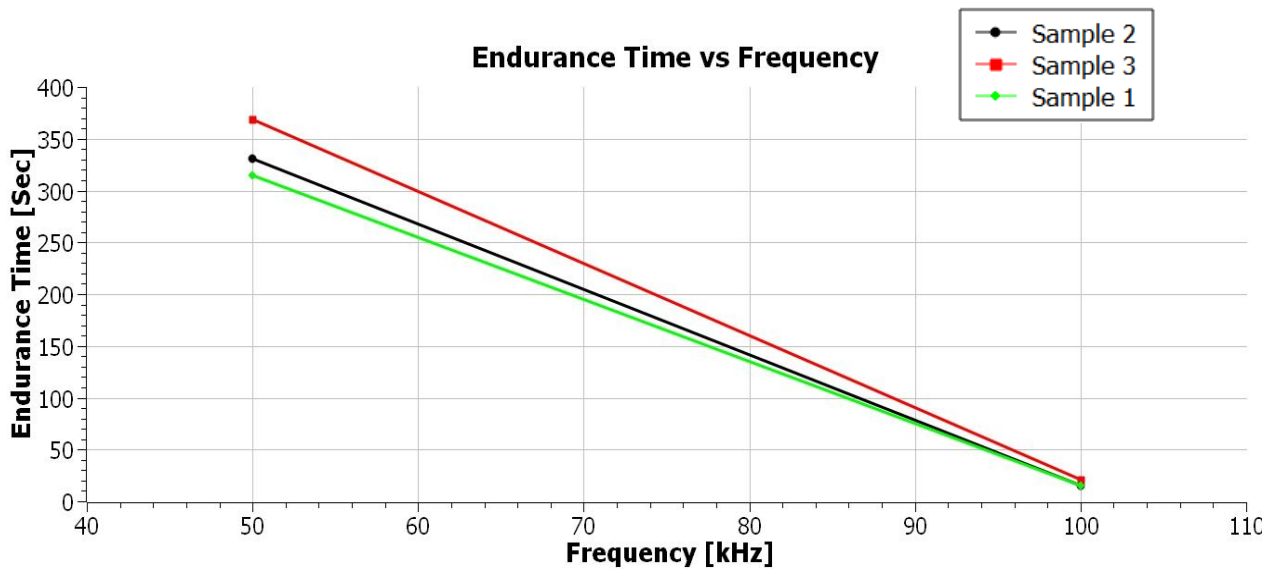


Figure 3.22: Effect of the repetitive square wave at 100 kHz and sinusoidal AC 50 kHz on the endurance of the twisted pairs at 1050V

From these results, if we just focus on the variation of frequency by considering other parameters (waveform shape and rise time) constant, we can easily conclude that as supply frequency increases, PDIV decreases, which decreases the endurance time of the inverter fed machine insulation, this is because the larger the frequency, the larger the number of PD per second, the shorter the lifetime.

4.2.3 Effect of humidity on the endurance of the twisted pairs:

The effect of humidity on the partial discharge phenomenon is very difficult to understand. The fundamental issue is that the presence of humidity changes the chemical kinetics of the air, modifying the interactions between it and the applied electric field. Furthermore, especially if there are solid-gas interfaces, excessive humidity

concentrations can substantially alter the distribution of the electric field in the air. The methods by which the quantity of water vapor in the air determines partial discharge initiation are yet unclear, especially when the combined effect of temperature is considered. The effect of humidity on the PD inception voltage was observed by many authors [59] [60] [61].

This study aims to investigate if humidity affects the insulation of inverter-fed motors. To investigate the effect of humidity, an endurance test on twisted pairs has been performed by using a repetitive square wave voltage supply at lower pressure (150 mbar). These tests are performed at different humidity while the voltage level should be kept constant to understand the effect of humidity on the endurance of the twisted pairs.

The experimental results described in [57] show that higher RH gives rise to PD events with higher PD magnitude. It has been well known that PD with a higher magnitude, generally, results in a shorter insulation lifetime [58]. As a result, as relative humidity rises, the endurance of the twisted pairs diminishes.

Endurance test has been performed on sample #2 TP at constant 700 V of a repetitive square wave under 150 mbar pressures. Figure 4.23 shows the graph between endurance time and humidity, where the humidity changes from 38% to 47% with a change in endurance time is from 32,488 to 20,000 seconds respectively. The results show that humidity has a significant impact on the endurance of twisted pairs. There's an inverse relationship between endurance time and humidity, as humidity increases, endurance decreases this is because the presence of humidity changes the chemical kinetics of the air causes the change of applied electric field distribution in the air.

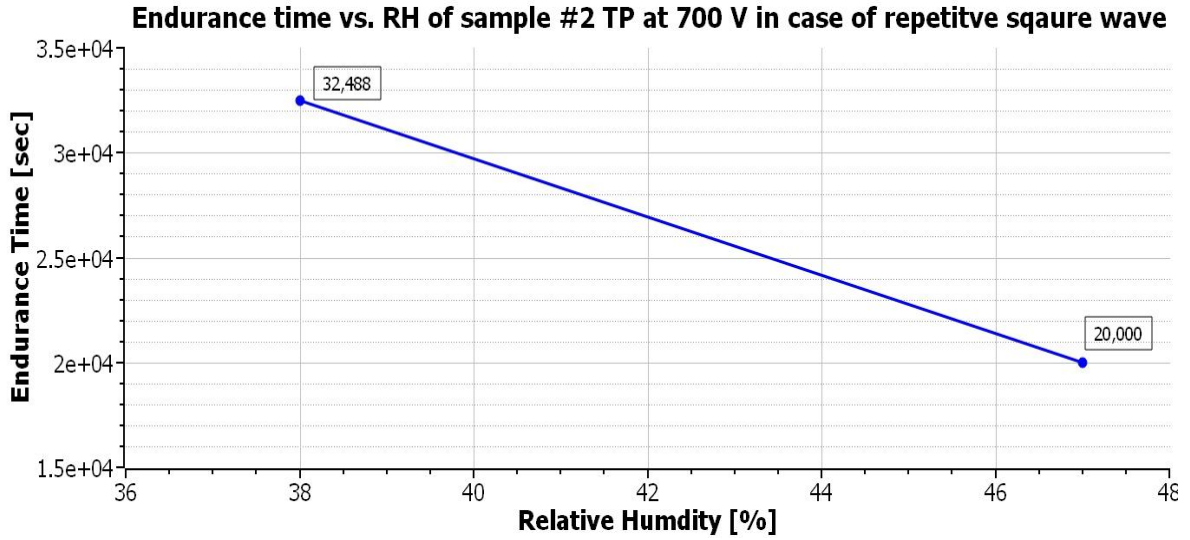


Figure 4.23: Endurance Time vs. RH of sample #2 TP at 700 V of a repetitive square wave under 150 mbar

To support the discussion above, sample #1 has been tested at three different values of humidity while keeping the same voltage level of 756 V at repetitive square waves under 150 mbar pressures. The results are similar to the one discussed above, but here the voltage level is a bit higher than the previous case and humidity is also different. In this case, humidity changes from 32.5% to 51% with the drop in endurance time are from 1934 seconds to 86 seconds respectively, as shown in figure 4.24.

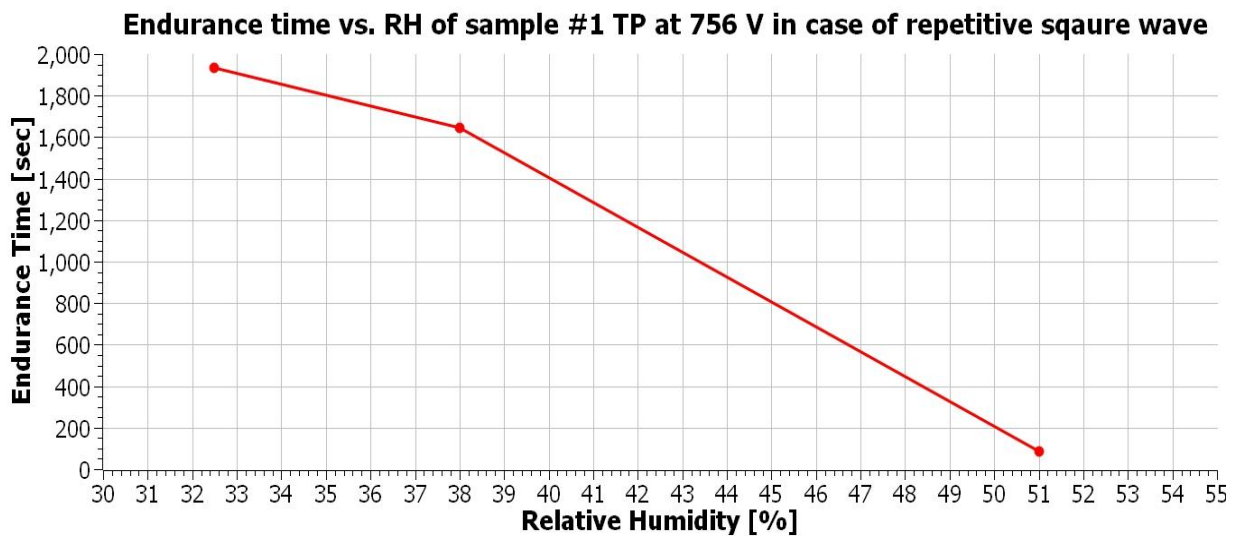


Figure 4.24: Endurance Time vs. RH of sample #1 TP at 756 V of a repetitive square wave under 150 mbar

Moreover, the effect of humidity on the endurance of samples #1 & 3 TPs at 756 V is shown in figure 4.25. The decrease of humidity from 38% to 32.5% in both samples increases endurance time, which can be analyzed in the figure below.

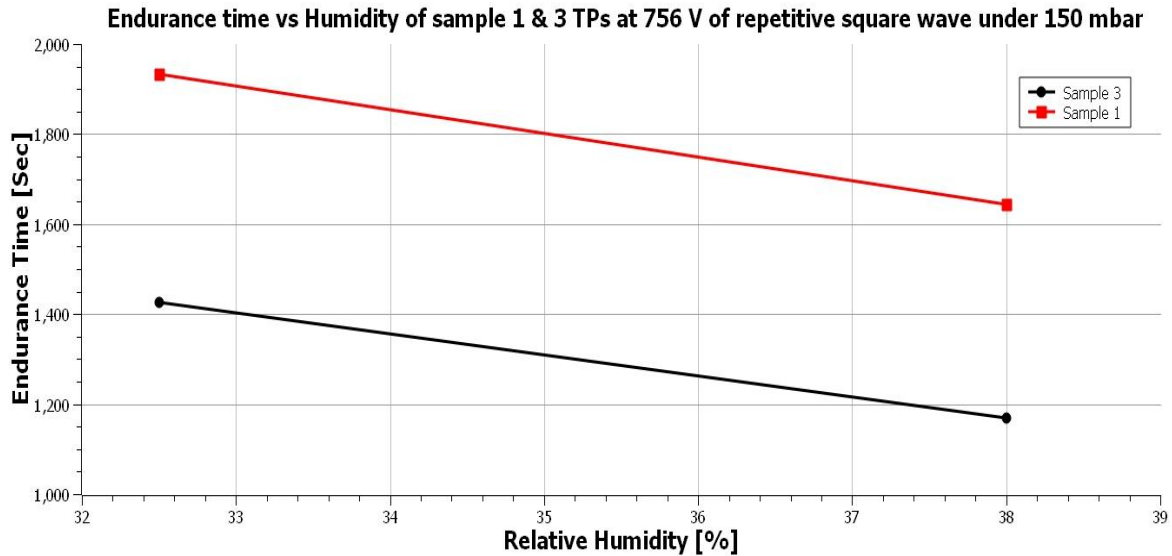


Figure 4.25: Endurance Time vs. RH of sample #1 & 3 TPs at 756 V of a repetitive square wave under 150 mbar.

All of the foregoing findings show that humidity has an impact on the PD inception voltage as well as the insulating material's durability (endurance). These tests were carried out on different days without the use of a climate chamber. Furthermore, temperature measurement was required with humidity, and temperature in all of these tests was recorded lower. This is because if the humidity and temperature both increase, the results will be different; the combined effect of temperature and humidity makes the results more complex, as stated in [60].

We can deduce from the foregoing findings that the corona-resistant wires utilized in these experiments can withstand PDs for a long duration. We saw in section 4.2.1 that a voltage level of (700 V \approx 1400 Vpk-pk) has an endurance time of 32488 sec 9 hours, which is not that much if compared to the duration of a transcontinental flight, these experiments have been performed at relatively large relative humidity (\sim 40%). If we consider lower humidity, longer times can be expected.

Chapter 5

Conclusion

The aim of this research is to analyze **the critical points in MEA converter to machine chain** by performing PD tests on PCBs (high voltage terminal part of the inverter) and endurance tests of the twisted pairs (turn/turn insulation of the inverter fed machine). The conclusion of this research provides the precise description of what we got with all the above experiments:

PD tests have been performed on various PCBs to understand whether this part is critical in the sense of PD occurrence or not? The answer to this question with all the findings from the experiments performed on PCBs is discussed below:

- The AC voltage stress at ambient conditions affects the PDIV of PCBs, as voltages increase PDIV decreases; it also decreases with the decrease of the gap between two conducting points (creepage distance). It is showed in figure 4.4 that the creepage distance of PCBs (E6 and C6) is the same and their PDIV is also the same, while the creepage distance of PCB D6 (short gap) is shorter so the PDIV is also lower as compared to other PCBs.
- The effect of PDIV due to the temperature rise describes that there is an inverse relationship between PDIV and temperature, when temperature increases from 25 to 120 °C, PDIV decreases and vice versa. The percentage decrease in PDIV is 40%, in the case of both PCBs (hole between plates (E6) and the gap between plates (C6) \approx 1.5 mm), whereas the percentage drops in PDIV is 45% in the case of PCB with small creepage distance of around 0.3 mm. It is also determined that the effect of temperature on PDIV is caused by something other than a reduction in air density. Non-linearity in the temperature normalization curve could be attributable to permittivity or another environmental effect, however, the influence of permittivity seems limited because the non-linearity is moderate.
- The effect of pressure on the PDIV of PCBs is shown in section 4.1.3 where it is observed that the pressure and PDIV have a direct relationship, if the pressure

goes down from (1013 – 200 mbar) PDIV decreases linearly while if we further decrease the pressure from 200 mbar, PDIV decreases in a faster way. The percentage decrease of PDIV of all the three PCBs at 200 mbar is 54 - 55%, while the reduction of PDIV at 100 mbar ranges between 65 - 70%. This is because when the pressure is lessened, the lower field intensity is required to trigger the initial electronic avalanche.

- In the case of DC supply voltage it is observed that in the case of PCB with a small creepage distance, the PDIV ranges between 1600 – 2700 V while in the case of the other two PCBs, the PDIV ranges between 3800 – 4600 V. If we go beyond this, breakdown occurs. Furthermore, it has also been observed that space charges have a significant impact on the measurement of PDIV. As a result, this section concludes that understanding the nature of space charges in the material is required before doing PDIV measurements in DC.
- The PDIV under repetitive square wave is found to be 8% higher than under AC waveform. This is because the repetitive square wave voltage is affected by an overshoot during the turn on and off flanks. The probability of PD inception during an overshoot is limited to the inherent randomness of free electrons able to start a PD. Since the applied voltage is ramped during the tests, this delay tends to provide a higher PDIV. Besides, the PCB permittivity at the largest frequencies of the inverter voltage might be lower than that at AC 50 Hz. Consequently, lower electric fields can be expected in the air, leading to larger PDIV values.

Following the completion of all PD testing on various types of PCBs, it is concluded that the converter part in the converter to machine chain is not critical. However, it is important to remember that the proper creepage distance in the high voltage terminal part of the inverter is necessary to avoid PDs and ensure the inverter to machine chain's reliability.

After the converter part, the behavior of turn/turn insulation of the inverter-fed machine when subjected to repetitive square wave/AC 50 kHz voltages are examined in order to determine how long the machine's insulation can tolerate the stress under aerospace

conditions. To understand the behavior of machine insulation, an endurance test has been performed on the twisted pairs, the results discussed below:

- Endurance time of all three samples of twisted pair decreases as the voltage level of repetitive square wave 100 kHz /sinusoidal AC 50 kHz supply increases, this implies that if we increase the voltage level of an inverter fed machine at a lower pressure, it will take less time to the breakdown. Moreover, the endurance time of the corona-resistant wire of sample #2 TP is higher than the other two samples because of its higher diameter.
- Sinusoidal AC 50 kHz voltage has a lower endurance time compared to the repetitive square wave 100 kHz voltage; this is due to the higher frequency of repetitive square voltages which decreases the endurance time of the twisted pairs if the rise time and wave shape are held constant.
- Humidity has a significant impact on the endurance of twisted pairs, as humidity increases, endurance decreases this is because the presence of humidity changes the chemical kinetics of the air causes the change of applied electric field distribution in the air.

After all of these tests, it can be concluded that the corona-resistant wire can withstand PDs for a long time in aerospace conditions. Also shown in figure 4.14 that a voltage level of (700 V \approx 1400 Vpk-pk) has an endurance time of 32488 sec 9 hours, which is not that much if compared to the duration of a transcontinental flight. If we consider lower humidity, longer times can be expected.

Acknowledgments

In the name of Almighty Allah, the most gracious and merciful, who gave me the confidence and fortitude to complete my thesis. My foremost expression of submission and gratitude goes to Almighty Allah without whose grace and mercy; this work would never be possible even in the slightest.

I would like to express my sincere gratitude to my supervisor, Prof. Andrea Cavallini for giving me the opportunity to do my master's thesis under him. His trust and direction, as well as his encouragement and support during difficult moments, have always pushed me to shape my research. I'd like to express my gratitude to my co-supervisor Alberto Rumi for his guidance and assistance throughout my experiments. Thank you to everyone in my lab for your help and for making it such a lovely place to work.

No words could ever sufficiently describe my gratitude to my parents for their unwavering support, love, prayers, and best wishes for my success. These are the sacrifices and encouragements they have made for my higher education that have helped me become the person I am today. Above all, I want to express my sincere gratitude to my uncle, Kishore Kumar, for his steadfast support and encouragement throughout my life; I believe it is because of him that I am here, as well as my brother, Sanjay Kumar, who has always treated me like a best friend. I'd also like to extend my gratitude to my fiancée for her unwavering faith and support in every step of my life.

Finally, I would like to thank my friends for their encouragement, fun times, and their presence. I would thank Dr. Usman Hadi, for his support and guidance.

Bibliography

- [1] Runsen Zhang and Shinichiro Fujimori, “The role of transport electrification in global climate change mitigation scenarios”, IOP Publishing, Environmental research letter, Environ. Res. Lett. 15 034019 (2020).
- [2] Pat Wheeler, “Technology for the More and All Electric Aircraft of the Future”, IEEE international Conference on Automatica (ICA-ACCA), ISBN: 978-1-5090-1148-3 (Oct 2016).
- [3] J.A. Rosero, J.A. Ortega, E. Aldabas, and L. Romeral, “Moving towards a more electric aircraft”, IEEE Aerospace and Electronic Systems Magazine (Volume: 22, Issue: 3, March 2007), pp: 3 – 9, ISSN: 1557-959X.
- [4] R.I Jones, “The More Electric Aircraft: the past and the future?”, IEE Colloquium on Electrical Machines and Systems for the More Electric Aircraft (Ref. No. 1999/180), 9 Nov. 1999.
- [5] Xin Zhao, Josep M. Guerrero, Xiaohua Wu, “Review of aircraft electrical power systems and architectures”, IEEE International Energy Conference (ENERGYCON) 2014, ISBN: 978-1-4799-2449-3.
- [6] C.C. Chan. “The state of the art of electric and hybrid vehicles”, Proceedings of the IEEE (Volume: 90, Issue: 2 Feb. 2002), pp. 247-275, ISSN: 1558-2256.
- [7] Giampaolo Buticchi; Serhiy Bozhko; Marco Liserre; Patrick Wheeler; Kamal Al-Haddad, “On-Board Microgrids for the More Electric Aircraft-Technology Review”, IEEE Transactions on Industrial Electronics (Volume: 66, Issue: 7, July 2019), pp 5588 – 5599, ISSN: 1557-9948.
- [8] Fei Fred Wang, Zheyu Zhang, “Overview of silicon carbide technology: Device, converter, system, and application”, CPSS Transactions on Power Electronics and Applications (Volume: 1, Issue: 1, Dec. 2016), pp: 13 – 32, ISSN: 2475-742X.
- [9] Mirza Batalović, Kemo Sokolija, Mesud Hadžialić, Nejra Batalović, “Partial discharges and IEC standards 60840 and 62067: Simulation support to encourage changes”, Hrčak Technical gazette, Vol. 23 No. 2, 2016, IEEE, pp: 589 – 598

- [10] El-Sayed M. El-Refaie, M. K. Abd Elrahman, and O. Zidane, “ Eighteenth International Middle East Power Systems Conference (MEPCON)”, IEEE, Dec 2016, ISBN: 978-1-4673-9063-7, Cairo, Egypt.
- [11] M.C. Ram kumar, P. Cools, A. Arun kumar, N. De Geyter, R. Morent, R. Morent, V.Kumar, S. Uday Kumar, P.Gopinath, S.K. Jaganathan, K.N. Pandiyaraj, Science direct, “Polymer coatings for biocompatibility and reduced nonspecific adsorption”, Publisher: Elsevier, Book: Functionalised Cardiovascular Stents, 2018, pp: 155-198.
- [12] Wikipedia, “Partial discharge”, https://en.wikipedia.org/wiki/Partial_discharge.
- [13] Rui Rui and Ian Cotton. “Impact of low pressure aerospace environment on machine winding insulation”. en. In: 2010 IEEE International Symposium on Electrical Insulation. San Diego, CA, USA: IEEE, June 2010, pp. 1 - 5. ISBN: 978-1-4244-6298-8.
- [14] IEC TS 60034-18-41, “Qualification and Acceptance test for Type I Electrical Insulation Systems Used in Rotating Electrical machines Fed form Voltage Converters”, Ed. 1 2006.
- [15] Francesco Guastavino and Andrea Dardano, “Life tests on twisted pairs in presence of partial discharges: influence of the voltage waveform”, IEEE Transactions on Dielectrics and Electrical Insulation (Volume: 19, Issue: 1, February 2012), pp: 45-52, ISSN: 1558-4135.
- [16] F. Guastavino, D. Cordano, E. Torello, and G. Secondo, “Electrical aging tests on different kind of insulating systems adopted for induction stator motor”, 2015 IEEE Conference on Electrical Insulation and Dielectric Phenomena (CEIDP), (December 2015), ISBN: 978-1-4673-7498-9.
- [17] Humidity and temperature test chamber DY200 T-DY200 C(T), Angelantoni Test Technologies. Online:<https://www.directindustry.com/prod/angelantoni-test-technologies/product-18270-1975826.html>.
- [18] Tektronix MDO3000 Mixed domain oscilloscope. Online: <https://www.tek.com/oscilloscope/mdo3000-mixed-domain-oscilloscope>.

- [19] Altanova group – products - Partial discharge tests. Online:
<https://www.altanova-group.com/en/products/partial-discharge-tests/altanova-catalogo>.
- [20] Hamamatsu, Photon counting head H11870 series, July 2021.
Online:https://www.hamamatsu.com/resources/pdf/etd/H11870_TPMO1061E.pdf
- [21] Hamamatsu – Counting unit C8855-01, July 2021
Online:https://www.hamamatsu.com/resources/pdf/etd/C885501_TACC1078E.pdf
- [22] Testo 635-1 – Temperature and Humidity measuring instrument – testo.com
Online:<https://static-int.testo.com/media/b7/04/6757c3682a28/testo-635-Data-sheet.pdf>
- [23] Altanova group – products - Partial discharge tests-laboratory equipments-capacitive divider. Online:<https://www.altanova-group.com/en/products/partial-discharge-tests/laboratory-equipment/capacitive-divider>
- [24] M. Kaufhold, "Failure Mechanism of the Interturn insulation of Low Voltage Electric Machines Fed by Pulse-Controlled Inverters". Proceedings of 1995 Conference on Electrical Insulation and Dielectric Phenomena, Oct 1995, ISBN:0-7803-2931-7
- [25] Weijun Yin. "Failure Mechanism of Winding Insulations in Inverter-Fed Motors", IEEE Electrical Insulation Magazine (Volume: 13, Issue: 6, Nov.-Dec. 1997), pp:18 – 23, ISSN: 1558-4402.
- [26] P. Wang, A. Cavallini, and G. C. Montanari, "Endurance testing of rotating machines insulation systems: Do sinusoidal and square voltage waveforms provide comparable results?", 2013 IEEE International Conference on Solid Dielectrics (ICSD), July 2013,ISSN: 2159-1687-6.
- [27] IEC TS 60034-18-42, Rotating electrical machines-Part 18-42: Qualification and acceptance tests for partial discharge resistant electrical insulation systems (Type II) used in rotating electrical machines fed from voltage converters, 2011.

- [28] IEC 62477-1 Safety requirements for power electronic converter systems and equipment - Part 1: General, 2012, IEC standard.
- [29] IEC 62477-2 Safety requirements for power electronic converter systems and equipment - Part 2: Power electronic converters from 1 000 V AC or 1 500 V DC up to 36 kV AC or 54 kV DC, 2018, IEC standard.
- [30] Andrea Cavallini. "Reliability of low voltage inverter-fed motors: What have we learned, perspectives, open points", 2017 International Symposium on Electrical Insulating Materials (ISEIM). Toyohashi: IEEE, Sept. 2017, pp. 13-22. ISBN: 978-4-88686-099-6.
- [31] Ian Cotton, Andrew Nelms, Mark Husband, "Higher voltage aircraft power systems", IEEE Aerospace and Electronic Systems Magazine (Volume: 23, Issue: 2, Feb. 2008), March 2008, pp: 25 – 32, ISSN: 1557-959X.
- [32] B. H. Nya, J. Brombach, D. Schulz, "Benefits of higher voltage levels in aircraft electrical power systems", 2012 Electrical Systems for Aircraft, Railway and Ship Propulsion, Oct. 2012, ISSN: 2165-9427
- [33] Johannes BROMBACH, Torben SCHRÖTER, Arno LÜCKEN, Detlef SCHULZ, "Optimizing the Weight of an Aircraft Power Supply System through a +/- 270 VDC Main Voltage", Wydawnictwo SIGMA-NOT, 2012, pp: 47 – 50, ISSN: 0033-2097.
- [34] Andy Yoon, Jianqiao Xiao, Danny Lohan, Faraz Arastu, Kiruba Haran, "High-Frequency Electric Machines for Boundary Layer Ingestion Fan Propulsor", IEEE Transactions on Energy Conversion (Volume: 34, Issue: 4, Dec. 2019), 20 September 2019, pp: 2189 – 2197, ISSN: 1558-0059.
- [35] Adolfo Dannier, Gianluca Brando, Ivan Spina, Angelo Raciti, Santi Agatino Rizzo, Giovanni Susinni, "High frequency converter topologies suitable for more electric aircraft", 2018 AEIT International Annual Conference, Oct. 2018, ISBN: 978-8-8872-3740-5.
- [36] Firman Sasongko, Peng Yaxin, Josep Pou, Rejeki Simanjanjorang, "One-Kilohertz Fundamental Frequency Operation of a SiC Power Converter for

- Future Aircraft System”, 2018 Conference on Power Engineering and Renewable Energy (ICPERE), Oct. 2018, ISBN: 978-1-5386-7456-7.
- [37] Shan Yin, King Jet Tseng, Rejeki Simanjorang, Yong Liu, Josep Pou, “A 50-kW High-Frequency and High-Efficiency SiC Voltage Source Inverter for More Electric Aircraft”, IEEE Transactions on Industrial Electronics (Volume: 64, Issue: 11, Nov. 2017), 24 April 2017, pp: 9124 – 9134, ISSN: 1557-9948.
- [38] Peng Wang, Hongying Xu, Jian Wang, Wanya Zhou, Andrea Cavallini, “The influence of repetitive square wave voltage rise time on partial discharge inception voltage”, 2016 IEEE Conference on Electrical Insulation and Dielectric Phenomena (CEIDP), Oct. 2016, ISBN: 978-1-5090-4654-6.
- [39] Doris Ragna Meyer, Andrea Cavallini, Luca Lusuardi, Davide Barater, Giorgio Pietrini, Alessandro Soldati, “Influence of impulse voltage repetition frequency on RPDIV in partial vacuum”, IEEE Transactions on Dielectrics and Electrical Insulation (Volume: 25, Issue: 3, June 2018), pp: 873 – 882, ISSN: 1558-4135.
- [40] J.C.G. Wheeler, “Effects of converter pulses on the electrical insulation in low and medium voltage motors”, IEEE Electrical Insulation Magazine (Volume: 21, Issue: 2, March-April 2005), pp: 22 – 29, April 2005, ISSN: 1558-4402.
- [41] Luca Lusuardi, Alberto Rumi, Andrea Cavallini, Davide Barater, and Stefano Nuzz, “Partial Discharge Phenomena in Electrical Machines for the More Electric Aircraft. Part II: Impact of Reduced Pressures and Wide Bandgap Devices”, IEEE Access (Volume: 9), pp: 27485 – 27495, February 2021, ISSN: 2169-3536.
- [42] Dalibor Filipovic-Grcic, Bozidar Filipovic-Grcic, and Ivan Novko, “An Improved Method for Performance Testing of Partial Discharge Calibrators”, ISH 2019: Proceedings of the 21st International Symposium on High Voltage Engineering, pp: 1334-1345.

- [43] Altanova group – products - Partial discharge tests-laboratory equipments-PD calibrator. Online: <https://www.altanova-group.com/en/products/partial-discharge-tests/sensors-and-accessories/pd-calibrator>.
- [44] Christopher Emersic, Robert Lowndes, Ian Cotton, Simon Rowland, Robert Freer, “Degradation of conformal coatings on printed circuit boards due to partial discharge”, IEEE Transactions on Dielectrics and Electrical Insulation (Volume: 23, Issue: 4, August 2016), pp: 2232 – 2240, September 2016, ISSN: 1558-4135.
- [45] M. Kaufhold, G. Borner, M. Eberhardt, and J. Speck, “Failure mechanism of the interturn insulation of low voltage electric machines fed by pulse-controlled inverters”, IEEE Electrical Insulation Magazine (Volume: 12, Issue: 5, Sept.-Oct. 1996), pp: 9 – 16, ISSN: 1558-4402
- [46] U. Fromm, “Interpretation of partial discharges at dc voltages”, IEEE Transactions on Dielectrics and Electrical Insulation (Volume: 2, Issue: 5, Oct 1995), pp: 61 – 70, Oct 1995, ISSN: 1558-4135.
- [47] A. Cavallini, F. Ciani, and G.C. Montanari, “The effect of space charge on phenomenology of partial discharges in insulation cavities”, CEIDP '05. 2005 Annual Report Conference on Electrical Insulation and Dielectric Phenomena, 2005., Oct. 2005.
- [48] A. Cavallini, L. Versari, and L. Fornasari, “Feasibility of partial discharge detection in inverter-fed actuators used in aircrafts”, 2013 Annual Report Conference on Electrical Insulation and Dielectric Phenomena, Oct. 2013, ISBN: 978-1-4799-2597-1.
- [49] Wang P, Cavallini A, Montanari G.C, and Guangning Wu, "Effect of rise time on PD pulse features under repetitive square wave voltages", IEEE Transactions on Dielectrics and Electrical Insulation, vol. 20, no. 1, pp. 245,254, February 2013.
- [50] Luca Lusuardi, Andrea Cavallini, Andrea Caprara, Fabrizio Bardelli, and Andrea Cattazzo, “The Impact of Test Voltage Waveform in Determining

the Repetitive Partial Discharge Inception Voltage of Type I Turn/Turn Insulation Used in Inverter-Fed Induction Motors”, 2018 IEEE Electrical Insulation Conference (EIC), June 2018, ISSN: 2576-6791.

- [51] Gian Carlo Montanari, Paolo Seri, and Robert Hebner, “Type Of Supply Waveform, Partial Discharge Behavior And Life Of Rotating Machine Insulation Systems”, 2018 IEEE International Power Modulator and High Voltage Conference (IPMHVC), June 2018, ISSN: 2576-7283.
- [52] Alberto Rumi, Andrea Cavallini, and Luca Lusuardi, “Impact of WBG Converter Voltage Rise-Time and Switching Frequency on the PDIV of Twisted Pairs”, 2020 IEEE 3rd International Conference on Dielectrics (ICD), July 2020, ISBN: 978-1-7281-8983-3.
- [53] S. Matsumoto, Nguyen Nhat Nam, D. Nagaba and T. Ogiya, "Partial discharge characteristics of twisted magnet wire under high frequency AC voltage", Proceedings of 2014 International Symposium on Electrical Insulating Materials, pp. 57-60, 2014.
- [54] Peng Wang, Neng Yang, Changjiang Zheng, and Ying Li, “Effect of repetitive impulsive and square wave voltage frequency on partial discharge features”, 2018 12th International Conference on the Properties and Applications of Dielectric Materials (ICPADM), May 2018, ISSN: 2160-9241.
- [55] Jun Jiang, Mingxin Zhao, haohai Zhang, Min Chen, Haojun Liu, and Ricardo Albarracín, “Partial Discharge Analysis in High-Frequency Transformer Based on High-Frequency Current Transducer”, MDPI journals, Energies, Volume 11, 2018.
- [56] Tarek S. Negm, Mostafa Refaey, and Ahmed A. Hossam-Eldin, “Modeling and simulation of internal Partial Discharges in solid dielectrics under variable applied frequencies”, 2016 Eighteenth International Middle East Power Systems Conference (MEPCON), Dec. 2016, ISBN: 978-1-4673-9063-7.
- [57] Peng Wang, Yanghao Gu, Qi Wu, Andrea Cavallini, Qin Zhang, Jiawei Zhang, Peiyi Li, and Ying Li, “Influence of Ambient Humidity on PDIV and

Endurance of Inverter-fed Motor Insulation”, 2019 IEEE Electrical Insulation Conference (EIC), June 2019, ISSN: 2576-6791.

- [58] Wang, G. C. Montanari and A. Cavallini, "Partial Discharge Phenomenology and Induced Aging Behavior in Rotating Machines Controlled by Power Electronics", IEEE Trans. on Indus. Electr., vol. 61, pp. 7105-7112, 2014
- [59] Fenger and Greg C. Stone. “Investigations into the effect of humidity on stator winding partial discharges”. In: IEEE transactions on dielectrics and electrical insulation 12.2 (2005), pp. 341–346.
- [60] Yusuke Kikuchi et al. “Effects of ambient humidity and temperature on partial discharge characteristics of conventional and nanocomposite enameled magnet wires”. In: IEEE Transactions on Dielectrics and Electrical Insulation 15.6 (2008), pp. 1617 - 1625.
- [61] Satoshi Matsumoto et al. “Partial discharge characteristics of twisted magnet wire under high frequency AC voltage”. In: Proceedings of 2014 International Symposium on Electrical Insulating Materials. IEEE. 2014, pp. 57–60.
- [62] Sky brary -Ram air turbine (RAT). Online:
[https://www.skybrary.aero/index.php/Ram_Air_Turbine_\(RAT\)](https://www.skybrary.aero/index.php/Ram_Air_Turbine_(RAT))